Chondrogenic differentiation of bone marrow-derived stromal cells in pellet culture and silk scaffolds for cartilage engineering – Effects of different growth factors and hypoxic conditions

Dissertation zur Erlangung
des naturwissenschaftlichen Doktorgrades der
Julius-Maximilians-Universität Würzburg

vorgelegt von

Martin Krähnke
aus Mainz

Würzburg 2019

Eingereicht bei der Fakultät für Chemie und Pharmazie am

_____

Gutachter der schriftlichen Arbeit

1. Gutachter: _____

2. Gutachter: _____

Prüfer des öffentlichen Promotionskolloquiums

1. Prüfer: _____

2. Prüfer: _____

3. Prüfer: _____

Datum des öffentlichen Promotionskolloquiums

_____

Doktorurkunde ausgehändigt am

_____

Contents

List of Figures

List of Tables

Chapter 1

Introduction

1.1 Tissue engineering

Starting in fields of reconstructive surgery, the replacement of missing function through rebuilding the body's structure via transplantation of tissue and organs has improved the quality of life of thousands of patients. However, the transplantation from one individual to another has severe constraints. The major problems of accessing enough tissue and organs as well as tissue rejection and destruction by the immune system of the host still remain to be solved. In order to overcome these issues, the field of tissue engineering has developed[1].
As an interdisciplinary research area, it combines fundamentals of engineering and biosciences[2,3]. The aim of tissue engineering, which has evolved into what is called today "regenerative medicine", is the regeneration and repair of biological tissue and organs in the organism which have been damaged by trauma or pathology[4]. New tissue is fabricated using living cells, which generally are associated with a matrix or scaffold material, either natural or synthetic, to guide tissue development. Several cell sources have been identified and can be employed, while especially stem cells have accelerated research in the last years and provide valuable therapeutic impulses. To improve the restoration of the tissue, specific signals such as growth factors can further be conjugated to the material or used during *in vitro* culture[1].
As one field of tissue engineering, articular cartilage engineering aims at the development of articular cartilage tissue substitutes to cure tissue defects resulting from trauma, injury or disease. Although traditional methods like autografts and allografts have been used in clinic to treat articular cartilage lesions, disadvantages associated with these therapies still exist, e.g. donor site mobility and limited cartilage tissue availability[5–7]. Therefore, it is worthwhile to develop an effective and simple method to successfully repair and regenerate articular cartilage tissue. As a rapidly growing field, cartilage tissue engineering approaches may provide alternative innovative solutions for articular cartilage repair and restoration by developing biomimetic tissue substitutes[8].

1.2 Articular Cartilage

Articular cartilage is a highly specialized connective tissue of diarthrodial joints. It plays a fundamental role in the function of the musculoskeletal system by allowing almost frictionless motion to occur between the articular surfaces of a synovial joint by providing a smooth, lubricated surface for articulation[9]. Articular cartilage distributes the transmission of loads over a large contact area and thereby minimizes the contact stresses and dissipates the energy associated with the biomechanical load[10,11]. These properties allow articular cartilage to remain healthy and functional over a long life time. However, due to the absence of blood vessels, articular cartilage has a limited capacity of intrinsic repair. In this regard, preserving articular cartilage in a healthy state is of major importance for joint health[12].

Structure and composition of articular cartilage

Articular cartilage is composed of chondrocytes and a dense extracellular matrix (ECM). The ECM primarily consists of water, collagen and proteoglycans and to a lesser amount of glycoproteins and non-collagenous proteins. Chondrocytes are highly specialized cells which are responsible for the development of articular cartilage and the maintenance of the ECM. They are metabolically active cells displaying a relatively slow state of matrix turnover[13]. Usually a few cells are arranged together in a territorial region called chondrons, surrounded by a network of thin collagen fibrils. The cells are embedded in their own produced ECM without vasculature, so their nutrient supply provided by the synovial fluid is given by a combination of diffusion and hydraulic transport processes during joint compression[14].

Articular cartilage structure exhibits a zonal organization and can be distinguished according to its collagen fiber ultrastructure orientation, ECM content and chondrocytic cell type: superficial zone - middle zone - deep zone - calcified zone (Figure 1.1)[9,15].

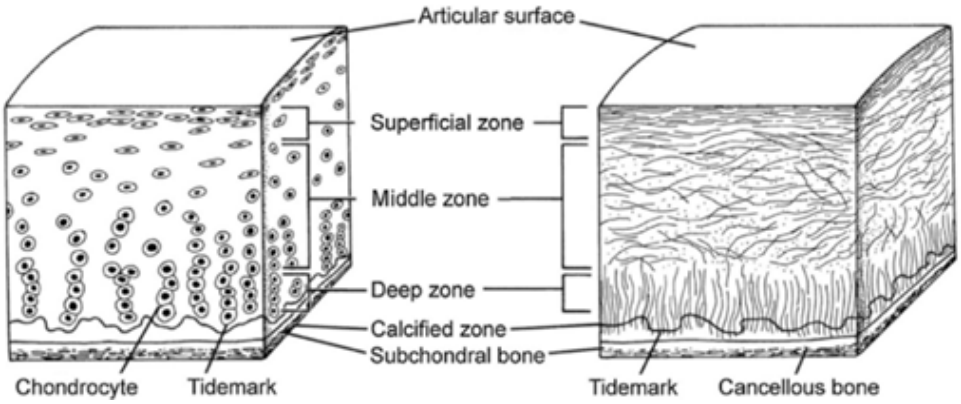

Figure 1.1: Structure of human articular cartilage. Cellular organization in the zones of human articular cartilage is shown on the left, the change of collagen fibril orientation in the different zones of cartilage is shown on the right. Reprinted from [16], Copyright (2017), with permission from Elsevier.

Zones

The organization of articular cartilage reflects its functional role. The superficial zone protects deeper layers from sheer stress and makes up 10% to 20% of articular cartilage thickness. To withstand sheer, tensile and compressive forces imposed by articulation, tightly packed collagen fibrils (primarily type II and IX collagen) and flattened chondrocytes which produce lubricin, are aligned parallel to the articular surface[12,17]. The middle zone or transitional zone, immediately under the superficial zone, represents 40% - 60% of the total cartilage volume. It contains less organized but thicker collagen fibrils and is rich in the proteoglycan aggrecan. Cell density is lower and cell morphology is rounded (Figure 1.1 left). The deep zone represents up to 30% of articular cartilage volume. Cell density is at lowest but the proteoglycan content and collagen fibril diameter is maximal[18]. The chondrocytes are arranged in columns parallel to the collagen fibrils and perpendicular to the surface of the joint. The tidemark delineates the boundary between deep zone and calcified cartilage, which merges into the subchondral bone. Chondrocytes in the calcified zone express the hypertrophic phenotype and synthesize collagen type X providing structural integrity and a great resistance to compressive forces. Furthermore, the calcified layer plays a significant role in securing the cartilage to bone by anchoring the collagen fibrils

of the deep zone to the subchondral bone[12,19].

Regional Organization

In addition to its zonation the matrix surrounding the chondrocytes consists of different regions depending of its composition and collagen fibril organization or diameter. Three regions can be distinguished: pericellular, territorial and interterritorial matrix region. All chondrocytes are surrounded by a thin ($\approx 2\,\mu$m) pericellular matrix. This matrix is rich in a number of proteoglycans and non-collagenous matrix proteins and non-fibrillar collagens[16]. The territorial matrix surrounds the pericellular matrix of each chondrocyte, in some region even clusters of chondrocytes. It consists of thin collagen fibrils forming a basket-like structure around the cells[20,21]. This basket-like network might provide protection for the chondrocytes against mechanical stress and substantial loads[9]. The interterritorial region makes up the largest volume of mature articular cartilage. Its matrix contains the largest diameter collagen fibrils in randomly oriented bundles contributing most to biomechanical properties of articular cartilage[22]. The fibers are oriented differently in the zones depending on the requirements: parallel to the articular surface in the superficial zone, obliquely in the middle zone and perpendicular to the joint surface in the deep zone[12,23].

Extracellular matrix

Articular cartilage extracellular matrix consists of two major components: tissue fluid, which accounts for 65% - 80% of total wet weight, and the framework of structural macromolecules (primarily collagens, proteoglycans, non-collagenous proteins and glycoproteins) which are responsible for tissue stiffness and stability account for the remaining wet weight[11].

Tissue Fluid

Water contributes up to 80% of wet weight of articular cartilage with 80% in the superficial zone to 65% in the deep zone. It contains proteins, metabolites

and high concentrations of cations like sodium and calcium to balance negatively charged proteoglycans. The interaction of water with the proteoglycans influences the mechanical properties and allows load-dependent deformation of cartilage[24]. In addition, the flow of water throughout the matrix and articular surface provides nutrition to the chondrocytes and medium for lubrication[25].

Collagens

Collagen is an ubiquitous component of articular cartilage and forms an extensive network throughout the territorial and interterritorial matrix. It contributes up to 60% of dry weight of articular cartilage. Collagen type II accounts for 90-95% of collagens in the ECM of articular cartilage and forms the primary component of the macrofibrillar framework[9]. Collagens type VI, IX, X and XI are also found to a lesser extent and help to stabilize this major collagen type II framework[26](see Table 1.1). Collagen type II is composed of three α_1II

Table 1.1: Different types of collagens and their particular functions. Reprinted from [23], Copyright 2008, with permission from Oxford University Press.

Type	Morphological location	Function
II	Principal component of macrofibril (90%–95%)	Tensile strength
VI	Pericellular matrix	Helps chondrocytes to attach to the matrix
IX	Cross-linked to surface of macrofibril	Tensile properties and interfibrillar connections
X	Closely related to the hypertrophied cells in calcified cartilage layer	Structural support and aids in cartilage mineralization
XI	Within or on macrofibrils	Nucleates fibril formation

chains that form a triple helix. The major amino acids are glycine, proline, hydroxyproline (G-X-Y) and alanine, with hydroxyproline stabilizing the triple helix via hydrogen bonds along the polypeptide chain. This structure provides articular cartilage with important tensile properties which help stabilizing the ECM[27].

Proteoglycans

Proteoglycans consist of a protein core with one or more attached glycosaminoglycan (GAG) chains (long unbranched polysaccharide units consisting of repeating disaccharides with a covalently bound negatively charged carboxylate or sulfate group)[9]. Glycosaminoglycans found in articular cartilage include hyaluronic acid, chondroitin sulfate, keratan sulfate and dermatan sulfate. They form long strings extended from the core protein and repel one another due to their negative charge[12]. Articular cartilage consists of a variety of proteoglycans like aggrecan, decorin, biglycan and fibromodulin. The largest proteoglycan of size and the most abundant by weight (90%) of articular cartilage is aggrecan (Figure 1.2). Up to 500 aggrecan molecules bind to a hyaluronate monofilament backbone which can be stabilized by link proteins[28]. This forms large negatively charged proteoglycan aggregates[29] which combined with collagens form a powerful, permeable, fiber-reinforced composite material that provides the osmotic properties needed to withstand compressive loads[10].
The non-aggregating proteoglycans are more described to interact with other collagens or modulate cell behavior. Decorin and fibromodulin for example stabilize the collagen network by binding to collagen type II but also seem to limit access of collagenases to their specific cleavage sites[30]. Furthermore, these proteoglycans can bind growth factors and regulate their activity by sequestering the growth factor (e.g. transforming growth factor beta (TGF-β)) into the ECM[31].

1.3 Matrix-modulating enzymes and ECM remodeling

The ECM serves as an important regulator of cellular and tissue functions that are essential for life. Its role goes far beyond providing physical support for tissue form, stability and biomechanic resilience: it is a dynamic structure that is constantly undergoing remodeling processes to control tissue homeostasis[9,32]. These remodeling processes for matrix homeostasis are regulated by a care-

ful balance between matrix synthesis, secretion, modification and enzymatic degradation[33]. The functional significance of the ECM becomes evident by multiple defects and diseases that are directly associated with a dysregulation of ECM components[34]. Cleavage of ECM components is the main process during ECM remodeling, regulates ECM composition and structure and furthers the release of signaling molecules like growth factors[35]. Important enzymes involved in regulating matrix homeostasis are matrix-degrading enzymes such as "a disintegrin and metalloproteinase with thrombospondin motifs" (ADAMTSs) and matrix metalloproteinases (MMPs) and their inhibitors (tissue inhibitor of MMPs (TIMPs)). MMP1, MMP3, MMP13, ADAMTS4 and ADAMTS5 have been reported to play a key role in normal cartilage turnover, cartilage degradation and osteoarthritis (OA)[36].

MMPs

MMPs belong to the family of Ca- and Zn-dependent endopeptidases and are able to degrade nearly all ECM components due to their wide substrate specificity. MMP activity is generally low in normal conditions but increases during remodeling and inflammation processes. So far, 23 human MMPs have been identified and according to their substrate specificity have been grouped into the major classes of collagenases, gelatinases, stromelysins and membrane-type MMPs (MT-MMP)[37,38]. Most of the MMPs are secreted as zymogens into the extracellular space where they are activated primarily by proteolytic cleavage of the self-inhibiting N-terminal prodomain or by oxidation of the thiol group[35]. In addition to its main function of ECM digestion, MMPs display multiple other features. Various MMPs can activate precursor proteins like pro-MMPs by cleavage or release neo-epitopes and cryptic cleavage fragments with new biological activity such as the collagen IVα3 chain fragment tumstatin which provides anti-angiogenic potential[39].

By subcellular relocation from the membrane or the cytosol into the nucleus, MMPs are involved in the regulation of proliferation and apoptosis by cleaving transcription factors and nuclear proteins[40–42]. Table 1.2 gives an overview of the MMPs that were analyzed in this work, its activators and targets. For more details please refer to Lu et al.[43].

Table 1.2: Properties of the major MMPs and ADAMTSs. Reprinted from [43], Copyright (2011), with permission from Cold Spring Harbor Laboratory Press.

Members	Alias	Activators	ECM targets	Other targets
MMP1	Collagenase-1	MMP3, 10, plasmin; kallikrein; chymase	Collagens I, II, III, VII, X; gelatins; aggrecan; tenascin; perlecan; entactin	IGFBP-2, -3, -5; pro-IL-1b; CTGF; MMP2, 9
MMP3	Stromelysin-1	Plasmin; kallikrein; chymase; tryptase	Aggrecan; decorin; gelatins; fibronectin; laminin; collagens III, IV, IX, and X; tenascin; perlecan	IGFBP-3; pro-IL-1b;; HB-EGF; pro-TGF-β; CTGF; E-cadherin; plasminogen; uPA pro-MMP1, 7, 8, 9, 13
MMP13	Collagenase-3	MMP2, 14 plasmin; kallikrein; chymase; tryptase	Collagens I, II, III, IV, IX, X, and XIV; aggrecan; fibronectin; tenascin; SPARC/osteonectin; laminin; perlecan	CTGF; pro-TGF-β; MCP-3
ADAMTS4	Aggrecanase-1	n.d.	Aggrecan; brevican; versican; fibronectin; decorin	n.d.
ADAMTS5	Aggrecanase-2	n.d.	Aggrecan; versican; brevican	n.d.

ADAMTS

The ADAMTS family consists of 22 members that, like MMPs, belong to the metzincins, the zink-dependent proteases, but only 12 members are active proteases[35]. The structure of all ADAMTS can be categorized starting from the N-terminus: a signal peptide, a pro-domain, a catalytic domain, the integrin binding disintegrin-like domain which prevents cell-cell interaction, a central thrombospondin (TS) repeat, a cysteine-rich domain, a spacer region and (except for ADAMTS4) one or more TS repeats[44]. An important difference between ADAMTS and MMPs is the ability of many ADAMTSs to bind to the ECM[45,46]. Even though the exact mechanism is not fully understood so far, it is believed that ECM binding is based on the TSP repeats, e.g. it was previously shown that ADAMTS4 binds aggrecan via its sole TSP motif[47].

ADAMTS are expressed as inactive proenzymes and activated by proprotein convertase cleavage (e.g. furin) either intracellularly in the ER[48], at the cell surface[49] or extracellularly[50]. Their functions include cleavage of matrix proteoglycans, collagen processing as procollagen n-proteinase and inhibition of angiogenesis[47]. ADAMTS1, 8, 9, 15, 16, 18 and especially ADAMTS4 and 5 are regarded as proteoglycanases due to their ability to degrade aggrecan, versican,

brevican and other proteoglycans[44] (Table 1.2).

Degradation of aggrecan and collagen and the generation of cartilage neoepitopes

In contrast to the aggrecanases among the ADAMTSs which only seem to be specific for aggrecan and the related proteoglycans versican and brevican, members of the MMP family are able to degrade both collagen and aggrecan structures. However, MMPs and ADAMTSs are the only enzymes known so far that cleave aggrecan *in vivo*. The most sensitive region for MMP and ADAMTS site-specific cleavage of aggrecan is the IGD domain, located between the G1 and G2 domain[51]. MMPs cleave aggrecan primarily at the $N_{341} \downarrow F_{342}$ bond which

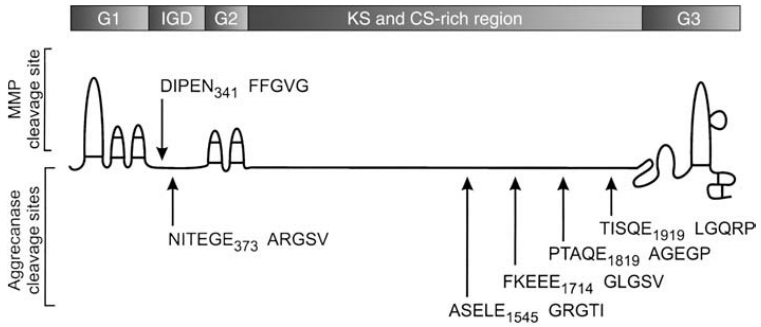

Figure 1.2: MMP and ADAMTS cleavage sites in the aggrecan core protein. The amino acid sequence cleaved by MMPs are shown above and those cleaved by the ADAMTSs are shown below the aggrecan core protein. The domain motifs are depicted at the top of the figure. Reprinted from [51], Copyright (2003), with permission from Springer Nature. For a more detailed description of the aggrecan core protein please see section 1.2.

generates the C-terminal $DIPEN_{341}$ and the N-terminal $F_{342}FGVG$ neoepitopes[51] (Figure 1.2). Even though the MMPs are believed to cleave in the C-terminal regions of aggrecan as well, the exact cleavage site still needs to be explored[52]. The aggrecanases cleave at the $E_{373} \downarrow A_{374}$ bond in the IGD generating the C-terminal NITEGE $_{373}$ and the N-terminal A_{374}RGSV neoepitope. ADAMTS4 and ADAMTS5 have various other cleavage sites in the CS-rich region[53,54] where they preferentially cleave *in vitro*[55].

The collagen type II triple helix in its fibrillar form is generally resistant to proteolytic degradation by proteases except for cathepsin K, cystein protease and MMPs (e.g. MMP1, 13, 14)[56,57]. Collagen degradation is initiated by primary collagen cleavage at specific sites in the triple-helix domain yielding short α-chain fragments. Subsequently the remaining α-chain fragments unwind and can be further degraded by collagenases, gelatinases and other enzymes[51]. As described for aggrecan, MMPs also cleave collagen type II at specific sites generating site specific neoepitopes. The CTX-II neoepitope for example is generated after MMP cleavage (MMP1, 3, 7, 9, 13) in the C-telopeptide domain of type II collagen fibrils[58] and gives information about cartilage damage and progress in OA as CTX-II levels are increased in the serum[59,60].

TIMP

ECM proteolysis needs to be tightly regulated to avoid excessive detrimental degradation and keep the destructive power of proteases under control. The tissue inhibitor of metalloproteinase (TIMP) family consisting of four members (TIMP1 - TIMP4) which are potent MMP and ADAMTS inhibitors that reversibly regulate MMP and ADAMTS activity[35]. They stoichiometrically bind 1:1 to the MMP active-site cleft and the resulting complex can be dispatched by macrophages after being recognized by the scavenger receptor[43]. Although most TIMPs are less specific when it comes to which MMP they inhibit[37], some TIMPs show preferential targets. TIMP1 for example inhibits almost every MMP except the MT-MMP, while TIMP3 preferentially binds aggrecanases like ADAMTS4 and -5[61] or MMP13[62,63]. In addition to its MMP activity regulatory functions during development and tissue remodeling processes, TIMPs show further properties like mesenchymal growth regulation, erythroid potentiating activity and cell growth-promotion[40].

The interaction between the proteolytic activity of metalloproteinases and their inhibitory counterparts, the TIMPs, is crucial for various biological events like apoptosis, cell proliferation[36] and differentiation[64]. By releasing biologically active molecules from the ECM or modulation and regulation of MMP signaling cascades the MMP/TIMP axis plays an important role in tissue development.

The TGF-β-induced chondrogenesis signaling pathways for example are supposed to be regulated by both the extracellular signal-related kinase and MMP signaling cascades. The potential function of these differentiation mechanisms highlight the regulatory role of MMPs during chondrogenic differentiation of mesenchymal stromal cells (MSC)[40].

1.4 Mesenchymal stromal cells

Mesenchymal stromal cells (MSCs) were first described by Friedenstein 1970 as colony-forming unit-fibroblasts[65] and later termed mesenchymal stem cells by Caplan 1991 due to their potential to differentiate along multiple mesenchymal lineages[66]. MSCs are multipotent stromal cells that can differentiate into a variety of cell types including chondrocytes, osteoblasts, adipocytes, myocytes and various other cell types[66,67]. They have a great capacity for self-renewal while maintaining their multipotency and offer multiple harvest sites like bone marrow or adipose tissue where they can be gained in larger amounts for musculoskeletal regeneration[68]. The most common method to isolate MSCs, which was also used in this thesis, is isolation via adherence to tissue culture plastic. They can further be concentrated using cell surface proteins, e.g. CD105 and CD45[69].
Microenvironmental cues comprising of growth factors, cell-cell and cell-matrix interactions as well as oxygen tension have the ability to induce and direct differentiation of MSCs[70]. In addition, MSCs might not only differentiate directly and function as a new cell type, but in response to particular conditions can also act as mediators and immunomodulators by releasing trophic factors on the pathological tissues that fulfill an endocrine and paracrine function[71,72].
Immunomodulatory activity is mediated by direct cell-cell contact and through secreted bioactive molecules that act on dendritic cells, B and T cells[73]. In the event of an injury, MSCs are activated and establish a regenerative microenvironment through their trophic activities to support the regeneration and refabrication of the injured tissue[74].
The multidifferentiation capacity together with the ability to self-renew and proliferate, relative abundance, immunomodulatory activity and the potential for

autologous transplantation, make MSCs attractive candidates for applications in tissue engineering and the treatment of degenerative diseases[68,70,75].

1.5 Chondrogenesis

Cartilage defects are currently treated by microfracture, mosaicplasty with autologous or allogeneic osteochondral grafts or by using cell-based autologous chondrocyte implantation (ACI)[76]. However, all treatment options that are available today do not result in a sufficient healing of the cartilage defect. While microfracture leads to a promising patient satisfaction in the first years[77], the formation of fibrocartilage at the defect site still leads to disappointing results in the long-term[78,79]. Furthermore, the application of autologous chondrocytes in articular cartilage repair is associated with the injury of healthy cartilage. In order to overcome these limitations and to improve the quality of regeneration, MSCs are regarded as a promising approach due to their high proliferation capacity and their potential to differentiate into chondrocytes[80].
Chondrogenesis is defined as the process of cartilage development which is regulated by the correct temporal and spatial expression of multiple secreted factors including insulin-like growth factors (IGFs), Wnts, fibroblast growth factors (FGFs) and members of the TGF superfamily (including bone morphogenetic proteins (BMPs) and growth/differentiation factors (GDFs))[81–84]. The formation of articular cartilage during appendicular skeletogenesis is initiated by prechondrogenic condensation and proliferation of chondroprogenitor mesenchymal cells in the early limb buds[85]. The chondroprogenitor cells express genes like *SOX9*, the major transcription factor for chondrogenesis and other members of the Sox family (*SOX5*, *SOX6*)[86,87]. The process of differentiation from MSCs into chondroblasts and further into chondrocytes is under the control of multiple factors including BMP2 and TGF-β1[88]. MSCs in the condensation differentiate into chondrocytes that produce cartilage-specific ECM including collagen type II, IX, XI and aggrecan core protein forming the cartilage tissue[89–91]. The initiation of MSC proliferation and differentiation is under control of Hox genes[92], which in turn are regulated by BMPs[93]. Over-expression of

BMPs leads to increased condensation size and cartilaginous anlagen through enhanced proliferation and matrix production mediated via the IHH-parathyroid hormone related pathway[94].

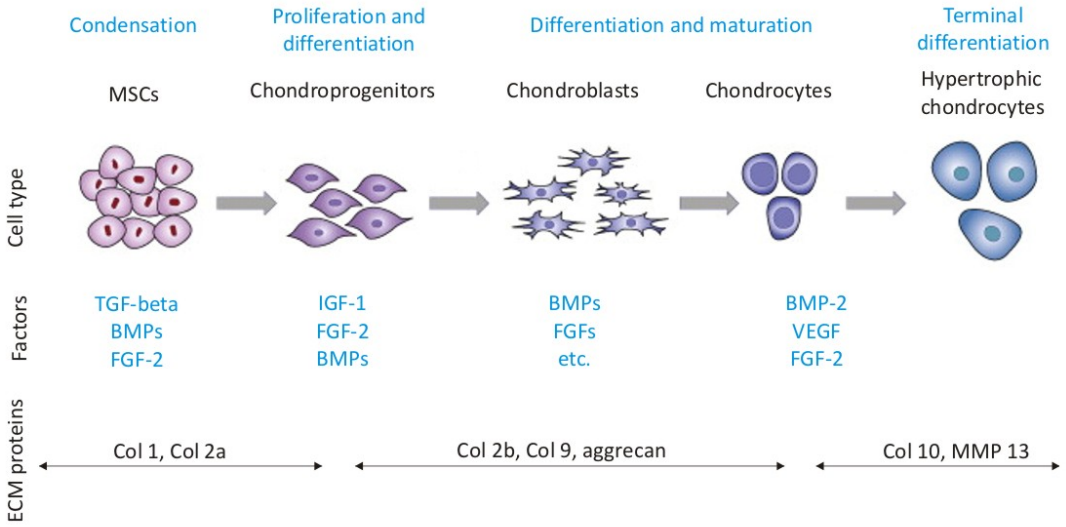

Figure 1.3: The different stages of chondrogenesis. Multipotent stem cells commit to the chondrogenic lineage[95].

The process of condensation is further regulated by cell-cell (among others via n-cadherin) and cell-matrix interactions which are important for differentiation into chondrocytes[96,97]. Interactions of the ECM and surface molecules (e.g. adhesion molecule N-CAM) are important in maintaining cell shape and condensation cohesion[94]. Proteoglycans in the ECM that play a critical role during chondrogenesis are syndecan, tenascin and fibronectin, the latter helps to sustain condensation[98]. With the disappearance of fibronectin and collagen type I, chondroprogenitor cells can transform into fully differentiated chondrocytes[99]. The formation of the synovial joint depends on the fate of differentiation of cells in the condensation[100]. They can differentiate into two different lineages of chondrocytes: one forms the growth plate and the other forms the articular cartilage at the rim of the bone. In articular cartilage the initial core cartilage enlarges through chondrocyte proliferation and matrix production, especially collagen type II and aggrecan and starts to form cartilage tissue in the anlagen. On the other hand, the growth plate cartilage determines the longitudinal growth

of long bones[94]. These two types of cartilage have to be distinguished distinctly, as articular chondrocytes found in the articular joint surface represent a stable and permanent phenotype which maintains joint function throughout life and produces all ECM components of articular cartilage necessary to provide the tissues functional properties. The transient chondrocytes found in the growth plates display a very dynamic phenotype, undergo proliferation, maturation, hypertrophy and apoptosis followed by the replacement by bone cells during endochondral ossification[101] (Figure 1.3).

As mentioned in the beginning, chondrogenesis is regulated by a variety of signals, growth factors and pathways, as well as cell-cell, cell-matrix interactions that are still far from being well investigated[94]. Due to this lack of knowledge, current cartilage engineering approaches using MSCs concentrate on selected factors that are known to play central roles in articular cartilage development and use knowledge from endochondral ossification to prevent hypertrophy from chondrogenically differentiated MSCs. One of the critical factors for chondrogenic differentiation of MSCs is the three-dimensional arrangement of the cells. The most commonly used culture system for chondrogenesis is the pellet culture system first described by Johnstone et. al in 1998[102]. The packed cellular aggregates allow close cell-cell contact in a 3D environment mimicking the precartilage condensation during embryonic development[102]. The pellets are further subjected to specific growth factors (e.g. BMPs, TGF-β, IGF), steroids (e.g. dexamethasone) and certain supplements to initiate chondrogenic differentiation[102,103]. TGF-β was shown to be one of the strongest pro-cartilage growth factors for the induction of chondrogenesis[104] and maintaining articular cartilage and the chondrocyte phenotype[105,106], whereas IGF-I is described to have functional roles in cartilage development and metabolism[107,108]. IGF-I and TGF-β action during chondrogenesis will be described in detail in section 1.7. During micromass culture in chondrogenic medium, MSCs increase expression of collagen type II and aggrecan[109], even though they continue to express collagen type I[110] and the hypertrophy marker collagen type X in long-term culture[111]. The great challenge when using MSC for articular cartilage repair is to generate cells with properties of permanent chondrocytes as found in

hyaline articular cartilage, including resistance to hypertrophy and terminal differentiation[112]. One critical cue that counteracts hypertrophy and promotes chondrogenic differentiation of MSCs is hypoxia.

1.6 Hypoxia

MSCs offer multiple harvest sites, e.g. fat tissue and bone marrow,[113] where they reside in their special niche for repair and remodeling functions[114]. One critical cue in their site-specific niches *in vivo* is oxygen; for example in bone marrow, oxygen concentrations from 1% to 7% have been reported[115,116]. Cells that are subject to low oxygen tensions (3%) show less DNA damage and senesce slower compared to normoxic conditions (21%) as previously shown for mouse embryonic fibroblasts[117]. This minor DNA damage results from a smaller amount of reactive oxygen species present under hypoxic conditions. Stem cells escape the oxidative stress by residing in their hypoxic niche[118]. Cartilage tissue itself is exposed to oxygen levels of 5% on the surface to less than 1% in the deep zone[119].
However, most of the research in cartilage tissue engineering so far has been performed with atmospheric oxygen tension (21%) of standard cell culture, which as it turns out in recent years, has profound influence on chondrogenesis. The issue of optimal cell culture conditions, especially regarding oxygen tension is receiving more and more interest in terms of different aspects like proliferation, survival and differentiation. MSCs are very well adapted to limited metabolic conditions[120]. In agreement to this, MSCs showed superior proliferation over several passages[116,121–123] in hypoxia compared to normoxia and are able to survive prolonged hypoxic stress in contrast to other cell types like cardiomyocytes due to their ability to switch to the glycolytic pathway for ATP production and their generally low consumption of ATP[124]. Remarkably, low oxygen conditions are necessary and promote the maintenance and preservation of full pluri- or multipotency as shown in studies using human embryonic stem cells (hES) or adipose- and bone marrow-derived MSC[125–127]. Hypoxia increased telomerase activity[128] and the expression of stemness markers like Rex1 and Oct4 suggesting

that oxygen tension can regulate quiescence in stem cells[125].
Mechanistically, the effects of hypoxia are thought to be primarily mediated by the main hypoxia inducible factor α (Hifα) isoforms Hif-1α and Hif-2α[129,130]. Hifα is stabilized under hypoxic conditions by impairing its oxygen dependent degradative hydroxylation[94,131]. Hifα dimerizes with Hifβ, translocates into the nucleus, and binds to Hif-responsive elements in the promoter region of Hif target genes[132]. Hif-1α and Hif-2α have both demonstrated to play important roles in chondrogenesis. Major Hif-1α target genes include the glucose-6-phosphate transporter which is important for glucose availability and therefore crucial for cell survival[133] or the chondrogenic master-regulator gene *SOX9*[134] which is also directly bound and targeted by Hif-2α[135] and is crucial in articular cartilage production and development[130,136].

Furthermore, it has been demonstrated that expanding and differentiating chondrocytes and MSCs in a hypoxic environment resulted in cultures with increased GAG and total collagen content[134,137–144]. Recently published studies have additionally indicated that hypoxia suppressed hypertrophic differentiation of chondrocytes and MSCs[145–147]. Thus, a low oxygen environment favors the chondrogenic potential of MSCs and simultaneously hinders differentiation into the adipogenic or osteogenic lineage[148].

1.7 Signaling factors during development and maintenance of articular cartilage

The interplay of oxygen tension, cell-cell-signaling, growth factors and other stimuli creates a complex signaling network that provides the key to develop complex geometries and tissues[100]. Various growth factors work in concert to regulate development and homeostasis of articular cartilage over the entire lifetime. They are membrane-bound polypeptides or secreted in the extracellular space that can stimulate gene expression, protein synthesis and differentiation[94,149]. As described in 1.5 beside Wnts and FGFs the growth factors IGF-I and TGF-β

are fundamental in cartilage formation, development and maintenance[150,151].

TGF-β

TGF-β plays a central role in all stages of chondrogenesis, including condensation, proliferation, ECM synthesis and differentiation[152–154]. It is involved in adhesion molecule (e.g. N-cadherin) and ECM protein (e.g. fibronectin) production which support mesenchyme condensation[155–157]. Furthermore, TGF-β promotes cell proliferation, cartilaginous matrix production and enhances gene expression of cartilage marker genes like *ACAN*, *COL2A* and the cartilage master regulator *SOX9*[158–160]. By inhibiting expression of collagen type X, MMP13, and osteocalcin TGF-β was reported to additionally delay hypertrophic progression of chondrocytes[161].
The three TGF-β isoforms TGF-β1, TGF-β2 and TGF-β3 are secreted in the inactive form and become activated by cleavage of the latency-associated peptide[162] while TGF-β3 was shown to have the highest chondrogenic potential of all three isoforms[163]. TGF-β signals are transduced by binding to a heteromeric complex of type I and II receptors with serine/threonine kinase domains that interact with each other causing type I receptor phosphorylation and activation[164]. The activated receptor phosphorylates receptor-associated Smads (Smad2 and Smad3) which binds to Smad4, translocates to the nucleus and regulates target gene transcription[165,166]. Alternative TGF-β mediated pathways, the so-called Smad-independent pathways, to regulate chondrogenesis include the extracellular signal-regulated kinase (ERK), mitogen-activated protein kinase (MAPK) and phosphatidylinositol 3-kinase (PI3K)/Akt signaling pathways[167,168]. TGF-β signaling is controlled by a variety of different intracellular mechanisms, e.g. by clathrin mediated endocytosis of receptor-bound TGF-β with subsequent degradation[169].

IGF-I and IGF-binding proteins

IGF-I is a key component in cartilage development. It has been shown to increase cell growth and proliferation in various cell types like adult chondrocytes[170,171] and MSCs and promotes the expression of chondrogenic marker genes, such as *COL2A* and *SOX9*[172]. IGF-I has been proven to be an important factor for

chondrocyte proliferation during early chondrogenesis[91] and strongly enhances protein and cartilaginous matrix synthesis including GAGs and collagen type II[173] while counteracting their degradation[108,174]. Several studies have demonstrated that IGF-I increases chondrocyte metabolism while maintaining the chondrogenic phenotype[175]. In addition, IGF-I and the IGF-I-receptor (IGF-IR) are expressed in developing and mature cartilage and were shown to be important promoters and regulators of matrix homeostasis and chondrogenic differentiation of MSCs[176,177].

IGF-I structurally shares great homology with insulin but binds the IGF-IR with more than 100 fold superior affinity than insulin[178]. The biological action after IGF-I binding to the IGF-IR is transduced via PI3K, MAPK and ERK signal pathways[179]. IGF-I acts independently from TGF-β signaling, but chondrogenic differentiation of MSCs can be enhanced when acting synergistically with TGF-β[91,172,180].

The truncated IGF-I analogue des(1-3)IGF-I (desIGF) which lacks the first three amino acids (Gly-Pro-Glu) at the N-terminus was reported to have enhanced potency relative to IGF-I in ovine articular chondrocytes regarding proteoglycan production or in *lit/lit* mice with respect to cell growth[181,182]. DesIGF is still able to activate the IGF-IR and binds it with the same affinity as IGF-I, but its affinity for IGF-binding proteins (IGFBP) is approximately 100 times reduced. Mutational studies have revealed that the Glu is responsible for the striking drop in affinity for the IGFBP[183].

IGFBPs modulate IGF-I bioavailability and function and modify its interaction with the IGF-IR[184]. The family of IGFBPs consist of six different isoforms (IGFBP-1 – IGFBP-6) that display a variety of functions[185]. IGFBPs exhibit tissue specific expression suggesting each to play a distinct role in regulating the biologic action of IGF-I in the target tissue. Depending on the cell type and conditions, the same binding protein can exert an IGF-I inhibiting or enhancing role[186]. For example, while IGFBP-3 has been shown to potentiate IGF-I action when IGFBP-3 was preincubated with the cells, it was inhibitory when co-treated with IGF-I[187]. As most cells express more than one IGFBP, the IGFBP regulation of each IGFBP plays an important role in regulating IGF-I effects.

Almost 98% of IGF in human circulation is bound to one of the six IGFBPs while IGFBP-3 accounts for 80% of all IGF binding[188]. IGFBP-2 to -5 were shown to be present in human cartilage with IGFBP-3 being the most prevalent produced IGFBP by chondrocytes in culture[189–193]. Through binding IGFs, IGFBP-3 modulates their biological functions, e.g. acting as a protein carrier across the capillary barrier, extending half-life or modulating of receptor presentation[151,186]. The exact mechanism of IGFBP action still remains poorly understood. Nevertheless, the tight local control of IGF-I bioavailability by IGF-I synthesis, IGFBP and their degradation by IGFBP-specific proteases, represents an intricate network that regulates the ability of IGF-I to interact with its receptor.

1.8 Growth factor immobilization for cartilage regeneration

Immobilization of growth factors to biomaterials is an emerging field to present growth factors to cells or the target tissue. It offers a variety of advantages such as prolongation of growth factor availability and activity, spatial control, improved stability and a reduced amount of growth factor needed to gain similar biological responses compared to delivery of the growth factor in a soluble form[194].

In general, there are tree main immobilization strategies: non-covalent, covalent and physical entrapment. Non-covalent immobilization is based on hydrophobic and polar interactions or hydrogen and ionic bonds, e.g. in heparin-based systems. Common cross-linking strategies for covalent growth factor immobilization include photo-initiated monoacrylated PEG-succinimidyl ester and N-ethyl-N'-(3-(dimethylamino)propyl)carbodiimide/N-hydroxysuccinimide (EDC/NHS) coupling[195]. EDC/NHS cross-linking offers high coupling efficiency, biocompatibility and little influence on growth factor bioactivity under mild conditions[196].

Growth factors can be immobilized to various biomaterials, such as bioactive glass[197], hydrogels[198,199] like PEG or chitosan and particles[200] like silicon or

poly(methyl methacrylate)(PMMA)[201]. PMMA is a biocompatible polymer that degrades very slowly in an aqueous environment[202] and displays high tensile and compressive strength[203]. Therefore, PMMA bone cements and microspheres loaded with antibiotics have been widely used in the treatment of bone and soft tissue infections[204].
In the present study TGF-β3 was coupled to carboxylated PMMA microspheres using EDC/NHS chemistry (chapter 3.4). The potential of the functionalized microspheres to induce chondrogenic differentiation of MSCs was evaluated in pellet culture and porous silk fibroin scaffolds.

1.9 Silk Fibroin: A natural biomaterial for tissue engineering applications

Regeneration of tissue defects using biomaterials, cells and growth factors is a key approach in the treatment of tissue or organ lesions. One potent scaffolding material utilized for these treatments is silk fibroin. In particular, silk fibers from cocoons of the silkworm *Bombyx mori* have widely been utilized as sutures in clinical applications for skin wounds or eye and oral surgeries[205,206]. In the last decade, silk fibroin has gained increased attention in biomedical science due to its outstanding processing and mechanical properties. Silk fibroin has high stability combined with impressive elasticity but offers a tunable biodegradability at the same time. Furthermore, silk fibroin provides a high biocompatibility and the ability of functional modification owing to the presence of easily accessible chemical groups[207]. Using different processing techniques, silk-based matrices with different morphologies such as films, hydrogels, non-woven nets or porous scaffolds can be fabricated[208]. The application of specific techniques, such as porogen leaching and freeze-drying, allows the production of scaffolds with defined optimized geometry and interconnectivity[208]. Porous silk-based constructs provide a robust matrix that can be seeded with cells of different origin, e.g. chondrocytes[209], osteoblasts[210] or MSCs[211] and the pore-interconnectivity allows a homogeneous cell distribution[212]. The unique

combination of elasticity and stability along with its biocompatibility makes silk fibroin an attractive biomaterial for cartilage engineering applications.

1.10 Goals of the thesis

Over the last decades, novel treatment options for articular cartilage lesions have improved the clinical outcome for numerous patients. However, issues like the formation of fibrocartilage at the cartilage defect site still lead to disappointing results in the long-term[78,79,213]. To solve these problems, cell-based approaches have increasingly gained attention in the development of treatments for articular cartilage lesions. Here, BMSCs belong to the most intensively investigated cell sources, both *in vitro* and *in vivo*, due to their high capacity for chondrogenesis[7]. Nevertheless, despite intensive research activity in this field, little progress has been made during the past decade. The exact mechanisms of articular cartilage development still remain poorly understood. Cartilage development and the process of differentiation from MSCs into chondrocytes is regulated by microenvironmental cues such as oxygen tension and by the correct temporal and spatial expression of multiple secreted factors including IGFs and members of the TGF superfamily, such as TGF-β[80–84,88]. In order to engineer cartilage tissue, a deeper understanding of developmental processes and microenvironmental cues that regulate chondrogenic cell fate and cartilaginous matrix development is a prerequisite. To study these mechanisms and aiming at the development of artificial cartilage tissue, the purpose of this thesis was the investigation of crucial factors that regulate chondrogenic cell fate, in particular IGF-I and oxygen tension, and the evaluation of a functionalized artificial 3D cartilage tissue construct.
The overall goals of the study included:

1. **Investigation of IGF-I as an important growth factor and oxygen tension as a key microenvironmental cue that promote chondrogenic differentiation and cartilaginous ECM development and maintenance of bone marrow-derived stromal cells.**

2. **Evaluation of a 3D scaffold based on silk fibroin in combination with TGF-β3-coupled PMMA microspheres, particularly the investigation of chondrogenesis in the engineered construct upon seeding with BMSCs.**

1.1 Investigation of IGF-I action on chondrogenic differentiation of BMSCs

The growth factor IGF-I plays a central role in cartilage development and was shown to increase cell growth and proliferation in various cell types like adult chondrocytes[91,171] and MSCs[172]. However, its use for chondrogenic differentiation of BMSCs is surprisingly rare and poorly understood. The few studies that dealt with the chondroinductive effects of IGF-I on BMSCs have either reported that IGF-I treatment has little effect[214,215] or additionally applied an insulin-containing standard cell culture supplement (ITS+ Premix) into the chondrogenic medium[214,216,217] which is assumed to mask IGF-I effects[172,218].
To shed light on its influence on chondrogenesis and ECM development of BMSCs, IGF-I effects were studied on the molecular and protein level in the pellet culture system without insulin. In this context, we additionally focused on the influence of IGFBP on IGF-I action and bioavailability. Therefore, we used the IGF-I analogue desIGF, whose affinity for IGFBPs is approximately 100 times reduced compared to IGF-I[172], and further applied a small molecule IGFBP inhibitor NBI-31772 to disrupt IGF-I/IGFBP interactions and release IGF-I from the IGF-I/IGFBP complex (**Chapter 3.1**).

1.2 Investigation of hypoxic conditions on ECM development during chondrogenesis of BMSCs

Besides growth factors, the ability of stem cells to differentiate along one lineage or another is dependent on microenvironmental cues[219]. One critical microenvironmental cue in mesenchymal progenitor fate, starting as early as embryogenesis, is oxygen tension[220]. Not only in bone marrow oxygen concentrations from 7% to 1% have been reported[115,116], also cartilage tissue itself is exposed to hypoxic conditions of 5% to less than 1%[119]. However, most of the research in cartilage tissue engineering and in basic research on BMSCs in this context so far has been performed with atmospheric oxygen tension (21%) of standard cell culture, which as it turned out in recent years has a serious impact on chondrogenesis.

Thus, the influence of low oxygen tension on IGF-I mediated chondrogenic differentiation of BMSCs was investigated with a focus on anabolic processes. Using the pellet culture system, the suitability of hypoxic conditions to improve cartilaginous ECM development in comparison to normoxic conditions was assessed by biochemical assays, histology and immunohistochemistry (**Chapter 3.2**).

Cartilaginous ECM development and maintenance is naturally driven by continuous dynamic remodeling. These remodeling processes for matrix homeostasis are regulated by a careful balance between matrix synthesis, modification and enzymatic degradation[33]. Having addressed the influence of hypoxia on anabolic processes in chapter 3.3, in a second step the hypoxic impact on matrix-modulating enzymes and the MMP-mediated aggrecan degradation was comprehensively investigated on the molecular and protein level employing two independent 3D cell culture systems, i.e. standard pellet culture and porous silk fibroin scaffold-based culture (**Chapter 3.3**).

2 Development of a functionalized 3D scaffold for cartilage tissue regeneration

Regeneration of tissue defects using a combination of biomaterials, progenitor cells and growth factors is a generally promising approach in the treatment of tissue lesions. Traditional chondrogenic approaches utilize soluble growth factor delivery which is limited in clinical applications[221]. However, a controlled delivery and localized presentation of growth factors during tissue development to avoid side effects is desirable. Hence, the goal of this study was to develop a functionalized implant that provides a locally restricted presentation of TGF-β3 for the chondrogenic differentiation of BMSCs towards cartilage defect repair. This work was conducted in collaboration with the group of Prof. Dr. Dr. Lorenz Meinel at the Department of Pharmaceutical Technology and Biopharmacy of Würzburg University (**Chapter 3.4**).
The developed 3D silk fibroin-based scaffolds were analyzed for pore intercon-

nectivity and biocompatibility. Subsequently, different cell seeding strategies were tested to guarantee a homogeneous cell distribution and to allow rapid and uniform tissue regeneration in the construct. Aiming at the development of a clinically suitable cartilage implant, the implant was loaded with TGF-β3-coupled PMMA microspheres and BMSCs to stimulate chondrogenic differentiation and cartilaginous tissue development. The tissue construct was assessed for chondrogenesis and ECM development using histology, immunohistochemistry, biochemical analysis and qRT-PCR (**Chapter 3.4**).

Chapter 2

Material and Methods

2.1 Material

Table 2.1: Overview of used instruments.

Instrument	Manufacturer	Head office
Accu-jet® pro	Brand	Wertheim, Germany
Amicon® stirred ultrafiltration cell 8010	EMD Millipore Corporation	Billerica, USA
Analytical scale	Ohaus	Zürich, Switzerland
Analytical scale XA 105	Mettler-Toledo	Columbus, USA
Centrifuge Rotina 420 R	Hettich	Tuttlingen, Germany
Centrifuge SIGMA 1-14	SIGMA Laborzentrifugen GmbH	Osterode, Germany
CO_2 Incubator	IBS Integra Biosciences	Fernwald, Germany
Cryostat CM 3050S	Leica	Wetzlar, Germany
FluorChem FC2 Imager	Alpha Innotec	San Leandro, USA
Freeze Dryer α	Martin Christensen GmbH	Osterode, Germany
Electrophoresis- and blotting chamber	Bio-Rad	München, Germany
Hemacytometer Neubauer	Paul Marienfeld GmbH	Lauda, Germany
Heating oven	Binder GmbH	Tuttlingen, Germany
Laminar flow box Typ-HS18	Heraeus	Hanau, Germany
Laminator	Severin	Sundern, Germany
Orbital shaker Unimax 1010	Heidolph	Schwabach, Germany
Mastercycler® Gradient	Eppendorf	Hamburg, Germany

Table 2.1: Overview of used instruments: continued.

Instrument	Manufacturer	Head office
Magnetic stirrer	VWR	Darmstadt, Germany
Microscope BX51/DP71 camera	Olympus	Hamburg, Germany
Microscope IX51/XC30 camera	Olympus	Hamburg, Germany
Mini-PROTEAN™ Tetra Cell System	Bio-Rad	München, Germany
MRX microplate reader	Dynatech Laboratories	Chantilly, USA
NanoDrop 2000c spectrophotometer	Thermo Fisher Scientific	Waltham, USA
pH-meter HI2210	Hanna Instruments	Kehl am Rhein, Germany
Pipettes Research® Plus	Eppendorf	Hamburg, Germany
Pipette multistep	Brand	Wertheim, Germany
PowerPac® basic power supply	Bio-Rad	München, Germany
Real-Time PCR Detection System CFX96T™	Bio-Rad	München, Germany
Tecan GENios pro spectrofluorometer	Tecan	Crailsheim, Germany
TissueLyser	Qiagen	Hilden, Germany
Thermomixer comfort MTP	Eppendorf	Hamburg, Germany
Thermomixer MHR 23	DITABIS	Pforzheim, Germany
JSM-7500F field emission scanning electron microscope	Joel	Tokyo, Japan

Table 2.1: Overview of used instruments: continued.

Instrument	Manufacturer	Head office
Ultrasonic homogenizer SonoPlus	Bandelin	Berlin, Germany
Vortex, IKA® MS3 basic	IKA®	Staufen, Germany
Water bath	Memmert	Schwabach, Germany

2.2 Consumables

Table 2.2: Overview of the consumables used.

Consumable	Manufacturer	Head office
Bottle top filter Nalgene®	Thermo Scientific	Waltham, USA
Coverslip 24x60 mm	MENZEL	Braunschweig, Germany
Cryovials CryoPure 2.0 mm	Sarstedt	Nümbrecht, Germany
Disposable forceps ratiomed	megro GmbH	Wesel, Germany
Falcon cell strainers 100 μm	BD Biosciences	Heidelberg, Germany
Hardshell PCR plates, 96-well, thin wall	Bio-Rad	München, Germany
Microseal® 'C' Film	Bio-Rad	München, Germany
Microtome blades	Feather	Osaka, Japan
6 & 12-well plates	Greiner Bio-One	Frickenhausen, Germany
96-well plate	TPP	Trasadingen, Switzerland
96-well plate black	Thermo Scientific	Waltham, USA
Parafilm	Pechiney	Chicago, USA

Table 2.2: Overview of the consumables used: continued.

Consumable	Manufacturer	Head office
PAP pen liquid blocker	Sigma-Aldrich	München, Germany
PCR-strips 8 tubes 0.2 mL	Carl Roth GmbH	Karlsruhe, Germany
PD-Tips	Brand	Wertheim, Germany
PES membrane 13 mm diameter (0.2 μm)	Nalge Nunc International Corporation	Rochester, USA
Pipette filter tips	Sartstedt	Nümbrecht, Germany
Pipette tips	Starlab	Hamburg, Germany
Pipettes serological	Greiner Bio-One	Frickenhausen, Germany
pH indicator paper	Carl Roth GmbH	Karlsruhe, Germany
Polypropylene Tubes 15 mL/50 mL	Greiner Bio-One	Frickenhausen, Germany
SafeSeal Micro Tubes 1.5 mL/2.0 mL	Sarstedt	Nümbrecht, Germany
Sample cup PE 2.5 mL	Hartenstein	Würzburg, Germany
Scalpels	Feather	Osaka, Japan
Slide-A-Lyzer Mini Dialysis Device (MWCO 10 kDa)	Thermo Fisher Scientific	Rockford, USA
SpectraPor dialysis tubes (MWCO 6–8 kDa)	Spectrum Labs	Rancho Dominguez, USA
SuperFrost® plus glass slide	R. Langenbrinck	Emmendingen, Germany
Syringe Filter Minisart® 0.2 μm	Sartorius AG	Göttingen, Germany

Table 2.2: Overview of the consumables used: continued.

Consumable	Manufacturer	Head office
Syringe filter Versapor (5 μm)	Pall Life Sciences	Washington, USA
Syringes	BD Biosciences	Heidelberg, Germany
Syringes Omnican40	B.Braun	Melsungen, Germany
Tissue culture flasks T175	Greiner Bio-One	Frickenhausen, Germany
Ultrafiltration membrane disk filters (25 mm)	PALL® Life Sciences Corporation	Ann Arbor, USA)
Whatman® cellulose chromatography paper	Simga-Aldrich	München, Germany
Whatman® nitrocellulose membrane	Simga-Aldrich	München, Germany

2.3 Chemicals

If not otherwise stated in the Materials and Methods sections, all chemicals and reagents applied for the preparation of buffers and solutions were obtained from Sigma-Aldrich (München, Germany).

Table 2.3: Overview of the chemicals used.

Chemical	Manufacturer	Head office
Amersham™ ECL™ Prime Western Blotting Detection Reagent	GE Healthcare	Freiburg, Germany
Ambion RNaseZAP	Life Technologies	Karlsruhe, Germany

Table 2.3: Overview of the chemicals used: continued.

Chemical	Manufacturer	Head office
Antibody diluent, Dako REAL™	Dako	Hamburg, Germany
Aqua ad iniectabilia	B. Braun	Melsungen, Germany
bFGF	BioLegend	London, UK
Brilliant III Ultra-Fast SYBR® Green QPCR Master Mix	Agilent	Santa Clara, USA
Chondroitinase ABC	Sigma-Aldrich	München, Germany
DAPI mounting medium	Dako	Hamburg, Germany
ImmunoSelect®		
Des(1-3)IGF-I	GroPep Bioreagents	Thebarton, Australien
Dulbecco's Phosphate-buffered saline (PBS) (-)Ca^{2+}, (-)Mg^{2+}	Gibco® Life Technologies	Karlsruhe, Germany
Distilled water (DNAse/RNAse free)	Gibco® Life Technologies	Karlsruhe, Germany
EnVision G|2 Doublestain System	Dako	Hamburg, Germany
Gold/palladium (SSCD)	Bal-Tec AG	Liechtenstein
IGF-I	R&D Systems	Wiesbaden, Germany
IGFBP inhibitor NBI-31722	Merck Millipore	Darmstadt, Germany
ImProm-II™ reverse transcriptation system Kit	Promega	Madison, USA
Keratanse	Seikagaku	Tokyo, Japan
Live/Dead Cell Staining Kit II	PromoKine	Heidelberg, Germany

Table 2.3: Overview of the chemicals used: continued.

Chemical	Manufacturer	Head office
Microplate BCA™ Protein Assay Kit	Thermo Scientific	Waltham, USA
Novex® sharp protein standard	Life Technologies	Karlsruhe, Germany
Papain	Worthingtion	Lakewood, USA
Phosphate buffered saline (Dulbecco A) tablets	Thermo Scientific	Waltham, USA
PMMA microspheres	PolyAn	Berlin, Germany
Powerblock	Biogenex	Fermont, CA, USA
Proteinase K (Digest-All 4)	Life Technologies	Karlsruhe, Germany
Sensolyte®520 Generic MMP activity Kit *Fluorimetric*	Anaspec	Fremont, CA, USA
Silk fibroin	Trudel silk	Zürich, Switzerland
Terralin Liquid® disinfectant	Schülke	Norderstedt, Germany
TGF-β1	Biolegend	London, UK
Tissue-Tek® O.C.T. compound	Sakura Finetek	Zoeterwonde, Netherlands
TRIzol® Reagent	Life Technologies	Karlsruhe, Germany
0.25% Trypsin-EDTA	Life Technologies	Karlsruhe, Germany

2.4 Scaffold and microsphere components

Carboxylated PMMA microspheres:	Commercially available poly(methyl methacrylate) microspheres (PolyAn, Berlin, Germany).
Silk fibroin scaffolds:	Silk fibroin scaffolds were produced with silk fibroin from cocoons of the silkworm *B. mori*. The silk fibroin scaffolds were provided by Eva Gador from the Department of Pharmaceutical Technology and Biopharmacy of Würzburg University of Prof. Dr. Dr. Lorenz Meinel (AK Meinel, Würzburg).
TGF-β3-coupled PMMA microspheres:	TGF-β3-coupled PMMA microspheres were provided by Eva Gador from the Department of Pharmaceutical Technology and Biopharmacy of Würzburg University of Prof. Dr. Dr. Lorenz Meinel (AK Meinel, Würzburg).

2.5 Antibodies

Table 2.5: Overview of the primary antibodies used.

Antibody	Type/Source	Applicat./Dilut.	Manufacturer
Anti-Collagen I	Polyclonal IgG rabbit	IHC 1:800 WB 1:1000	Abcam (ab34710)
Anti-Collagen II	Monoclonal IgG mouse	IHC 1:100 WB 1:250	Acris (Clone II-4C11)
Anti-CTX-II	Polyclonal IgG rabbit	IHC 1:200	USCN Life Science
Anti-DIPEN	Monoclonal IgG mouse	IHC 1:100	MD Biosciences
Anti-GAPDH	Monoclonal IgG mouse	WB 1:1000	Merck Millipore (Clone 6C5)
Anti-MMP13	Polyclonal IgG rabbit	IHC 1:100	Abcam

Table 2.6: Overview of the secondary antibodies used.

Antibody	Type/Source	Applicat./Dilut.	Manufacturer
Alexa Fluor 488 anti-rabbit	Polyclonal IgG goat	IHC 1:400	Dianova (711-545-152)
Cy3 anti-mouse	Polyclonal IgG donkey	IHC 1:500	Dianova (715-165-150)
Cy3 anti-rabbit	Polyclonal IgG goat	IHC 1:500	Jackson Immuno (711-165-152)
HRP anti-rabbit	Polyclonal IgG goat	WB 1:2000	Dako (P0448)
HRP anti-mouse	Polylonal IgG mouse	WB 1:1000	Dako (P0161)

2.6 Primers

Table 2.7: Overview of the qPCR primers used.

Gene	Gene Symbol	Unique Assay ID	Manufacturer
ADAMTS4	*ADAMTS4*	QT00032949	Qiagen
ADAMTS5	*ADAMTS5*	QT00011088	Qiagen
Aggrecan	*ACAN*	QT00001365	Qiagen
Collagen II	*COL2A1*	QT00049518	Qiagen
GAPDH	*GAPDH*	QT00079247	Qiagen
MMP1	*MMP1*	QT00014581	Qiagen
MMP3	*MMP3*	QT00060025	Qiagen
MMP13	*MMP13*	QT00001764	Qiagen
RPL13a	*RPL13A*	QT00089915	Qiagen
Sox9	*SOX9*	QT00001498	Qiagen
TIMP1	*TIMP1*	QT00084168	Qiagen
TIMP3	*TIMP3*	QT00046382	Qiagen

2.7 Cell Culture Media

Proliferation medium:	Dulbecco's Modified Eagle's Medium/Ham's F-12 (DMEM/F12; ThermoFisher, MA) supplemented with 10% fetal bovine serum (FBS) and 1% penicillin-streptomycin (PS; 100 U/mL penicillin, 0.1 mg/mL streptomycin; ThermoFisher, MA), and 5 ng/mL basic fibroblast growth factor (bFGF; BioLegend, London, UK).
Cryopreservation medium:	Proliferation medium, supplemented with 10% DMSO.
Seeding and chondrogenic medium:	The different seeding and chondrogenic differentiation medium used in each chapter is described in detail in 2.9.2.

2.8 Buffers and Solutions

Citric acid buffer:	25 g citric acid monohydrate, 6 mL glacial acid, 60 g sodium acetate trihydrate, 17 g NaOH, bring volume to 500 mL with ddH_2O. Add 100 mL ddH_2O, and 150 mL 2-propanol. Adjust carefully to pH 6, and store at 4°C under toluene.
Chloramine T solution:	141 mg chloramine T, 8 mL citirc acid buffer, and 1 mL 2-propanol.
DAB solution:	1.5 g p-dimethylamino-benzaldehyde (DAB), 6 mL 2-propanol, and 2.6 mL 60% perchloric acid.

DMMB solution:	16 mg dimethylmethylene blue (DMMB) is dissolved for 16 hours in 5 mL absolute ethanol. Afterwards it is added to a prepared NaCl-glycine solution, consisting of 900 mL ddH_2O, 3.04 g glycine, 2.37 g NaCl. Adjust to pH 3.0 and bring volume to 1 L with ddH_2O.
High salt phosphate buffer:	12 mM phosphate, 1.5 M sodium chloride, pH 7.4.
MES buffer:	0.1 M MES, 0.5 M sodium chloride, pH 6.
Papain digestion buffer:	20 mL PBE buffer, 17 mg L-cysteine, 3 U/mL papain, and sterilize with a 0.2 μm syringe-filter.
PBE buffer:	6.53 g Na_2HPO_4, 6.48 g NaH_2PO_4, 10 mL 500 mM EDTA in 900 mL ddH_2O. Adjust to pH 6.5 and bring volume to 1 L with ddH_2O and sterilize with a 0.2 μm bottle top filter.
PBS:	10 PBS (Dulbecco A) tablets in 1 L ddH_2O.
PBST:	0.1% Tween® 20 in 1 x PBS.
Resolving gel buffer:	1 M Tris, adjust to pH 8.8.
Running buffer:	25 mM Tris, 192 mM glycine, 0.1% SDS.
Stacking gel buffer:	0.5 M Tris-HCl, adjust to pH 6.8.
TBST buffer:	20 mM Tris, 150 mM sodium chloride, 0.1 % Tween® 20, pH 7.4.
TEN buffer:	0.1 M NaCl, 1 mM EDTA, 10 mM Tris, adjust to pH 7.4.
Transfer buffer:	25 mM Tris, 192 mM glycine, 10% methanol.
WB blocking solution:	5% nonfat dried milk powder in PBST.

2.9 Methods

2.9.1 Isolation and culture of cells

Human bone marrow-derived MSCs were isolated by extensive washing with PBS of trabecular bone surgically removed from patients (age 57-65 years) undergoing total hip arthroplasty. Written informed consent was obtained from each patient and the study was approved by the local ethics committee. The isolated cells were centrifuged (300 g, 10 min), resuspended in expansion medium consisting of Dulbecco's Modified Eagle's Medium / Ham's F-12 (DMEM/F12; ThermoFisher, MA, USA) with 10% fetal bovine serum (FBS) and 1% penicillin-streptomycin (PS; 100 U/mL penicillin, 0.1 mg/mL streptomycin), and seeded in T175 cm^2 culture flasks (Greiner Bio-One, Frickenhausen, Germany). Non-adherent material was removed after 48 h by washing with PBS. During proliferation, the expansion medium was supplemented with 5 ng/mL basic fibroblast growth factor (bFGF; BioLegend, London, UK) and changed every 3-4 days until cells reached 80% confluence. MSCs were passaged using trypsin-EDTA at 0.25% (Invitrogen, Karlsruhe, Germany) and second passage cells (P2) were employed in the experiments.

2.9.2 Pellet culture and chondrogenic differentiation of MSCs

Pellet formation: MSCs (P2) were suspended in seeding medium [DMEM high glucose, 1% PS, 10 nM dexamethasone, 50 μg/mL ascorbic acid-2-phosphate, 1 mM sodium pyruvate, 40 μg/mL proline, supplemented with

(1) Chapter 3.1: TS-Mix (final concentrations: 6.25 μg/ml transferrin, 6.25 μg/mL selenious acid, 5.35 μg/mL linoleic acid, 1.25 mg/mL bovine serum albumin)].
(2) Chapter 3.2: TS-Mix].
(3) Chapter 3.3: 1 μg/mL IGF-I (R&D Systems, Wiesbaden, Germany), TS-Mix].
(4) Chapter 3.4: ITS+ Premix].

2 x 10^5cells were seeded per well in 96-well plates (conical bottom), centrifuged at 300 g for 5 min, and allowed to form dense cell pellets overnight (except for chapter 3.1: Cells were allowed to form pellets for 2 days) in an incubator (37°C, 5% CO_2, 21% O_2). The day of chondrogenic induction is defined as day 0 (Figure 2.1).

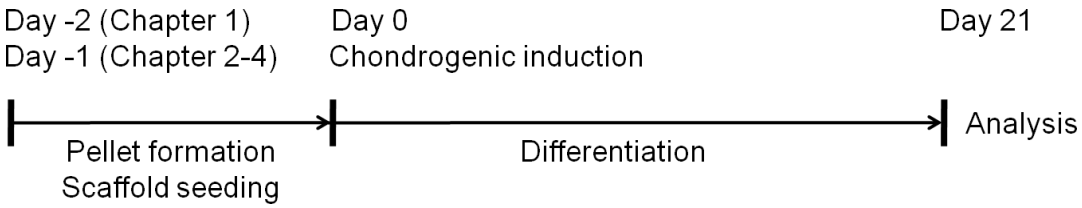

Figure 2.1: Experimental setup. BMSCs were seeded on silk scaffolds (day -1) or were allowed to form dense cell pellets (day -2 in chapter 3.1 or day -1 in chapter 3.2–3.4). Chondrogenic differentiation was induced by applying a hormonal cocktail on day 0. Scaffolds and pellets were subsequently analyzed on the cellular and molecular level.

Pellet culture and chondrogenic differentiation:
(1) Chapter 3.1: Pellets were cultured in chondrogenic medium [seeding medium of chapter 3.1 supplemented with 10 ng/ml recombinant human transforming growth factor-β1 (TGF-β1, BioLegend, London, UK), different concentrations of IGF-I or des(1-3)-IGF-I (GroPep Bioreagents, Thebarton, Australien) in the presence or absence of the IGFBP inhibitor NBI-31772 (Merck Millipore, Darmstadt,Germany)] for 21 days (37°C, 5% CO_2).
(2) Chapter 3.2: Pellets were cultured in chondrogenic medium [seeding medium of chapter 3.2 supplemented with 10 ng/ml TGF-β1, different concentrations of IGF-I] either under normoxic (21% O_2) or hypoxic (2% O_2) conditions for 21 days (37°C, 5% CO_2).
(3) Chapter 3.3: Pellets were cultured in chondrogenic medium [seeding medium of chapter 3.3 supplemented with 10 ng/ml TGF-β1] either under normoxic (21% O_2) or hypoxic (2% O_2) conditions for 21 days (37°C, 5% CO_2).
(4) Chapter 3.4: Pellets were cultured in seeding medium of chapter 3.4 under normoxic conditions (21% O_2) for 21 days (37°C, 5% CO_2).

Medium was changed every 2-3 days.

2.9.3 Culture of MSC-silk fibroin scaffold constructs

Preparation of silk fibroin scaffolds with one porosity

Silk fibroin-based 3D scaffolds (3 mm diameter, 2 mm height) were produced at the Department of Pharmaceutical Technology and Biopharmacy of Würzburg University of Prof. Dr. Dr. Lorenz Meinel, by Eva Gador with defined porosity using paraffin as porogen, as previously described[222] with some modifications. 60 mg of 315-710 μm paraffin spheres were weighed into 1 mL syringes. For reaching interconnectivity of the pores the syringes were incubated at 37°C for 1 h in a heating oven (Binder GmbH, Tuttlingen, Germany). After cooling to room temperature 55 μL 20% (w/v) SF solution was pressed over the paraffin mold until all pores between the paraffin spheres were filled with silk fibroin solution. The constructs were flash frozen in liquid nitrogen for a minimum of 5 min and lyophilized at −30°C for 36 h in a laboratory freeze-dryer alpha 1-4 (Martin Christ GmbH, Osterode, Germany). Lyophilized scaffolds were treated with 90% (v/v) methanol for 30 min to reach water insolubility and allowed to air dry in a fume hood before leaching paraffin two times with n-hexane for 12 h. The resulting porous silk fibroin scaffolds were dried under vacuum for a minimum of 12 h[223].

Preparation of silk fibroin scaffolds with two porosities

Silk fibroin scaffolds (3 mm diameter, 4 mm height) were produced at the Department of Pharmaceutical Technology and Biopharmacy of Würzburg University of Prof. Dr. Dr. Lorenz Meinel, by Eva Gador as previously described[222] with some modifications. 30 mg of 100–160 μm paraffin spheres were weighed into 1 mL syringes. For reaching interconnectivity of the pores, the syringes were incubated at 45°C for 45 min in a heating oven (Binder GmbH, Tuttlingen, Germany). After cooling to room temperature 30 mg of 315–710 μm paraffin spheres were weighed into 1 mL syringes on the melted 100–160 μ paraffin spheres. For reaching interconnectivity of the pores the syringes were incubated at 37°C for 1 h in a heating oven (Binder GmbH, Tuttlingen, Germany). When

the paraffin mold reached room temperature again 55 μL 20% (w/v) silk fibroin solution was pressed over the paraffin mold until all pores between the paraffin spheres were filled with silk fibroin solution. The constructs were flash frozen in liquid nitrogen for a minimum of 5 minutes and lyophilized at -30°C for 36 h in a laboratory freeze-dryer alpha 1-4 (Martin Christ GmbH, Osterode, Germany). Lyophilized scaffolds were treated with 90% (v/v) methanol for 30 min to reach water insolubility and allowed to air dry in a fume hood before leaching paraffin two times with n-hexane for 12 h. The resulting porous biphasic silk fibroin scaffolds were dried under vacuum for a minimum of 12 h. Finally, the dried biphasic silk fibroin scaffolds were cut into 2 mm thick slices for each layer using a racer blade[223].

Scaffold seeding and culture

The scaffolds were seeded using a syringe-based method. The scaffold was pre-wetted overnight in expansion medium and plugged in a syringe (Omnican 40, B.Braun, Melsungen, Germany). 8 x 10^5 MSC (P2) were resuspended in 20 μl expansion medium and soaked into the scaffold. By moving the plunger of the syringe a homogeneous cell distribution was obtained. Cells were incubated for 4 h (37°C, 5% CO_2, 21% O_2) to allow proper cell attachment. The scaffolds were taken out of the syringe and incubated in seeding medium over night. The seeded constructs for chapter 3.3 were cultured in chondrogenic medium either under normoxic (21% O_2) or hypoxic (2% O_2) conditions for 21 days in medium as described above for pellet culture of chapter 3.3. Scaffold seeding for chapter 3.4 will be described in detail in the second subsection following.
To test scaffold seeding efficiency, further seeding approaches were tested:

Unilateral: The scaffold was pre-wetted overnight in expansion medium. 8 x 10^5 MSC (P2) were resuspended in 20 μl expansion medium and dropwise added from top on the scaffold. Excess suspension that leaked out of the scaffold was added from top for a few times again.
Bilateral: The scaffold was pre-wetted overnight in expansion medium. 8 x 10^5 MSC (P2) were resuspended in 20 μl expansion medium. 10 μl of cell suspension was added dropwise from top on the scaffold, the scaffold was turned over and

10 μl of cell suspension was added dropwise from top again. This procedure was repeated with excess suspension that leaked out of the scaffold for a few times.

Immobilization of TGF-β3 on PMMA microspheres

PMMA microspheres (4.6 μm; 8.3 μmol COOH/g; PolyAn, Berlin, Germany) were used as carrier for immobilization of TGF-β3. Immobilisation of TGF-β3 to the PMMA microspheres was performed by Eva Gador at the Department of Pharmaceutical Technology and Biopharmacy of Würzburg University of Prof. Dr. Dr. Lorenz Meinel. EDC/NHS chemistry was used to covalently immobilize the growth factor on the PMMA microspheres. TGF-β3 (a kind gift of Novartis Pharma AG, Basel, Switzerland) was dialyzed (Slide-A-Lyzer Mini Dialysis Device, MWCO 10 kDa, Thermo Fisher Scientific, Rockford, USA) against 5 mM citrate buffer, pH 3.8. The PMMA microspheres were sterilized in 70 % (v/v) ethanol, subsequently washed with ddH_2O and resuspended in MES buffer. 3 mM EDC and 6 mM NHS were given to 50 μL of the microsphere suspension and incubated for at least 15 min to activate carboxyl groups. Following activation, the microspheres were washed with MES buffer and TGF-β3 (9.64 ng/μL) was added to the microsphere suspension. The reaction mixture was vortexed shortly and then mixed at room temperature for 2 h. To finish the coupling reaction the microspheres were thoroughly washed for three times with TBST buffer and three times with high salt phosphate buffer to remove unbound TGF-β3. Finally, the microspheres were washed with PBS, resuspended in PBS and counted with a Neubauer hemocytometer (Brand GmbH, Wertheim, Germany) to determine the number of beads per μL bead suspension. Each solution was sterilized by sterile filtration (0.2 μm, PES membrane, 13 mm diameter, Nalge Nunc International Corporation, Rochester, USA)[223].

Microsphere loading of silk scaffolds and pellets

A suspension of TGF-β3-coupled-PMMA microspheres (AK Meinel, Würzburg, Germany) equivalent to a loading of 78 ng TGF-β3 was given to 8 x 10^5 MSC (P2), brought to a final volume of 30 μl with expansion medium without bFGF and soaked into the scaffold with one porosity. The same amount of microspheres was used for the adsorbed group as well as the blank group without growth

factor and coupling reagent which served as negative control. By moving the plunger of the syringe a homogeneous cell distribution was obtained. Cells were incubated for 4 h (37°C, 5% CO_2, 21% O_2) to allow proper cell attachment. The scaffolds were cut out of the syringe and incubated in seeding medium for chapter 3.4 for 21 days (37°C, 5% CO_2, 21% O_2).
For microsphere loaded pellets, a suspension of TGF-β3-coupled-PMMA microspheres equivalent to a loading of 18 ng TGF-β3 was given to 2 x 10^5 cells (P2) suspended in seeding medium per well in 96-well plates (conical bottom), centrifuged at 300 g for 5 min, and allowed to form dense cell pellets overnight in an incubator (37°C, 5% CO_2, 21% O_2). The blank group without growth factor and coupling reagent served as negative control. The pellets were incubated in seeding medium for chapter 3.4 for 21 days (37°C, 5% CO_2, 21% O_2)

2.9.4 RNA isolation and qRT-PCR analysis

Pellets (6 per sample were pooled with n=3) or constructs (n=3) were homogenized employing a TissueLyser from Qiagen (Hilden, Germany) prior to total RNA extraction using TRIzol® Reagent (Invitrogen, Karlsruhe, Germany) according to the manufacturer. First strand cDNA was synthesized using the ImProm™-II Reverse Transcription System (Promega, Madison, USA). Quantitative real-time PCR (qRT-PCR) analysis was performed with an MJ Research Opticon2 Cycler (BioRad, Hercules, CA, USA) using the MESA GREEN qPCR MasterMix Plus with MeteorTaq polymerase (Eurogentec, Seraing, Belgium) and QuantiTec® Primer Assays (Qiagen) for *MMM1*, *MMP3*, *MMP13*, *ADAMTS4*, *ADAMTS5*, *TIMP1*, *TIMP3*, *ACAN*, *COL2A1*, *RPL13A* with cycling parameters as previously described[224] with slight modifications. In brief, qRT-PCR was performed with the following cycling conditions: 1) 50°C for 2 min 2) 95°C for 10 min followed by 3) 40 cycles at 95°C for 15 seconds, 60°C for 30 seconds and 72°C for 30 seconds 4) 72°C for 10 min. mRNA expression levels were normalized to the housekeeping gene *RPL13A*. Fold increase in expression levels for each gene was determined using the $2^{\Delta\Delta CT}$-method. The obtained values were further normalized to the expression at day 0.

2.9.5 Biochemical assays

Pellets (2 per sample were pooled with n=3) and MSC-silk scaffold constructs (n=3) were harvested after 10 or 21 days of cultivation and prepared for biochemical analysis and histology as previously described[225]. Briefly, scaffolds were disintegrated using the TissueLyser. Pellets and disintegrated constructs were digested in 0.5 mL or 1 mL of a papainase solution with 3 U/mL in buffer (100 mmol Na_2HPO_4, 10 mmol Na_2EDTA, pH 6.5) for 16 h at 60°C.

Determination of DNA content

DNA content of samples was determined using Hoechst 33258 dye (Polysciences, Warrington, USA) as previously described[226]. 10 μL of papain digested sample was added to 200 μL of Hoechst 33258 dye solution and the DNA amount was measured fluorometrically with a Tecan GENios pro spectrofluorometer at an excitation wavelength of 365 nm and an emission wavelength of 458 nm. Salmon testis was used as standard.

Determination of GAG content

Sulfated GAG content of samples was determined spectrophotometrically at 525 nm after reaction with dimethylmethylene blue dye (DMMB)[227] by using bovine chondroitin sulfate as standard adapted to 96-well plate format. 10 μL of papain digested sample were added to 40μL of PBE-cysteine buffer. 200 μL DMMB solution is added and the GAG content was analyzed using a MRX microplate reader.

Determination of hydroxyproline content

Hydroxyproline content of pellets and constructs was determined spectrophotometrically at 550 nm after acid hydrolysis and reaction with chloramine-T and p-dimethylaminobenzaldehyde[228]. The assay was adapted to 96-well plate format. 100 μL of papain digested sample was added to 36% of HCl and hydrolyzed for 16 h at 105°C. HCl is allowed to evaporate under the bench and the samples were resuspended in 500 μL ddH_2O. Afterwards, 50 μL of chloramine T-solution was added to 100 μL of resuspended sample and incubated for 20 min at RT.

50 μL of DAB solution is added and incubated for 30 min at 65°C. Hydroxyproline content is analyzed using a MRX microplate reader using L-hydroxyproline as standard. The total collagen amount was calculated using a hydroxyproline to collagen ratio of 1:10[229].

Determination of general MMP activity

General MMP activity was measured using the SensoLyte® 520 Generic MMP activity Kit *Fluorimetric* (Anaspec, Fremont, CA, USA). 6 pellets per sample (n=3) were pooled and processed according to the protocol of the manufacturer. In Brief, tissue samples were homogenized and the MMP activity was monitored at an excitation wavelengths of 490 nm and an emission wavelengths of 520 nm after proteolytic cleavage of 5-FAM/QXL™ 520 FRET peptide by MMPs.

2.9.6 Histology and immunohistochemistry

For histological and immunohistochemical evaluation, pellets and constructs were fixed in 3.7% buffered formalin, dehydrated by increasing sucrose concentrations from 10% to 60% and embedded in Tissue-Tek O.C.T. Compound (Sakura, Torrance, CA, USA). Samples were cut into 7 μm-thick sections. 6 sections at 70 μm intervals of pellets (n=3) and 10 sections at 140 μm intervals of scaffolds (n=3) were taken on a slide. The sampling scheme ensured the evaluation of lateral to medial cross-sections to at least middle sectional areas of the pellets and the BMSC-seeded constructs.

Safranin O staining for GAG

To stain for GAG, sections were treated with aqueous 0.2% safranin O solution, counter-stained with 0.02% fast green and mounted with Glycergel® Mounting Medium (Dako, Hamburg, Germany).

HRP-based immunohistochemical staining

Immunohistochemical staining for collagen type I and II was performed using the EnVision G|2 Doublestain System (Dako) according to the protocol of the manufacturer with slight modifications. Prior to the blocking step with 10%

goat serum (Dako) in PBS for 30 min to prevent unspecific binding, sections were incubated in proteinase K for 7 min. As primary antibody the collagen type II alpha 1 chain antibody (clone II-4C11, 1:100, Acris, Herford, Germany) and the collagen type I alpha 1 chain antibody (1:800, Abcam, Cambridge, UK) was utilized. Samples were counterstained with haematoxylin for 3 min.

Fluorescence-based immunohistochemical staining

Immunohistochemical staining for MMP-generated aggrecan neoepitope DIPEN and MMP-generated collagen type II fragment was performed as previously described[230,231]. In brief, 7 μm sections were rehydrated in PBS and digested with 0.1 units/mL protease-free chondroitinase ABC and 0.1 units/mL of keratanase I (Seikagaku, Tokyo, Japan), prior to overnight incubation with primary mouse antibody to the MMP-generated aggrecan neoepitope DIPEN (1:100, MD Biosciences, Zürich, Switzerland) or polyclonal rabbit antibody to cross-linked C- telopeptide of type II collagen (CTX-II) (1:200, USCN Life Science, Huston, TX, USA). For immunohistochemical staining for MMP13, antigen retrieval was performed by 7 min proteinase K digestion followed by a 30 min block (Powerblock, Biogenex, Fermont, CA, USA) before overnight incubation with polyclonal rabbit anti-MMP13 antibody (1:100, Abcam, Cambridge, UK). Samples for collagen I and II fluorescence staining were processed as described in subsection "HRP-based immunohistochemical staining.
Slides were thoroughly washed with PBS, and a Cy3-conjugated AffiniPure donkey anti-mouse or Cy3-conjugated AffiniPure goat anti-rabbit secondary antibody (Jackson Immuno Research, West Grove, PA, USA) was added for 2 h in the dark. Nuclei were counterstained with IS Mounting Medium DAPI (Dako). Equivalent concentrations of species-matched immunoglobulins on identically treated sections were used as negative controls. The stained slides were imaged using an Olympus BX51 fluorescent and bright-field microscope and the CellSens™ imaging software from Olympus (Olympus, Hamburg, Germany).

2.9.7 Quantitative image analysis

Positive DIPEN-, CTX-II- and MMP13-labeled structures were quantified as relative immunolabeled area [immunolabeled area per cell] using NIH ImageJ Fiji Software based on the Jensen protocol[232]. Briefly, all images of the stained markers were acquired with the same marker-specific exposure time. For each marker, a specific threshold value was selected to allow the segmentation of the specific signal from the background and thereafter was kept constant along all measurements. Subsequently, the selected area was analyzed and measured (n=4–8 images). To determine total cell numbers the nuclei were counted by means of the particle analyzer of the NIH ImageJ Fiji Software. Analogue to the immunolabeled area a threshold was set to segment the specific signal from background noise, the image was binarized, the objects (nuclei) separated and subsequently counted[232]. The quantified immunolabeled area was normalized to total nuclei.

2.9.8 Scanning electron microscopy

Porosity, interconnectivity and seeding of silk scaffolds was investigated by SEM. Samples were bisected through the center and fixed in 6% glutaraldahyde in PBS. The constructs were subsequently rinsed in PBS, dehydrated in a series of graded aceton and dried using critical point drying (CPD). The scaffolds were sputtered with gold and analyzed at 5 kV using a JSM-7500F field emission scanning electron microscope (Joel, Tokyo, Japan).

2.9.9 Live/dead staining

Cell viability was evaluated using the live/dead cell staining kit from PromoKine (Heidelberg, Germany). The scaffolds were washed three times with PBS and stained by applying 0.5 mL of staining solution containing 4 μM ethidium bromide homodimer III (EthD) and 2 μM calcein acetoxymethyl ester (calcein) in PBS to the scaffolds per well. After 1 hour, the dye was removed, the constructs were washed with PBS and cut vertically to the scaffold surface in half. The middle section was subsequently analyzed using a fluorescence microscope (ex/em

460-490 nm/520 nm and ex/em 510-550 nm/590 nm, respectively) and processed with the Olympus CellSens™ software. Living cells were stained in green, dead cells were stained in red.

2.9.10 Quantification of protein content

Total protein content was quantified using the BCA Protein Assay Kit (Thermo Scientific, Rockford, USA). The assay was performed according to the protocol of the manufacturer. Spectroscopic quantification was performed at 562 nm using a MRX microplate reader (Dynatech Laboratories, Chantilly, Virginia). Albumin served as standard for total protein calculation.

2.9.11 Sodium dodecyl sulfate polyacrylamide gel electrophoresis (SDS-PAGE)

For immunodetection of collagens by Western blot analysis 10 μg of isolated protein were separated by SDS-PAGE on 8% polyacrylamide gels. The composition of the gels is listed below:

Table 2.10: Separating gel

Components	Volume for two gels
30% acrylamide	4.08 ml
1 M TRIS pH 8.8	5.7 ml
10% SDS	150 μl
H_2O	4.92 ml
10% APS	150 μl
TEMED	7.5 μl

The stacking gel solution was poured into the gel tray directly after dissolving all components. After polymerization the separating gel was poured on top of the stacking gel and a gel comb was inserted to form wells. For separating proteins by SDS-PAGE the Bio-Rad Mini-PROTEAN ™ Tetra Cell System (Bio-Rad, München, Germany) was used. Prior to loading the gel was inserted into the tank according to the instruction manual and the tank was filled with

Table 2.11: Stacking gel

Components	Volume for two gels
30% acrylamide	0.9 ml
0.5 M TRIS-HCL pH 6.8	1.5 ml
10% SDS	60 μl
H_2O	3.42 ml
10% APS	60 μl
TEMED	6 μl

running buffer (25 mM Tris, 192 mM glycine, 0.1% SDS). Samples were loaded into the wells of the stacking gel with respective volumes of 10 μg protein and 1 μl of a protein ladder (Novex™ sharp protein standard, Life Technologies) was loaded onto the gel. The gel was run at 30 A.

2.9.12 Western Blot

After SDS-PAGE, the proteins on the gel were transferred to a nitrocellulose membrane by tank blotting using the Bio-Rad Mini-PROTEAN ® Tetra Cell System (BioRad). The gel holder cassette was inserted into the buffer tank filled with transfer buffer (25 mM tris base, 192 mM glycine, 10% methanol) and the proteins were transferred by applying 300 mA for 2 h.
After transferring the proteins to the nitrocellulose membrane, the membrane was blocked with 5% (m/V) nonfat dried milk powder in PBST (0.1% Tween® 20) on an orbital shaker for 1 h at RT. The membrane was incubated with the primary antibody collagen type II alpha 1 chain antibody (clone II-4C11, 1:5000, Acris, Herford, Germany) or collagen type I alpha 1 chain antibody (1:5000, Abcam, Cambridge, UK) diluted with PBST, containing 5% nonfat dried milk powder, and incubated at 4°C overnight under agitation.
The membrane was washed three times with PBS for 10 min on an orbital shaker. The HRP-conjugated secondary antibody, goat-anti-rabbit IgG (P0448, 1:2000, Dako) was added to the membrane and incubated for 1 h at RT. The membrane was washed three times with PBS for 10 min. Finally, the immunoreactive proteins were detected by chemiluminescence using the Amersham ECL Prime

Western Blotting Detection Reagent (GE Healthcare, Buckinghamshire, UK).

2.9.13 Quantification of IGFBP-3 using ELISA

IGFBP-3 in cell culture supernatant was quantified using the Quantikine® Human IGFBP-3 Immunoassay from R&D Systems (Minneapolis, USA). Samples from cell culture medium were collected between day -2 and 0 and 19 and 21 of culture and stored at $-30°C$ until analysis. IGFBP-3 levels were normalized to the total DNA content of the respective samples.

2.9.14 Statistical analysis

Data are presented as mean values ± standard deviation (SD). Statistical differences between groups were assessed by One-way ANOVA with Tukey's post hoc test, Two-way ANOVA with Sidak's post hoc test or unpaired Student's t-test. Values of $p < 0.05$ were considered statistically significant. Statistical analysis was performed using GraphPad Prism, Version 6.0 (GraphPad Software, La Jolla, CA). For the experiments, if not otherwise stated, the number of samples per group was n=3.

Chapter 3

Results and Discussion

3.1 Differential effects of IGF-I and des(1-3)IGF-I during chondrogenic differentiation of bone marrow-derived stromal cells

The process of cartilage development from MSCs into chondroblasts and further into chondrocytes is regulated by the correct temporal and spatial expression of multiple secreted factors including IGF-I and members of the TGF superfamily (including TGF-β)[81–84,88]. IGF-I is a key component in cartilage development and has been shown to increase cell growth and proliferation in various cell types like adult chondrocytes[170,171] and MSCs[176,177].

However, even though IGF-I plays a central role in chondrogenesis, its use for chondrogenic differentiation of BMSCs is surprisingly rare and poorly understood. BMSCs belong to the most intensively investigated tissue sources, both *in vitro* and *in vivo*, due to their high capacity for chondrogenesis[7] and are therefore still regarded as possible cell source with regard to cartilage regeneration. The few studies that have investigated the chondroinductive effects of IGF-I on BMSCs in the commonly used pellet culture system until today either have shown that IGF-I treatment has no effect[214,215] or additionally applied the insulin containing standard cell culture supplement (ITS+ Premix) into the chondrogenic medium[214,216,217]. Since the affinity of insulin for the IGF-IR is around two orders of magnitude lower compared to IGF-I, supraphysiological levels of insulin (approximately 100 times higher) are used which we and others assume to cause nonspecific stimulation of the IGF-IR and superpose or mask IGF-I effects[172,218]. To avoid IGF-I masking effects, our study was performed in the absence of insulin.

IGF-I action is, among others, regulated by IGFBPs which modulate IGF-I bioavailability and function and modify its interaction with the IGF-IR[184]. Since IGFBPs are involved in the attenuation of IGF-I-dependent ECM synthesis in chondrocytes[181,233], we postulated that IGFBPs might play an important role in IGF-I mediated chondrogenic differentiation of BMSCs as well.

Therefore, the aim of our study was to investigate the effects of IGF-I on

the chondrogenic potential of BMSCs and as a second step the influence of IGFBPs on IGF-I biological action and its bioavailability. To demonstrate the involvement and to assess the influence of IGFBPs on IGF-I action and bioavailability, we (1) used the truncated IGF-I analogue desIGF whose affinity for IGFBPs is approximatly 100 times reduced compared to IGF-I and (2) utilized a small molecule IGFBP inhibitor NBI-31772 to disrupt IGF-I/IGFBP interactions and displace IGF-I from the IGF-I/IGFBP complex.
BMSCs were cultured with IGF-I or desIGF for 21 days and were additionally exposed to NBI-31172. Chondrogenic differentiation was evaluated and the expression of chondrogenic marker genes was analyzed.

3.1.1 Chondrogenic differentiation of BMSCs in pellet culture

Cellular response of BMSCs during chondrogenic differentiation towards IGF-I and its truncated analogue desIGF at increasing concentrations was investigated in 3D pellet culture by biochemical analysis and histological and immunohistochemical staining. Biochemical analysis for major ECM components revealed

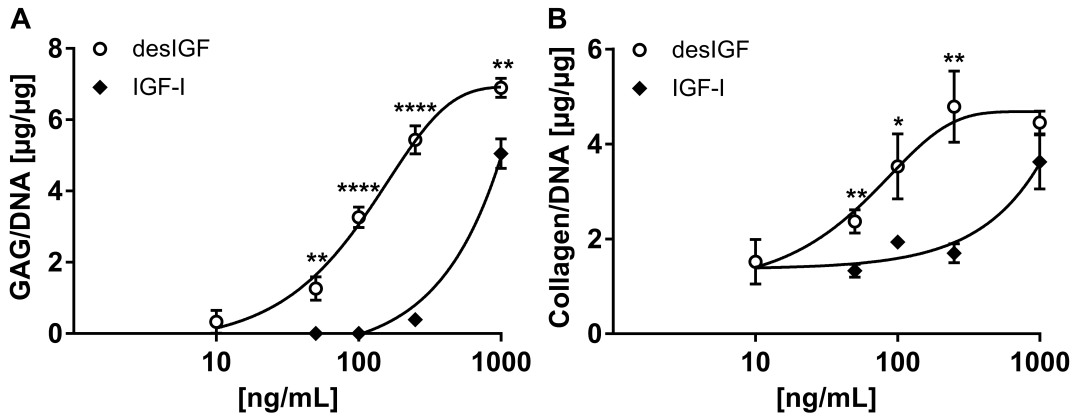

Figure 3.1: IGF-I and desIGF induced proteoglycan and total collagen production of BMSC pellets in a dose-dependent manner. Pellets were cultured for 21 days in chondrogenic medium and were treated with increasing concentrations of IGF-I or desIGF. Biochemical analysis for (A) GAG and (B) total collagen content. Asterisks denote statistically significant differences between the groups at the same concentration (*p<0.05, **p<0.01, ***p<0.001, ****p<0.0001).

enhanced GAG and total collagen production at increasing growth factor concentration after 21 days of chondrogenic differentiation (Figure 3.1 A+B). DesIGF turned out to be distinctly more potent than IGF-I, i.e. distinctly lower concentrations of desIGF were needed to elicit a response similar to IGF-I. For example, 50 ng/mL desIGF induced a higher GAG and collagen production than 100 or 250 ng/mL IGF-I, while 250 ng/mL desIGF exhibited a similar GAG content as 1000 ng/mL IGF-I. Furthermore, 100 ng/mL desIGF showed an equal amount of total collagen in the ECM as 1000 ng/mL IGF-I. The higher potency of desIGF was well reflected in the safranin O staining for GAGs and especially in the immunohistochemical staining for collagen type II (Figure 3.2 A+B).

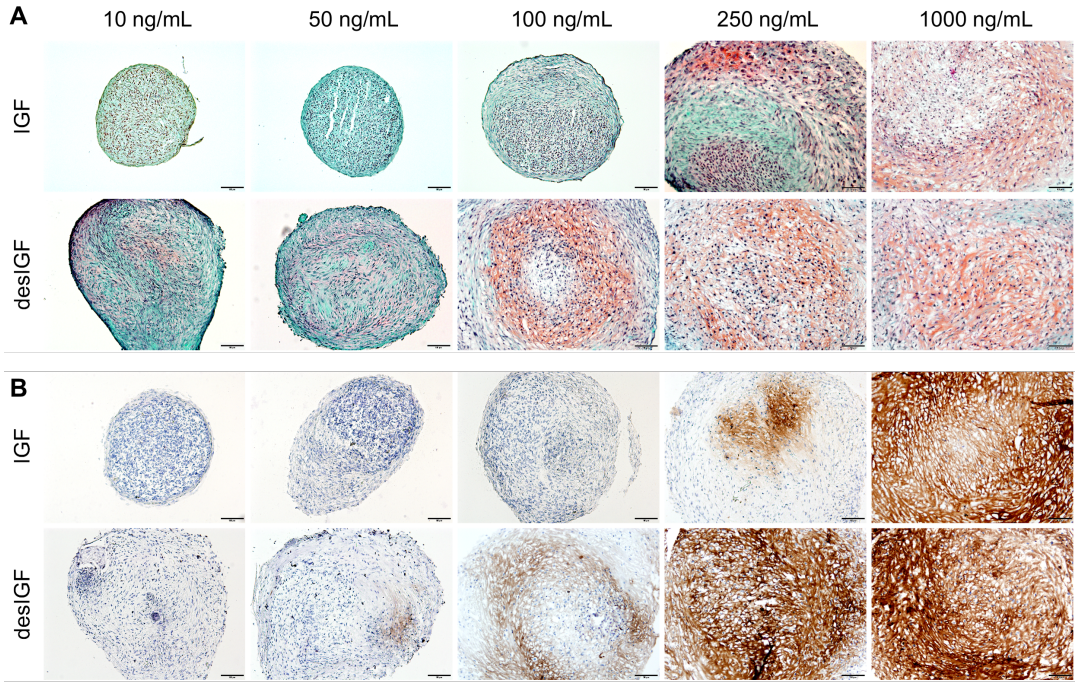

Figure 3.2: Histological and immunohistochemical staining for key cartilage ECM components. BMSC pellets were cultured for 21 days in chondrogenic medium in the presence of increasing concentrations of IGF-I or desIGF. (A) Safranin O staining for GAG in red and (B) immunohistochemical staining for collagen type II in brown, nuclei were stained with haematoxylin in blue-violet. Scale bar 100 μm.

GAG deposition in the ECM was higher at 10 ng/mL desIGF compared to 100 ng/mL IGF-I as shown in the safranin O staining. Collagen type II was present at 50 ng/mL desIGF, whereas in the IGF-I group a collagen type II signal was detected at a concentration of 250 ng/mL.

3.1.2 Quantification of IGFBP-3 secretion

DesIGF has no or only little affinity for IGFBPs and was shown here to be distinctly more potent than IGF-I with regard to chondrogenesis in BMSC pellet culture. Therefore, we hypothesized that high IGF-I doses were necessary to induce chondrogenic differentiation of BMSCs owing to enhanced IGF-I binding by IGFBPs which resulted in reduced IGF-I availability for receptor binding. As a first step to investigate the effects of IGFBPs during chondrogenesis of BMSCs, the secretion of the major IGFBP secreted by BMSCs, IGFBP-3, was analyzed at day 0 and after 21 days of chondrogenesis (Figure 3.3). No IGFBP-3

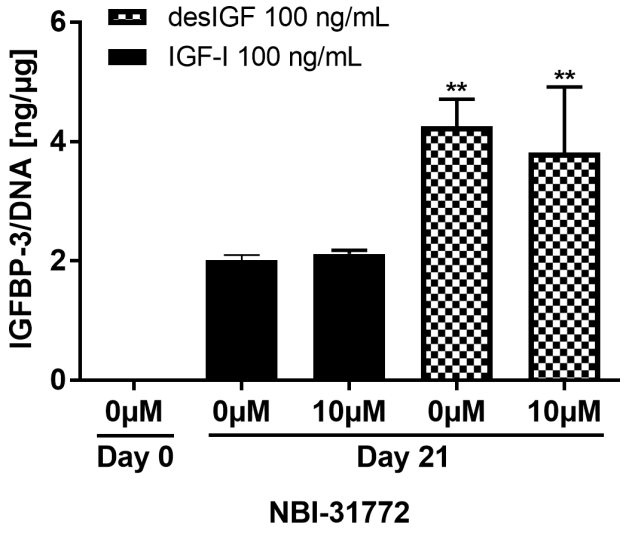

Figure 3.3: IGFBP-3 secretion of BMSCs. Culture media (conditioned between day -2 – 0 and 19 – 21) were evaluated using ELISA for BMSC pellets cultured in chondrogenic media for 21 days with or without the IGFBP inhibitor NBI-31772. Pellets were formed from day -2 – 0 in chondrogenic medium without IGF-I or desIGF. Growth factor and inhibitor supplementation started at day 0. Asterisks denote statistically significant differences between the different growth factors (**$p<0.01$).

secretion was observed at the beginning of the culture (day -2 – day 0, including pellet formation, without IGF-I and desIGF). In contrast, distinct secretion of IGFBP-3 was observed in chondrogenic culture (between day 19 – 21), in the presence of either IGF-I or desIGF. DesIGF-induced IGFBP-3 production significantly exceeded (2 fold) IGF-I-induced IGFBP-3 production. The IGFBP inhibitor NBI-31772 had no effect on IGF-I-dependent IGFBP secretion.

3.1.3 Effect of the IGFBP inhibitor NBI-31772 on proteoglycan synthesis of BMSCs

The small molecule, non-selective IGFBP inhibitor NBI-31772 prevents or disrupts binding of IGF-I to IGFBPs. Due to the IGF-I-capturing properties of IGFBPs, we postulated that IGF-I-dependent proteoglycan synthesis could be restored by NBI-31772-triggered release of bound IGF-I or prevention of IGF-I binding by IGFBPs. Indeed, continuous application of NBI-31772 during

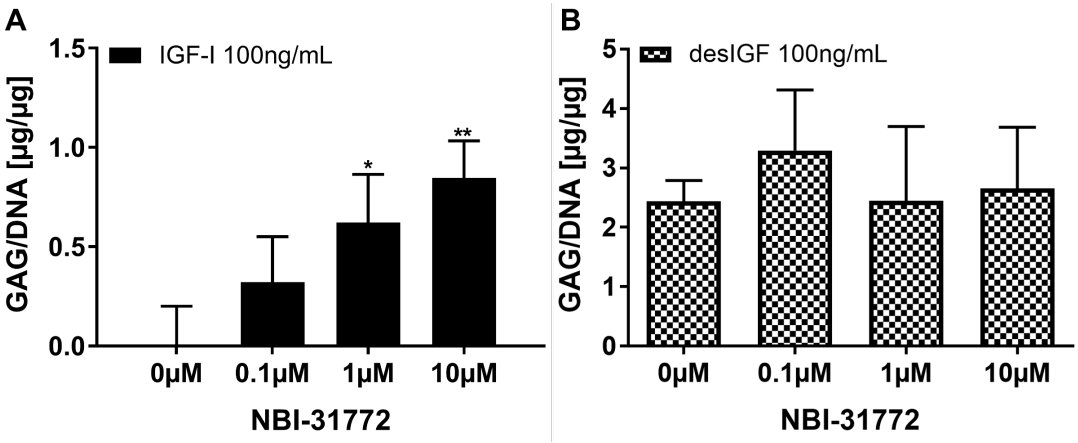

Figure 3.4: Effect of the small molecule IGFBP inhibitor NBI-31772 on GAG production of chondrogenically differentiating BMSCs in pellet culture. BMSCs were cultured in chondrogenic medium supplemented with 100 ng/mL of (A) IGF-I and (B) desIGF for 21 days in the presence of different concentrations or without the IGFBP inhibitor. (A+B) Biochemical analysis of the GAG content of the ECM. Asterisks denote statistically significant differences between the groups referring to the 0 μM control specimen (*p<0.05, **p<0.01).

cell culture increased proteoglycan synthesis of pellets cultured with IGF-I

(100 ng/mL) in a dose-dependent manner (Figure 3.4 A). As expected, since desIGF does not bind to IGFBPs, proteoglycan synthesis remained unaffected by NBI-31772 (Figure 3.4 B). The application of NBI-31772 alone had no affect on proteoglycan synthesis (data not shown). These observations were further

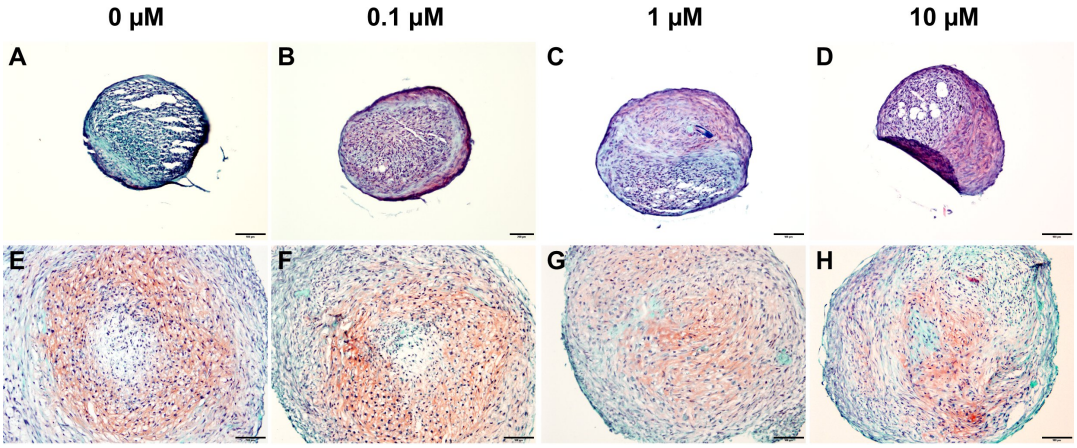

Figure 3.5: Evaluating the effects of the small molecule IGFBP inhibitor NBI-31772 on GAG production of chondrogenically differentiating BMSCs in pellet culture using histology. BMSCs were cultured in chondrogenic medium supplemented with 100 ng/mL of (A-D) IGF-I or (E-H) desIGF for 21 days in the presence of different concentrations (0.1–10 μM) or absence of the IGFBP inhibitor NBI-31772.

supported by histological staining for GAGs. While the application of the IGFBP inhibitor NBI-31772 enhanced safranin O staining dose-dependently in the IGF-I group, an increase of GAG production in the desIGF group could not be detected (Figure 3.2).

3.1.4 Gene expression of chondrogenic marker genes

To evaluate gene expression during chondrogenic differentiation of BMSCs, qRT-PCR was performed at day 21 (Figure 3.6). Expression of the cartilage specific marker genes *ACAN* and *COL2A* was significantly increased after exposure to desIGF (2.5 fold and 17 fold respectively) compared to IGF-I. Furthermore, *COL2A* showed a distinctly elevated expression (18 fold) in the IGF-I specimen after NBI-31772 exposure compared to the control group. In contrast, BMSCs

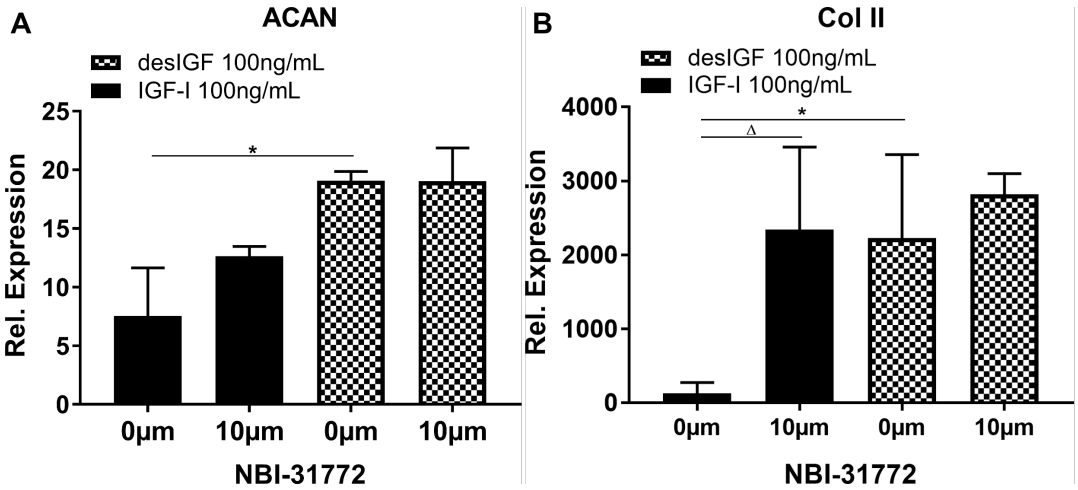

Figure 3.6: Effect of the small molecule IGFBP inhibitor NBI-31772 on gene expression of chondrogenically differentiating BMSCs in pellet culture. (A) Aggrecan and (B) collagen type II gene expression. BMSCs were cultured in chondrogenic medium supplemented with 100 ng/mL IGF-I or desIGF for 21 days in the presence (10 μM) or absence of the IGFBP inhibitor NBI-31772. mRNA expression levels were normalized to the housekeeping gene *RPL13A*. The obtained values were further normalized to the expression at day 0. Asterisks denote statistically significant differences between IGF-I and desIGF (*$p<0.05$), triangle denote significant differences between IGF-I and IGF-I in the presence of 10 μM NBI-31772 ($^{\triangle}p<0.05$).

cultured with desIGF revealed no differences in *ACAN* and *COL2A* expression after NBI-31772 administration.

3.1.5 Discussion

IGF-I is regarded as one of the most critical growth factors in cartilage development and homeostasis[234,235]. However, the role of IGF-I in chondrogenic differentiation of BMSCs is rare and still poorly understood. Therefore, in this study we investigated effects of the growth factor IGF-I during chondrogenic differentiation of BMSCs in standard pellet culture in the presence of TGF-β. We additionally compared the chondroinductive effects of IGF-I with its truncated analogue desIGF. In this context, the influence of IGFBPs on IGF-I action and bioavailability was further assessed.

Biochemical analysis of GAG and total collagen content demonstrated that IGF-I stimulated GAG and total collagen synthesis in pellets in a dose-dependent manner (Figure 3.1 A+B). This was well in aggreement with a report showing strongly enhanced protein and cartilaginous matrix synthesis including GAGs and collagen type II in articular chondrocytes[173]. Biochemical data was further confirmed utilizing histological and immunohistochemical staining for the major cartilaginous matrix components collagen type II and GAG (Figure 3.2). The co-administration of IGF-I and TGF-β, an important growth factor that plays a central role in all stages of chondrogenesis[152–154], has been shown to synergistically increase cartilaginous matrix synthesis in other types of MSCs as well[175,218,236]. It was suggested that TGF-β triggers the primary chondroinductive stimulus which is complemented and enhanced by IGF-I[237].
In general, we found that high doses of IGF-I were mandatory to induce chondrogenic differentiation of BMSCs in pellet culture, which was in accordance with previously published literature for different types of MSCs, e.g. synovial-derived stromal cells[238,239] or adipose-derived stromal cells (ASCs)[215,240] also suggesting higher IGF-I doses to be required for chondrogenesis of MSCs in pellet culture. However, it is important to note, that all mentioned studies additionally used insulin in the chondrogenic medium. We assume that the presence of insulin (approximately 100 times more than physiological level) might have caused nonspecific stimulation of the IGF-IR or may have masked IGF-I action, effects that likely distort interpretation of the results. Our data might provide an

explanation for studies using mesenchymal stromal cells (e.g. BMSCs or MSCs from umbilical cord) that did not observe proliferative or chondroinductive effects of IGF-I due to insufficient IGF-I doses ranging between 1 to 100 ng/mL IGF-I[214,215,241–243].

To unravel the question about high IGF-I doses necessary to induce chondrogenesis of BMSCs in pellet culture, we hypothesized that an enhanced IGF-I binding by IGFBPs is responsible for a reduced bioavailability of IGF-I for IGF-I-dependent chondrogenesis which had already been seen in the decline of IGF-I-dependent ECM synthesis in chondrocytes due to IGFBPs[181,233]. In order to indirectly analyze the involvement of IGFBPs, we utilized the IGF-I analogue desIGF to avoid interactions with IGFBPs during chondrogenic differentiation of BMSCs. DesIGF lacks the tripeptide Gly-Pro-Glu at the N-terminus[183] reducing its affinity for IGFBPs 100 times[244], but it is still able to activate the IGF-IR and binds it with the same affinity as IGF-I[172]. When BMSCs were cultured in the presence of desIGF, biochemical analysis revealed superior chondrogenesis compared to IGF-I (Figure 3.1). DesIGF turned out to be significantly more potent, e.g. 250 ng/mL desIGF induced the same GAG content in the ECM as 1000 ng/mL IGF-I (Figure 3.1 B). With regard to collagen synthesis, 100 ng/mL desIGF showed an equal amount of total collagen in the ECM as 1000 ng/mL IGF-I. In accordance with biochemical assays, pellets cultured in the presence of desIGF displayed enhanced histological staining for GAGs and immunohistochemical staining for collagen type II at low doses compared to IGF-I. These findings were well in agreement with former studies reporting enhanced desIGF potency (about 10-fold) relative to IGF-I with regard to GAG and collagen synthesis in chondrocytes due to a reduced binding by IGFBPs and thus an increased desIGF availability[181]. Higher potency of desIGF in comparison to IGF-I was additionally shown for proliferation of rat myoblasts with a ten-fold increased cell growth[182].

To further elucidate the modulatory impact of IGFBPs on IGF-I biological action or bioavailability for IGF-I-dependent GAG synthesis during chondrogenic differentiation of BMSCs in pellets, we used the IGFBP inhibitor NBI-31772, a

small non-peptide molecule that binds to IGFBPs and prevents IGF-I binding to IGFBPs or disrupts IGF-I/IGFBP interactions[245],thus, increasing the level of IGF-I available to bind to its receptor. Among others, IGFBPs govern IGF-I action via modulating IGF-I bioavailability and function and through modifying its interaction with the IGF-IR[184]. The affinity of IGFs for IGFBPs is thereby higher than the affinity of IGFs for their own receptor. MSCs express several IGFBPs with IGFBP-3 being the most prevalent produced in culture[151] which was reported to block IGF-I effects when supplemented to the medium[246]. Since the level of secreted IGFBPs has been shown to regulate IGF-I-dependent anabolic response of chondrocytes[246], we postulated that IGFBPs might also affect IGF-I-dependent GAG synthesis of BMSCs.
The secretion of IGFBP-3 during chondrogenic differentiation of BMSCs in pellet culture in the presence of IGF-I was demonstrated using ELISA. BMSCs exposed to desIGF elicited increased IGFBP-3 secretion, while NBI-31772 did not influence IGFBP-3 secretion. Remarkably, by applying NBI-31772, proteoglycan synthesis in cultures in the presence of IGF-I could be increased in a dose-dependent manner as demonstrated in biochemical assay (Figure 3.4 A). NBI-31772 seemed to partially rescue IGF-I chondroinductive action by displacing IGF-I from the IGF-I/IGFBP complex or by preventing IGF-I from IGFBP binding which results in an effective counteraction of the IGFBP induced reduction of IGF-I bioavailability. As expected, cultures in the presence of desIGF remained unaffected due to the strongly decreased affinity of desIGF for IGFBPs. These findings were in agreement with a previous study reporting increased proteoglycan synthesis in human osteoarthritic chondrocytes after NBI-31772 treatment[233]. Since the affinity of NBI-31772 for all six IGFBPs was shown to be similar[245], we assume NBI-31772 to disrupt IGF-I binding to all exogenous IGFBPs, subsequently enabling IGF-I to bind to the IGF-IR and induce proteoglycan synthesis.

The analysis of chondrogenic marker gene expression revealed similar expression patterns for the evaluated genes (Figure 3.6). Consistent with findings in biochemical assays and immunohistochemical staining, desIGF treatment also induced stronger up-regulation of *ACAN* and *COL2A* in comparison to IGF-I.

Due to its reduced IGFBP binding properties, the application of NBI-31772 did not influence desIGF-mediated gene expression. In contrast, BMSCs cultured in the presence of IGF-I and exposed to NBI-31772 showed enhanced *COL2A* expression compared to the specimen receiving IGF-I only, increasing *COL2A* expression to expression levels similar to the desIGF group.

To confirm IGF-I and desIGF chondroinductive effects in a more clinically relevant model system, we used a hyaluronic acid (HA) based hydrogel for chondrogenic differentiation of BMSCs. These experiments were conducted as part of the doctoral thesis of Rasmus Ahlbrecht (data not shown here). Consistent with the pellet culture results shown here, both growth factors stimulated GAG and collagen synthesis in a dose-dependent manner, while desIGF also displayed enhanced potency (approximately 10 fold) in HA hydrogels as demonstrated in biochemical assays and histological and immunohistochemical staining. Noteworthy, in comparison to pellet culture, significantly lower doses of growth factors were required to induce chondrogenesis in HA hydrogels. IGF-I triggered substantial major cartilaginous matrix component synthesis at IGF-I doses lower than 100 ng/mL. The obtained results correlate well with former studies using similar IGF-I doses for MSCs or chondrocytes in fibrin[175,247,248] or agarose gels[180]. Reduced IGF-I doses necessary to induce chondrogenesis are assumed to be based on MSC interaction with HA and its structural properties. HA hydrogels have been proven to be an effective biomaterial to support chondrogenesis of BMSCs[249,250] and increase chondrogenic marker gene expression including *COL2A*, *ACAN* and *SOX9*[251,252]. The ECM mimicking environment of the HA hydrogel and the biological cues provided by the HA seemed to enhance chondrogenesis and might have fostered IGF-I sensitivity of MSCs. BMSCs in HA hydrogels exhibited a similar IGFBP-3 secretion pattern as seen in pellet culture, but the IGFBP modulatory actions and NBI-31772 impact on chondrogenesis in HA hydrogels remain to be investigated.

In conclusion, this study emphasizes the importance of IGF-I during chondrogenesis of BMSCs. To the best of our knowledge, this is the first study to comparatively analyze the chondrogenic potential of IGF-I and its analogue

desIGF on BMSCs. High doses of IGF-I were shown to be necessary to induce chondrogenic differentiation of BMSCs compared to desIGF due to an IGFBP induced reduction of IGF-I action and bioavailability. Hence, our results corroborate the central role of the IGF-I/IGFBP system in chondrogenesis of BMSCs in two independent 3D culture systems and should be taken into account in future approaches to cartilage regeneration employing BMSCs.

3.2 Low oxygen tension enhances IGF-I induced chondrogenesis of bone marrow-derived stromal cells

Oxygen tension is a developmentally important stimulus in cartilage tissue development. Articular cartilage tissue is exposed to low oxygen tension of 5% on the surface to less than 1% in the deep zone[119]. However, most of the research in cartilage tissue engineering so far has been performed with atmospheric oxygen tension of 21% of standard cell culture, which has profound influence on chondrogenesis. The issue of cell culture conditions, especially regarding oxygen tension is receiving more and more interest in terms of different aspects like proliferation, survival and differentiation. For example, cells that were subject to low oxygen tension (3%) showed less DNA damage and senesced slower compared to cells that were exposed to atmospheric oxygen tension (21%) as previously shown for mouse embryonic fibroblasts[117]. This minor DNA damage results from a smaller amount of reactive oxygen species present under low oxygen concentrations.

MSCs are very well adapted to low oxygen tension and thus to limited metabolic conditions[120]. They have been shown to exhibit superior proliferation over several passages[116,121–123] in hypoxia compared to normoxia and are able to survive prolonged hypoxic stress in contrast to other cell types like cardiomyocytes due to their ability to switch to the glycolytic pathway for ATP production and their generally low consumption of ATP[124]. Remarkably, low oxygen conditions promote the maintenance and preservation of full pluri- or multipotency as shown in studies using human embryonic stem cells (hES) or adipose- and bone marrow-derived MSC[125–127]. In recent years, it has been demonstrated that expanding or differentiating chondrocytes and MSCs in a hypoxic environment resulted in an increased GAG content of the ECM[134,137–144]. Further studies have also indicated that hypoxia suppressed hypertrophic differentiation of chondrocytes and MSCs[145–147].

Thus, oxygen tension appears to be an important regulatory factor in the

proliferation, differentiation and matrix production of chondrocytes and BMSCs. However, the hypoxic impact on chondrogenesis of BMSCs in the presence of one of the most important growth factors for chondrogenesis, IGF-I, has not been specifically addressed so far. Consequently, the aim of this study was to investigate hypoxic effects on IGF-I mediated chondrogenic differentiation and cartilaginous matrix development of BMSCs in pellet culture. According to the convention of literature on that topic we refer 21% oxygen as normoxia and low oxygen tension as hypoxia even though high oxygen tension should rather be termed hyperoxia and low oxygen tension ($< 5\%$) should more accurately be termed physioxia (physiological) as recently suggested[253–255].

3.2.1 Chondrogenic differentiation of BMSCs

BMSCs were cultured in chondrogenic media at different IGF-I concentrations and exposed to normoxic and hypoxic conditions . Major ECM components were analyzed by biochemical analysis and immunohistochemical and histological staining. When BMSCs were cultured in an hypoxic environment, a significant increase in proteoglycan and collagen deposition could be detected after 21 days by quantitative glycosaminoglycan and total collagen analysis compared to normoxic conditions (Figure 3.7 A+B). For example, 250 ng/mL IGF-I induced a stronger GAG production under hypoxic conditions than 1000 ng/mL IGF-I under normoxic conditions. Furthermore, BMSCs cultured with 100 ng/mL IGF-I under hypoxic conditions showed an increased total collagen content in the ECM than BMSCs cultured with 1000 ng/mL IGF-I under normoxic conditions. In contrast to chapter 3.1, 100 ng/mL IGF-I induced GAG production in both groups. Increased GAG production under hypoxic conditions was further

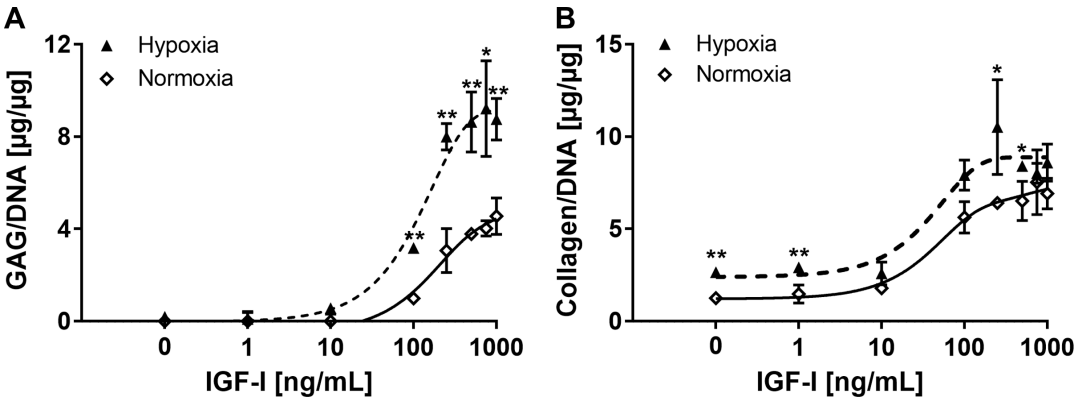

Figure 3.7: IGF-I dose-response for GAG and collagen production. BMSCs were cultured in chondrogenic medium for 21 days under normoxic and hypoxic conditions. Biochemical analysis of (A) GAG and (B) total collagen content. Asterisks denote statistically significant differences between the groups (*$p<0.05$, **$p<0.01$).

confirmed in the safranin O staining (Figure 3.8 A), e.g. 500 ng/mL IGF-I in the hypoxic group showed a stronger staining for GAG compared to 1000 ng/mL IGF-I in the normoxic group. Additionally, hypoxic exposure led to stronger staining for collagen type II at lower IGF-I concentrations in comparison to

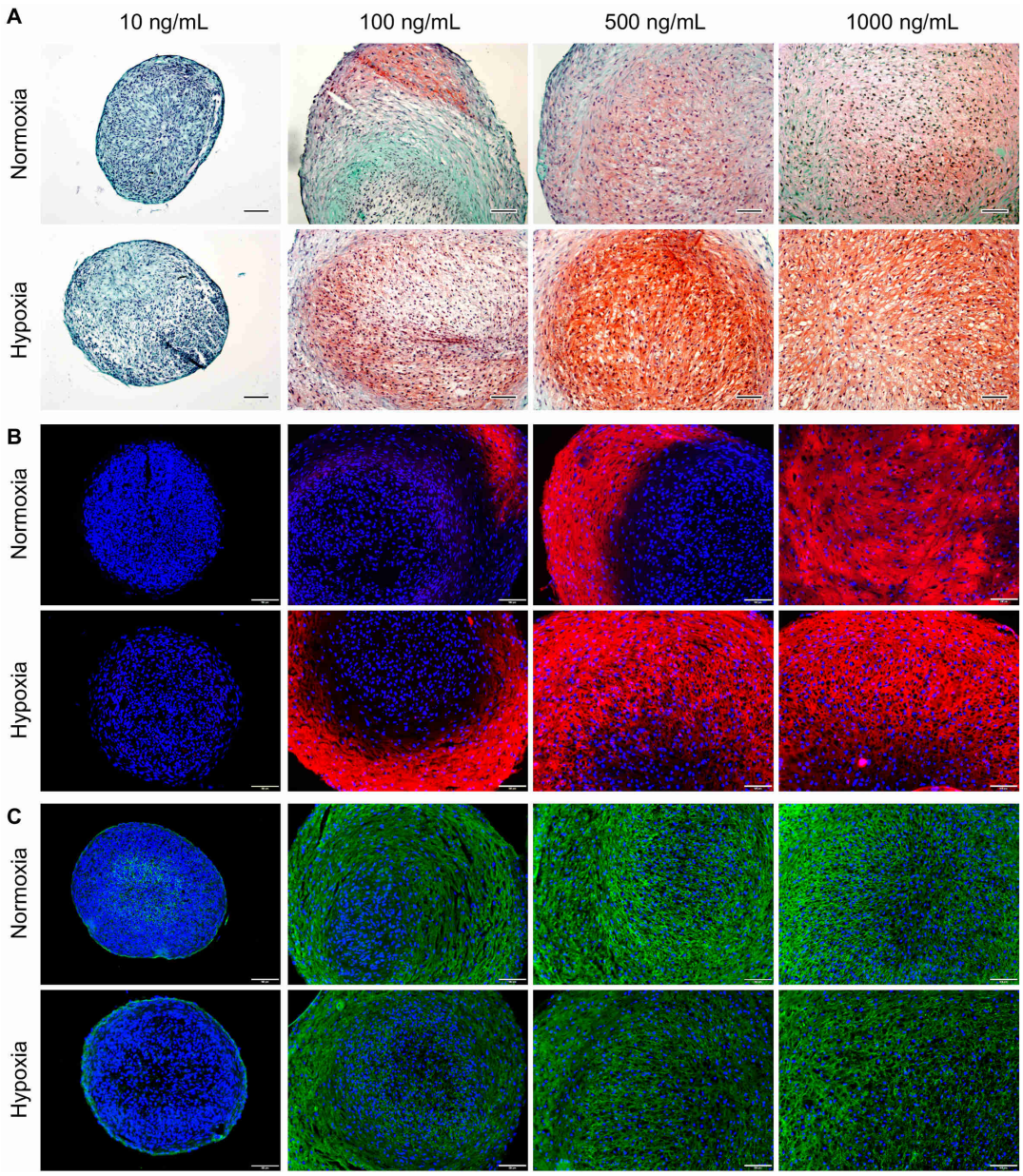

Figure 3.8: Histological and immunohistochemical staining for cartilaginous ECM components. BMSCs were cultured in chondrogenic medium for 21 days under normoxic and hypoxic conditions and treated with increasing IGF-I concentrations. (A) Safranin O staining for GAG in red. Immunohistochemical staining for (B) collagen type II in red and (C) collagen type I in green. (B+C) Nuclei were stained with DAPI in blue. Scale bar 100 μm.

normoxia (Figure 3.8 B) which was further confirmed in histomorphometric quantification (Figure 3.9 A). For example, BMSCs cultured under hypoxic conditions in the presence of 100 ng/mL IGF-I showed similar collagen type II staining like BMSCs cultured under normoxic conditions in the presence of 500 ng/mL IGF-I. In contrast, immunohistochemical staining for collagen type I

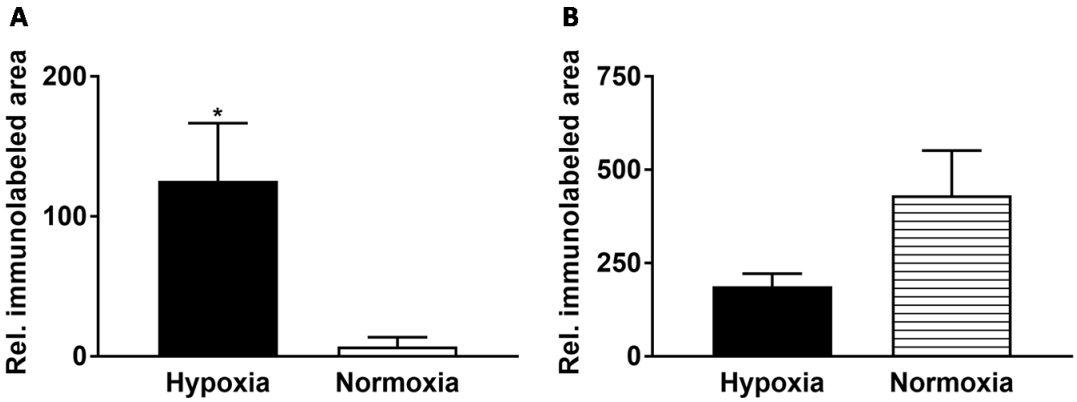

Figure 3.9: Histomorphometric quantification of relative collagen type I and II immunolabeled area. BMSCs were cultured in chondrogenic medium for 21 days under normoxic and hypoxic conditions and treated with 100 ng/mL IGF-I. Histomorphometric quantification of (A) collagen type II and (B) collagen type I. Asterisks denote statistically significant differences (*$p<0.05$).

did not reveal distinct differences after hypoxic exposure (Figure 3.8 C), even though a trend towards reduced collagen type I expression could be observed in the immunohistochemical staining and the histomorphometric quantification (Figure 3.9 B).

3.2.2 Quantification of IGFBP-3 secretion

IGFBP-3 secretion by BMSCs was functionally assessed after 21 days of chondrogenic differentiation using ELISA. It was shown that BMSCs produced significantly less (reduction by half) amounts of IGFBP-3 at 100 ng/mL IGF-I under hypoxic conditions than under normoxic conditions.

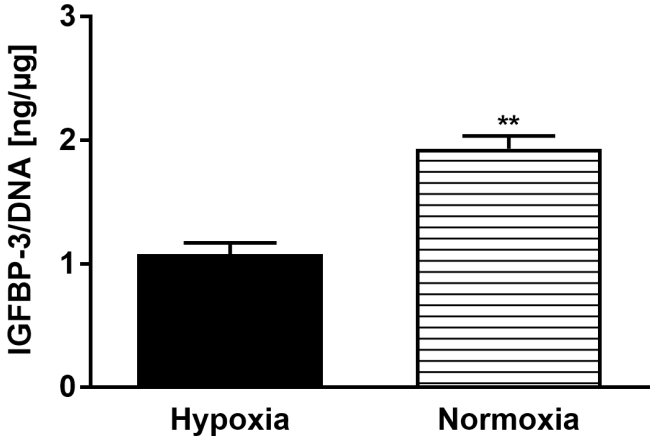

Figure 3.10: IGFBP-3 secretion of BMSCs was evaluated using ELISA. Culture media (conditioned between day 19 and 21) of BMSCs cultured in chondrogenic media for 21 days under normoxic and hypoxic conditions in the presence of 100 ng/mL IGF-I. Asterisks denote the statistically significant difference between the groups (**$p<0.01$).

3.2.3 Discussion

Engineering artificial cartilage tissue is still a challenging task. Thus, a deeper understanding of basic mechanisms that regulate cartilage development and function appears desirable. Since oxygen tension is an important cue in cartilaginous matrix development and homeostasis, the aim of this study was to investigate hypoxic effects on chondrogenic differentiation of BMSCs in association with IGF-I in comparison to standard cell culture conditions.

The role of IGF-I during chondrogenic differentiation of BMSCs has been described in detail in section 3.1 and will therefore be touched upon more briefly in the discussion of this section. Consistent with our data demonstrated in 3.1 for normoxic conditions, chondrogenic differentiation of BMSCs also was IGF-I-dependent under hypoxic conditions. IGF-I is a key growth factor in cartilage development and is described to enhance production of key ECM components such as GAGs and collagens, especially collagen type II, in MSCs and articular chondrocytes[172,173,248,256,257]. Consistent with these studies, IGF-I stimulating action on GAG and collagen synthesis with increasing IGF-I doses was confirmed under hypoxic conditions as well (Figure 3.7). Interestingly, different to chapter 3.1, 100 ng/mL IGF-I induced GAG production in both groups, probably due to donor dependency.
The absolute GAG and total collagen content in the ECM was increased in BMSCs cultured under low oxygen tension as shown in biochemical assays. This was well in agreement with previously published data that showed superior chondrogenic differentiation of MSCs with enhanced cartilaginous matrix synthesis under hypoxic conditions[134,140,258,259]. The latter was also shown for other cell types like chondrocytes[135,142]. Improved chondrogenesis under hypoxia was additionally validated by histological and immunohistochemical analysis (Figure 3.8). Pellets cultured in an hypoxic environment already displayed enhanced GAG and collagen type II staining at low IGF-I doses. Histomorphometric analysis of collagen type II staining supported this data (Figure 3.9 A). Contradictory results have been published concerning the hypoxic impact on collagen type I synthesis in chondrocytes. While on the one hand collagen type I expression

was reported to be decreased under hypoxia[253], another study could not find differences in collagen type I expression[260]. In agreement with the latter and another previously published report for MSCs[258], we could not detect distinct differences in collagen type I expression between different oxygen tensions. However, low oxygen tension seems to shift the collagen type II to collagen type I (Col II/Col I) ratio towards a more collagen type II producing state for low IGF-I doses. Similar effects have been observed on the gene regulatory level after hypoxic exposure during chondrogenic differentiation of MSCs and the culture of articular chondrocytes[261].

As discussed in section 3.1, IGF-I activity and bioavailability is tightly regulated by IGFBPs, IGFBP-specific proteases and the ability of IGF-I to interact with the IGF-IR. One possible mode of action of hypoxia to enhance chondrogenesis of BMSCs in the presence of IGF-I might be via down-regulating IGF-I binding by IGFBPs. This may increase IGF-I bioavailability and biological activity and foster IGF-I-dependent GAG and collagen synthesis. In fact, using ELISA for the major IGFBP-3, a significant decrease in IGFBP-3 secretion by BMSCs during chondrogenesis was demonstrated under hypoxic conditions (Figure 3.10). Our findings were in a certain manner unexpected as other studies could not find differences or even reported stronger IGFBP-3 secretion by BMSCs or bovine aortic endothelial cells when cultured under low oxygen tension, respectively[262,263]. This divergence was presumably due to the different cell types and the experimental set up used, as on the one hand IGFBP-3 secretion and action is highly cell specific and on the other hand in contrast to our study, BMSCs were not chondrogenically differentiated at different oxygen tensions but solely cultured under normoxic or hypoxic conditions. To analyze whether enhanced secretion of IGFBP-3 and a corresponding reduced availability of free IGF-I was responsible for reduced chondrogenesis of BMSCs in the presence of IGF-I under normoxic conditions, future studies may focus on IGFBP-3 inactivation via neutralizing antibodies.
Another mode of action how hypoxia fostered GAG and collagen production might be via IGF-I stimulated increased Hif-1α expression which in turn itself is further stabilized under low oxygen tension and improved Hif-1α specific

target gene expression, e.g. *SOX9*, as demonstrated in various cell types such as chondrocytes[264], human umbilical vein endothelial cells[265] and periosteal cells[266].

Interestingly, recent data indicated a hypoxia-triggered suppression of ASC mineralisation and osteogenic differentiation via IGFBP-3 up-regulation[267], which is the exact opposite IGFBP-3 expression pattern of our findings and illustrates the complexity of IGFBP action. Other aspects that regulate IGF-I effects during chondrogenic differentiation of BMSCs include reduced IGF-I proteolysis and enhanced IGF-IR binding or expression[185,186]. Since IGF-IR is expressed in developing and mature cartilage[176,177], hypoxia might increase IGF-IR expression as described for lung cells[268] and the A549 cell line[269] on the mRNA level and act through increased signal transduction via IGF-IR associated pathways. In preliminary western blot analysis, we were able to show trends of increased IGF-IR expression under hypoxic conditions (data not shown), but these data remain to be confirmed.

In summary, our results indicate that hypoxic exposure during chondrogenic differentiation of BMSCs improves cartilaginous tissue formation in the presence of IGF-I. Further studies are necessary to investigate possible effects of hypoxia on the IGF-I/IGFBP axis during chondrogenesis, cartilaginous matrix development and homeostasis of BMSCs.

3.3 Hypoxia affects ECM-modulating enzyme expression and reduces proteoglycan degradation during chondrogenic differentiation of BMSCs in different 3D cell culture systems

Hypoxic culture conditions have been shown to beneficially influence chondrogenic differentiation of MSCs (Chapter 3.2) and promote matrix synthesis of articular chondrocytes[134,135,139]. However, previous research has mainly focused on the stimulatory effects of hypoxia on GAG and collagen synthesis during chondrogenic differentiation of MSCs without addressing catabolic activity, even though ECM development and maintenance is driven by continuous dynamic remodeling. These remodeling processes for matrix homeostasis are regulated by a careful balance between matrix synthesis, secretion, modification and enzymatic degradation[33]. Important enzymes involved are matrix-degrading enzymes such as "a disintegrin and metalloproteinase with thrombospondin motifs" (ADAMTSs) and matrix metalloproteinases (MMPs) and their inhibitors (tissue inhibitor of MMPs (TIMPs)). MMP1, MMP3, MMP13, ADAMTS4 and ADAMTS5 have been reported to play a key role in normal cartilage turnover, cartilage degradation, and osteoarthritis[36].

As hypoxia was recently shown to reduce cartilage breakdown and to decrease the expression of numerous degradative enzymes in human articular chondrocytes[135,144,253], we postulated that hypoxia might also play a considerable role in diminishing ECM breakdown during chondrogenic differentiation of MSCs as well.

Therefore, in this study we investigated the effects of hypoxia on matrix-modulating enzymes during *in vitro* chondrogenic differentiation of MSCs. In particular, we hypothesized that low oxygen tension not only supports ECM development, but also protects cartilaginous ECM from degradation, especially by attenuating MMP activity contributing to higher proteoglycan content in the

ECM. To test this hypothesis, bone marrow-derived MSCs were differentiated in pellet culture in chondrogenic medium either under normoxic (21%) or hypoxic (2%) conditions. ECM development was assessed, and expression and activity of ECM-modulating enzymes, including MMP breakdown products, were analyzed. Key findings were further corroborated in MSC loaded 3D silk fibroin-based scaffolds under normoxic and hypoxic conditions.

3.3.1 Chondrogenic differentiation of BMSCs

BMSCs were cultured in chondrogenic media and exposed to normoxic and hypoxic conditions. In order to confirm enhanced extracellular matrix development under hypoxic conditions, major ECM components were analyzed by histological and immunohistochemical staining and biochemical analyses. Indeed, after exposure of BMSCs to a hypoxic environment, a significant increase in proteoglycan deposition after 10 and 21 days was detected by safranin O staining, as compared to normoxic conditions. This was well supported by quantitative glycosaminoglycan analysis (Figure 3.11 A + 3.12 A). Furthermore,

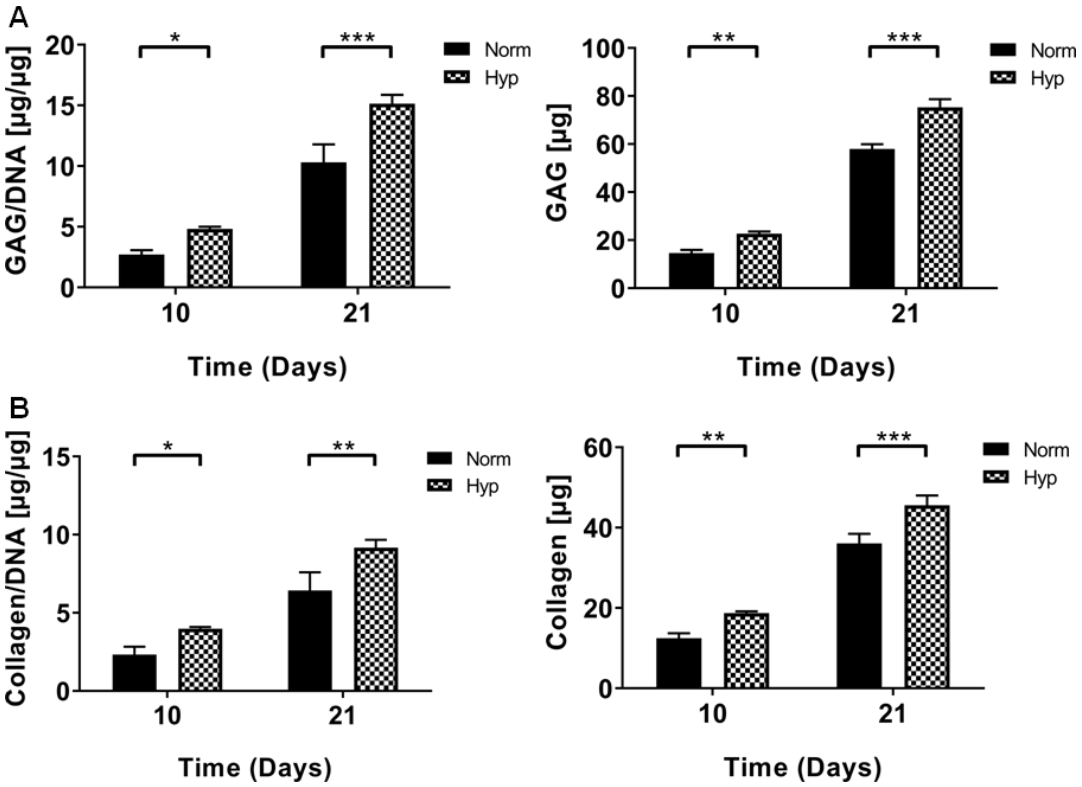

Figure 3.11: Quantitative analysis of (A) GAG and (B) total collagen content. BMSCs were cultured in chondrogenic medium under normoxic (21% O_2) and hypoxic (2% O_2) conditions for 21 days in pellet culture. Data is represented as mean ± SD (n=3). Asterisks denote statistically significant differences between the groups (*p<0.05, **p<0.01, ***p<0.001).

hypoxic exposure led to stronger staining for collagen type II after 10 days

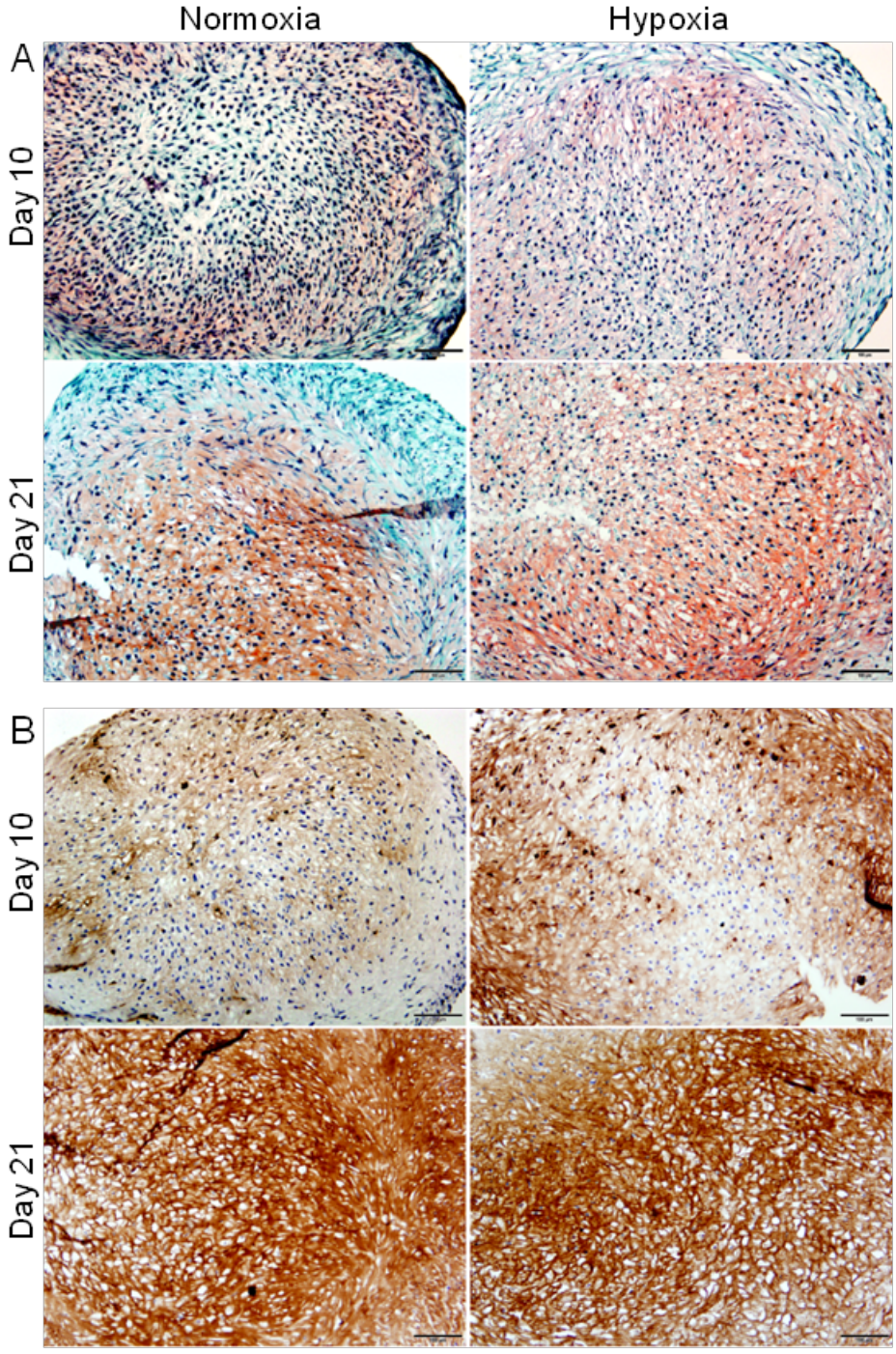

Figure 3.12: Chondrogenic differentiation of BMSC cultured in chondrogenic medium under normoxic (21% O_2) and hypoxic (2% O_2) conditions after 10 and 21 days in pellet culture. (A) Safranin O staining (GAG is shown in red, nuclei in dark blue) and (B) immunohistochemical staining for collagen type II (the presence of collagen type II is shown in brown, nuclei in blue). Scale bar 100 μm.

and to a significantly higher content of total collagen, as demonstrated by immunohistochemistry and biochemical assay, respectively (Figure 3.11 B + 3.12 B).

3.3.2 Gene expression of extracellular matrix-modulating enzymes

Gene expression analysis of ECM-modulating enzymes was performed on days 5, 10, and 21 in pellets using qRT-PCR (Figure 3.13). Expression of the prominent cartilage-degrading enzyme MMP13 was strongly decreased under hypoxic conditions, with a 26-fold and a 6-fold reduction at day 10 and day 21, respectively, as compared to normoxic conditions. *MMP3* also showed a distinctly lower expression at day 10 (7-fold) upon exposure to hypoxia. In contrast, *MMP1* and *ADAMTS4* showed only minor differences (*MMP1*, 2.5-fold increase at day 5; *ADAMTS4*, 1.8-fold increase at day 21), and for *ADAMTS5*, an increase under hypoxic conditions was determined at day 21 (6-fold), although gene expression was comparably low. With regard to enzymes inhibiting the activity of MMPs, similar expression was observed for *TIMP1*, whereas for *TIMP3*, a distinctly higher expression was observed under hypoxia, as compared to normoxic conditions (4-fold and 10-fold, at days 5 and 21, respectively). In addition to ECM-modulating enzymes, also expression of aggrecan and collagen type II was analyzed. For both, distinctly increased expression was detected under hypoxic conditions (up to 11-fold for aggrecan at day 21 and up to 2.8-fold and 4.7-fold for collagen type II, at day 10 and 21).

3.3.3 MMP13 protein expression and general MMP activity

In order to determine whether the expression of MMP13 was also decreased on the protein level in a hypoxic environment, immunohistochemical staining for MMP13 was performed. Consistent with the qRT-PCR results for *MMP13* gene expression, MMP13 protein expression was strongly reduced after 10 and 21 days of culture under hypoxic conditions as well (Figure 3.14). Histomorphometric quantification of the relative immunolabeled area showed an 8-fold and a 6.5-fold

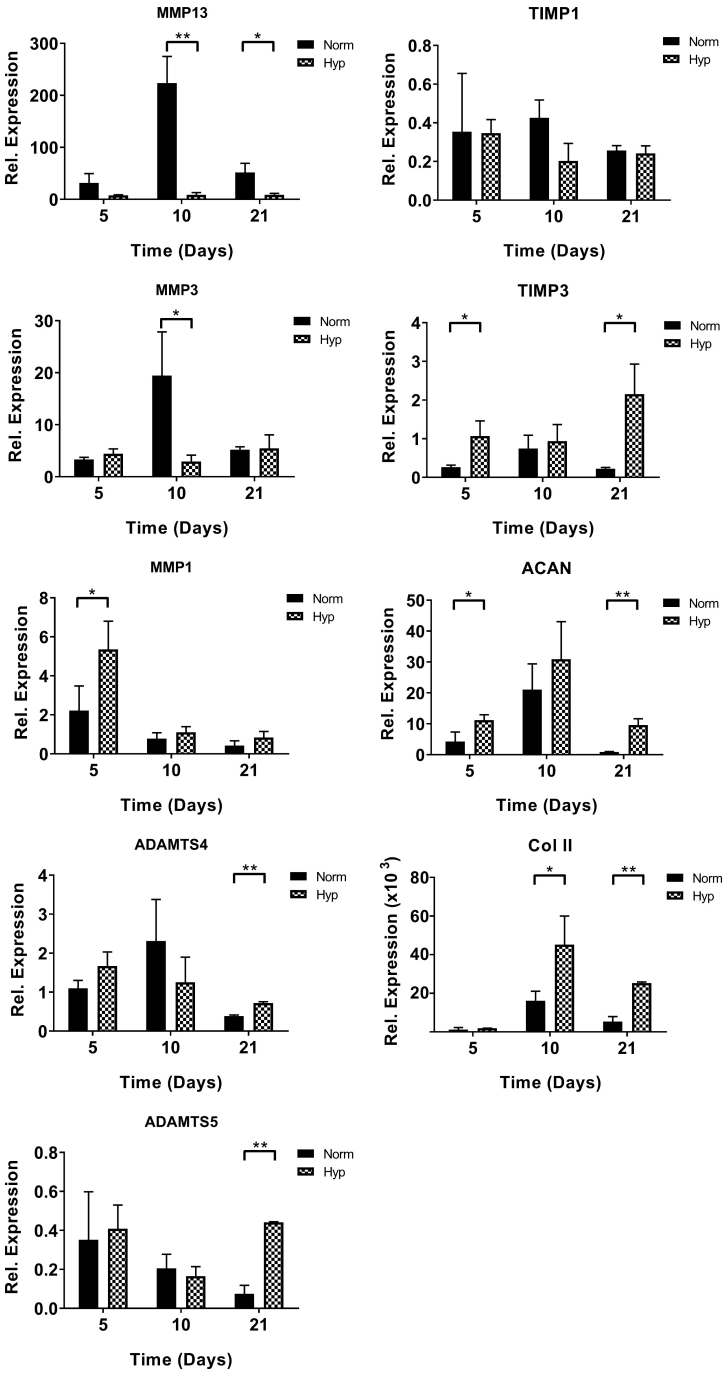

Figure 3.13: Examination of matrix-modulating enzyme gene expression using qRT-PCR. BMSCs were cultured for 21 days under hypoxic and normoxic conditions in chondrogenic medium. Gene expression levels of the different genes were normalized to *RPL13A* as housekeeping gene; the obtained values were further normalized to expression at day 0. Data represented as mean ± SD (n=3). Asterisks denote statistically significant differences between the groups (*$p<0.05$, **$p<0.01$).

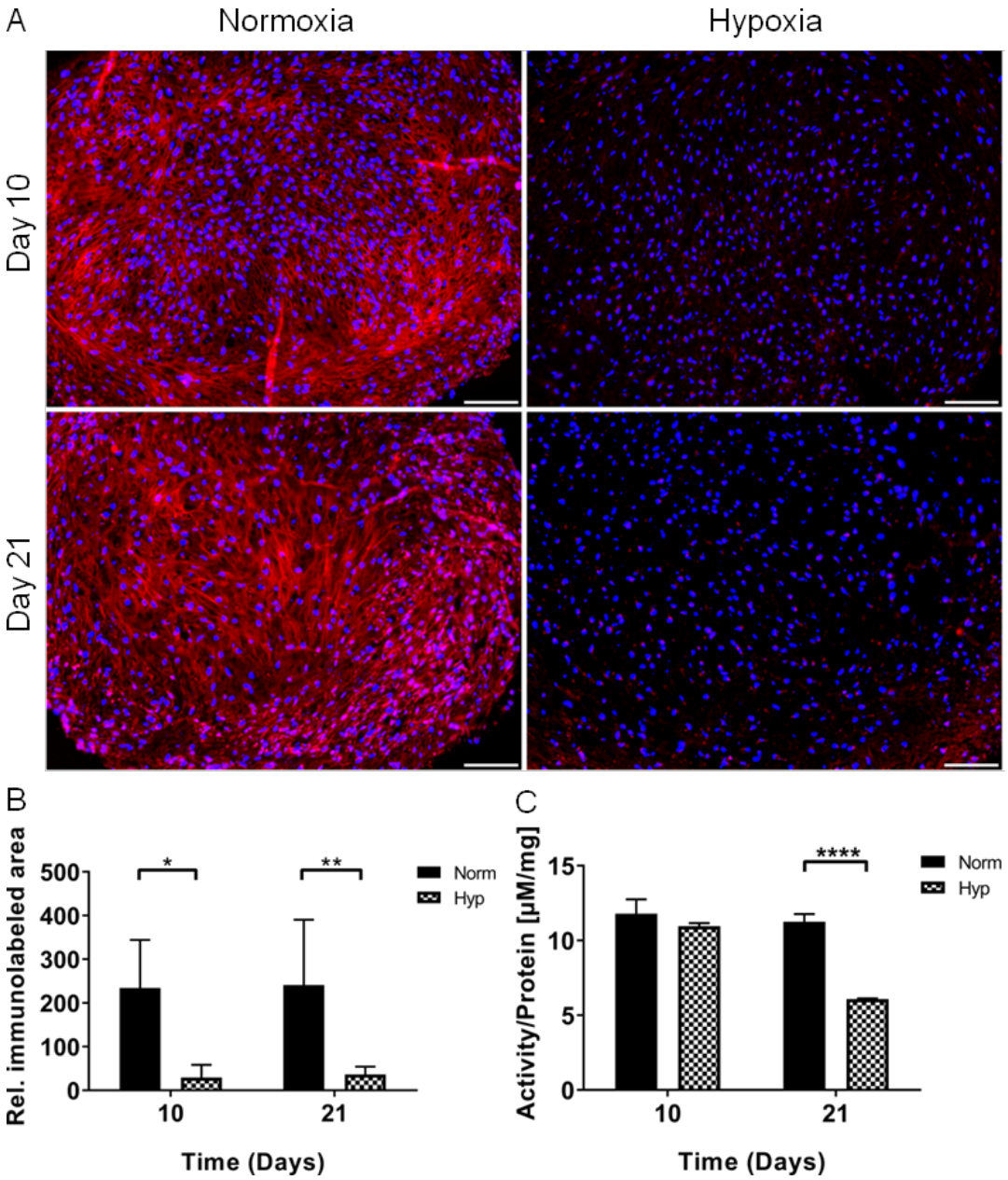

Figure 3.14: Immunohistochemical evaluation of MMP13 expression and determination of general MMP activity of BMSCs cultured for 21 days in chondrogenic medium under normoxic and hypoxic conditions. (A) Immunohistochemical staining for MMP13 (MMP13 in red, nuclei were stained with DAPI in blue). Scale bar 100 μm. (B) Histomorphometric quantification of relative MMP13-immunolabeled area. (C) Evaluation of general MMP activity (n=3). Data represented as mean ± SD. Asterisks denote statistically significant differences between the groups (*p<0.05, **p<0.01, ****p<0.0001).

decrease at day 10 and day 21, respectively, as compared to normoxic conditions (Figure 3.14 B). Furthermore, a FRET-based assay was employed to assess total MMP activity. At day 21, in the hypoxic group MMP activity dropped to 54% of values obtained for the normoxic group (Figure 3.14 C).

3.3.4 ECM degradation during chondrogenic differentiation of MSCs

To further characterize whether the attenuated MMP expression is reflected by reduced ECM breakdown during chondrogenic differentiation of MSCs, an immunohistochemical analysis for MMP-generated aggrecan-neoepitope DIPEN and cross-linked C-telopeptide of type II collagen (CTX-II) was performed. Immunohistochemical staining revealed that hypoxia distinctly reduced MMP-mediated aggrecan cleavage (Figure 3.15 A). This was further supported by histomorphometric analysis demonstrating an 8-fold and 37.5-fold decrease of relative immunolabeled area for aggrecan neoepitope DIPEN at days 10 and 21, respectively, as compared to the normoxic group (Figure 3.16 A). Differences in collagen type II degradation could not be detected between normoxia and hypoxia (Figure 3.15 B and 3.16 B).

3.3.5 MMP expression and ECM degradation in 3D scaffolds

To verify the key findings in a clinically more relevant context, we further investigated the hypoxic impact on ECM-modulating enzymes in 3D silk fibroin-based scaffolds. Consistent with pellet culture, histological evaluation of chondrogenic differentiation showed a more intensive staining for GAG under hypoxic conditions (Figure 3.17 A). Also well in agreement with the observations in pellets, qRT-PCR analysis of BMSCs cultured in silk scaffolds under hypoxia demonstrated an increased expression of *TIMP3* and a significant down-regulation of *MMP13*, as compared to normoxic conditions (Figure 3.17 B). This was well reflected on the protein level by distinctly weaker immunohistochemical staining for MMP13 in the hypoxic group (Figure 3.17 C). Also, again confirming the findings in the pellet culture, a distinctly reduced aggrecan cleavage was de-

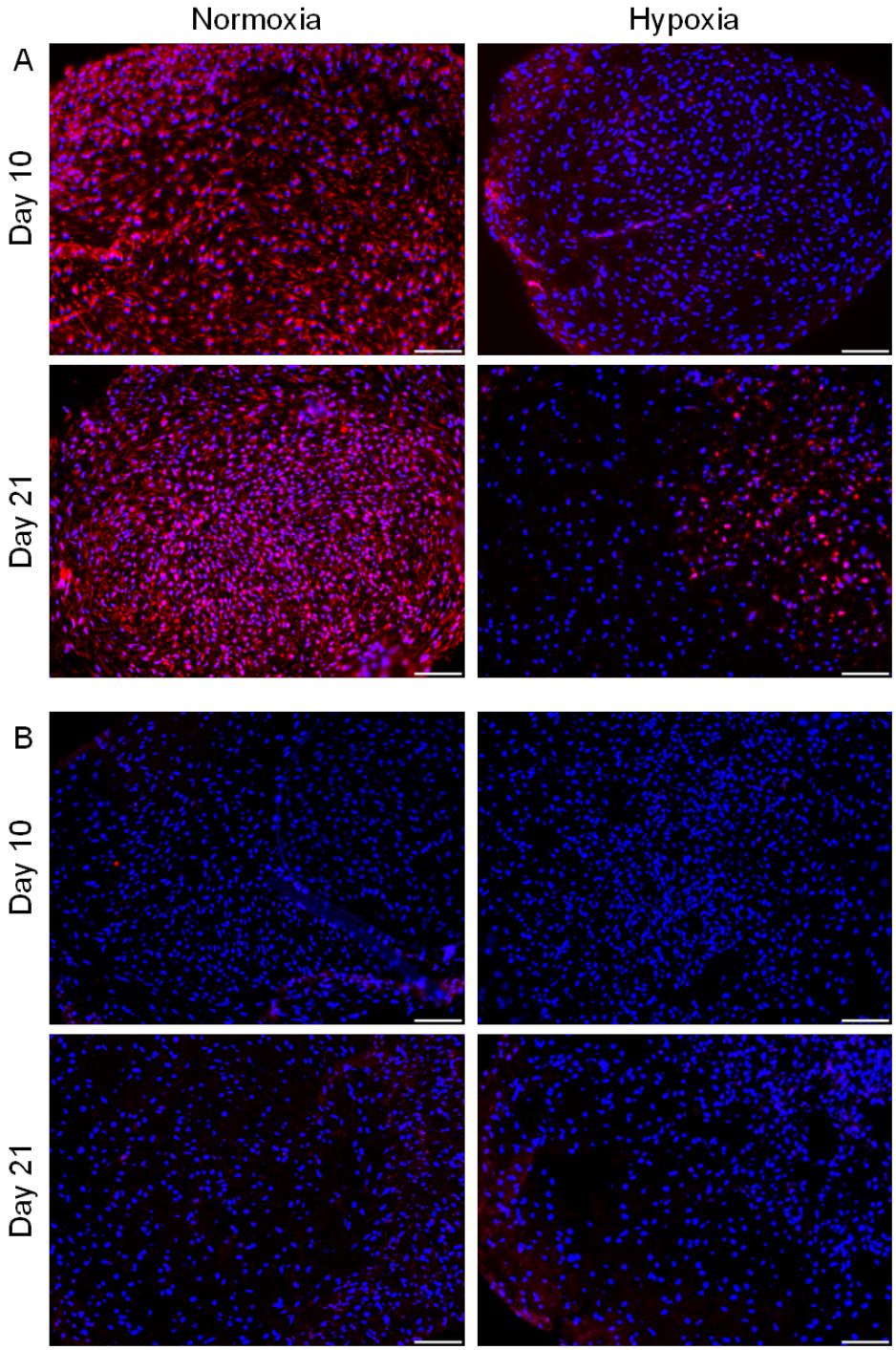

Figure 3.15: Immunohistochemical staining for MMP-mediated ECM degradation products. BMSCs were cultured in chondrogenic medium for 21 days under normoxic and hypoxic conditions. (A) MMP-generated aggrecan neoepitope DIPEN, a marker for aggrecan degradation and (B) cross-linked C-telopeptide of type II collagen (CTX-II), a marker for collagen type II degradation (DIPEN and CTX-II in red, nuclei were stained with DAPI in blue). Scale bar 100 μm.

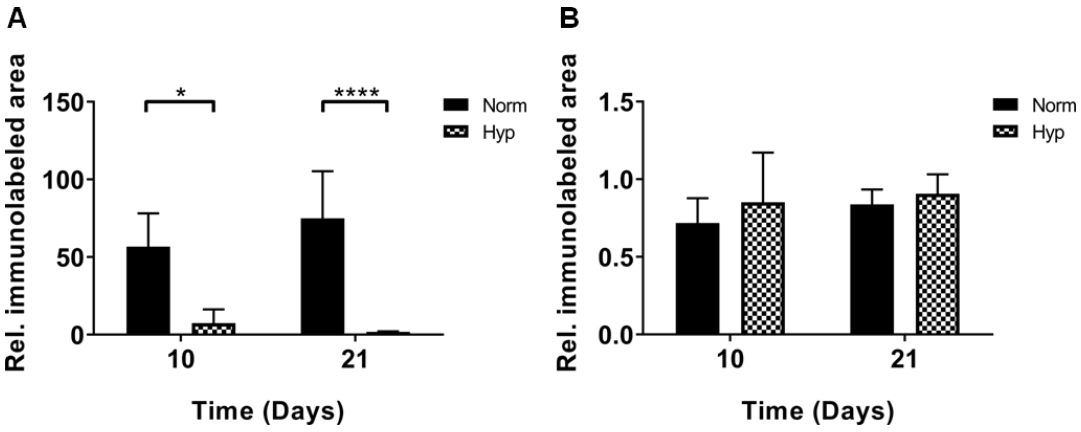

Figure 3.16: Histomorphometric quantification of relative (A) DIPEN- and (B) CTX-II-immunolabeled area. Data represented as mean ± SD. Asterisks denote statistically significant differences between the groups (*$p<0.05$, ****$p<0.0001$).

tected by staining for MMP-generated aggrecan-neoepitope DIPEN in scaffolds exposed to hypoxia as well (Figure 3.17 D).

3.3.6 Discussion

In this study we investigated differential effects of normoxic and hypoxic conditions on the expression and activity of ECM-modulating enzymes during chondrogenic differentiation of BMSCs and the resulting impact on ECM development. We hypothesized that low oxygen tension does not only promote cartilaginous ECM synthesis, but as a second mode of action protects cartilaginous ECM from degradation.

Previous studies have demonstrated that hypoxic culture conditions favor chondrogenic differentiation of MSCs and promote matrix synthesis by articular chondrocytes and BMSCs[134,135,138,139]. Consistent with this data, in our study BMSC pellets cultured under hypoxic conditions exhibited enhanced collagen type II (day 10), total collagen, and GAG content (day 10 and 21, respectively) in the ECM (Figure 3.11 and 3.12). Improved chondrogenesis under hypoxia was further confirmed by significantly increased mRNA gene expression for *ACAN* and *COL2A* (Figure 3.13), which was well in agreement with recently reported findings in hypoxic culture of MSC[141].

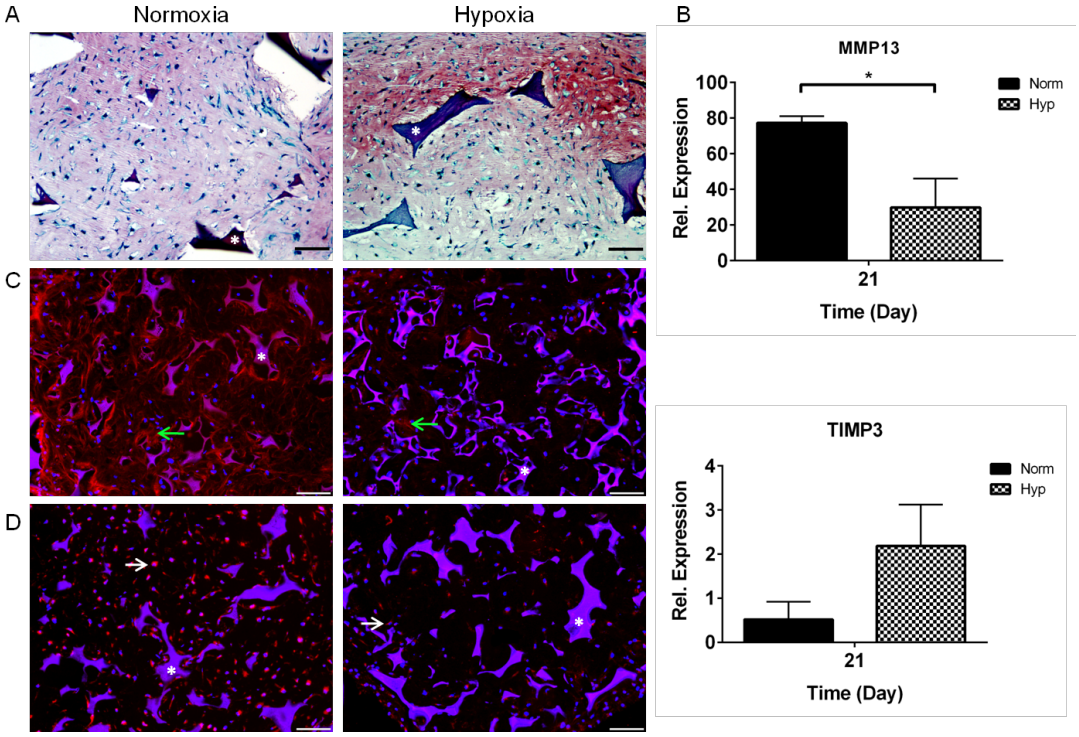

Figure 3.17: Chondrogenic differentiation of BMSCs in 3D silk fibroin-based scaffolds and evaluation of the hypoxic impact on ECM-modulating enzymes during chondrogenesis. BMSCs were cultured in chondrogenic medium for 21 days under normoxic and hypoxic conditions. (A) Safranin O staining for GAG (GAG in red, nuclei in dark blue). (B) qRT-PCR analysis of *MMP13* and *TIMP3* expression (gene expression levels of the different genes were normalized to *RPL13A* as housekeeping gene; the obtained values were further normalized to expression at day 0). Immunohistochemical staining for (C) MMP13 and (D) DIPEN (MMP13 and DIPEN in red, nuclei stained with DAPI in blue). Green arrows denote MMP13 staining, white arrows denote DIPEN staining, asterisks denote scaffolds. Scale bar 100 μm. Data represented as mean ± SD (n=3). Asterisks denote statistically significant differences between the groups (*$p<0.05$).

While the potent hypoxic actions on matrix synthesis of chondrocytes and MSCs during proliferation or differentiation are well described, the potential regulatory effects of hypoxia on matrix degradation have still to be investigated. Matrix turnover, the cleavage and rearrangement of collagen fibrils and glycosaminoglycans like aggrecan, is particularly important during chondrogenesis while the extracellular matrix matures. However, little is known about the expression and activity of matrix-modulating enzymes like MMPs and ADAMTSs and even less about the hypoxic impact on these enzymes during chondrogenic differentiation of MSCs. MMPs have been shown to be regulated during chondrogenesis, while inhibiting general MMP enzyme activity by applying broad-spectrum pan-Inhibitors prevents matrix maturation suggesting an essential role during chondrogenic differentiation of MSCs for MMPs[270]. In contrast, recently published data has shown that aggrecan cleavage mediated by ADAMTS does not play a role in chondrogenic differentiation of MSCs[271], therefore we focused on MMP mediated aggrecan digestion in this study. Only a few studies investigating other cell types like chondrocytes address the question of hypoxic effects on catabolic matrix-modulating enzymes during matrix development and maintenance. The application of a more physiological oxygen tension (5% or 1%) has been shown to reduce catabolic enzyme activity in chondrocytes resulting in decreased accumulation of type II collagen fragments and a more native hyaline cartilage-like collagen fibril organization[135,144].

Therefore, this study focused on the impact of hypoxia on matrix-modulating enzymes during chondrogenic differentiation of MSCs. Indeed, under hypoxia reduced ECM degradation caused by attenuated MMP activity was observed. This became particularly evident in the immunohistochemical staining for the MMP-generated aggrecan neoepitope DIPEN which was distinctly weaker in the hypoxic group. Quantification of DIPEN staining using histomorphometry revealed a strong decrease of aggrecan fragments (Figure 3.15 A and 3.16 A). These results were consistent with the attenuated general MMP activity detected in the generic MMP activity assay (Figure 3.14 C). Hypoxia was shown to almost halve the general MMP activity compared to normoxia on day 21.

MMPs digest aggrecan at the interglobular domain (IGD), located between the

G1 and G2 domains, which is particularly sensitive to proteinases like MMPs and ADAMTSs. These enzymes cleave at specific sites in this region, MMPs predominantly at the N341↓F342 bond which generates the C-terminal DIPEN341 and N-terminal 342FFGVG neoepitope[51]. The neoepitope DIPEN is described to be cell-associated and adjacent to the lacunae detected by immunolocalization in human and animal cartilage[272]. This was confirmed in our immunohistochemical staining during chondrogenic differentiation of MSCs, as positive DIPEN staining was cell-associated as well (Figure 3.15 A). The majority of DIPEN neoepitopes resident on G1 fragments of the aggrecan core protein derived from MMP cleavage, remain in the tissue bound to hyaluronan. Interestingly, the corresponding 342FFGVG neoepitope with the adherent keratan sulfate and chondroitin sulfate rich regions are not retained in the cartilage. Instead, they are released from cartilage, *in vivo* and *in vitro*[51]. Considering the fact that the DMMB assay only measures sulfated GAGs like chondroitin sulfate and keratan sulfate[227] it is very likely that the increased GAG content of the ECM that was seen in the DMMB assay in the hypoxic group is at least in part based on a decreased ECM breakdown as shown in reduced immunohistochemical staining for DIPEN neoepitopes. This link strengthened our initial hypothesis about the attenuating hypoxic impact on MMPs and its contribution to a higher GAG content in the ECM.

Interestingly, there was no evidence to suggest MMP-mediated collagen type II degradation as shown in immunostaining for CTX-II fragments. No differences could be found between normoxic and hypoxic conditions (Figure 3.15 B and 3.16 B); the staining intensity in general was at a very low level. This data was supported by CTX-II ELISA as CTX-II fragments could not be detected in lysed cartilaginous ECM (data not shown). These findings were, to a certain extent, unexpected, as MMPs are generally known to act on both aggrecans and collagen substrates[51], in particular MMP13, which is the collagenase with the highest affinity for collagen type II[273] and which was shown to be expressed in higher levels under normoxic conditions (Figure 3.14). Furthermore, recent studies have demonstrated a suppression of collagen type II destruction under hypoxic conditions in chondrocytes[135,144]. As possible reasons, we assume that in the

present study on the one hand the collagen type II network was still maturing and possible degenerative processes had not started yet, therefore, a detectable amount of CTX-II fragments was not accumulated. Thus, differentiation should be investigated for a longer period of time. On the other hand, the different cell types investigated in the different studies might explain the discrepancy between the contrasting results.
Altogether, the detected strongly reduced MMP-induced aggrecan cleavage and the attenuated general MMP activity clearly indicate a direct effect of reduced oxygen tension on MMP-mediated cartilaginous matrix breakdown. These findings correlate well with a recent report demonstrating that low oxygen tension can down-regulate TNF-α-mediated expression of degradative enzymes in chondrogenic pellet culture of MSCs[274]. Whether the increased GAG content in the ECM is also related to an attenuated cleavage of other substrates such as versican[275] remains to be investigated, as MMPs naturally also cleave GAGs other than aggrecan.

The investigation of specific ECM-modulating enzymes revealed different expression patterns for different genes during MSC chondrogenesis. In accordance with previously published data, *ADAMTS4* was up-regulated and *ADAMTS5* down-regulated during chondrogenic differentiation in normoxia[271], however, a consistent difference to the hypoxic group could not be detected. *MMP1* was slightly up-regulated under hypoxia at an early point of time, whereas, in contrast, *MMP3* and especially *MMP13*, which has been demonstrated to play a pivotal role in cartilage degeneration[62,276], showed a strong down-regulation under hypoxia (Figure 3.13). MMP13 protein expression was further assessed using histochemical staining (Figure 3.14) and was shown to be significantly weaker expressed under hypoxic conditions corresponding to its mRNA expression profile. Our results are consistent with recently published reports, demonstrating a down-regulation of *MMP13* expression and a decreased MMP13 concentration in cell culture supernatant in adipose-derived stromal cells and ATDC5 cells after hypoxic exposure in the context of hypoxia-induced inhibition of hypertrophic differentiation[277].
TIMP3 is considered to be the most potent endogenously produced inhibitor of

cartilage breakdown by inhibiting MMPs such as MMP13[278], and it has been indicated that MSCs can generally provide a matrix-protective microenvironment mediated via TIMP secretion[220,279]. Here, we found *TIMP3* to be significantly up-regulated under hypoxia, *TIMP1* was unaffected. Thus, taken together, the protection from cartilage destruction offered by hypoxia may be mediated, at least in part, by down-regulation of *MMP13* and *MMP3* (and other MMPs not tested in this study) and up-regulation of its endogenous inhibitor *TIMP*3.

In further experiments, it could be demonstrated that the observed hypoxic effects were independent of the 3D culture system. MSCs were cultured in 3D silk fibroin-based scaffolds which have previously been demonstrated to provide high biocompatibility and favorable mechanical characteristics, rendering them promising candidates for cartilage engineering applications[280,281]. In our study, constructs cultured under hypoxic conditions exhibited enhanced GAG content in the ECM as observed by stronger safranin O staining (Figure 3.17 A) and biochemical quantification (data not shown). Regulation of expression of the key matrix-modulating enzymes *MMP13* (down-regulated under hypoxia) and *TIMP3* (up-regulated) were very similar in silk scaffolds, as compared to pellet culture (Figure 3.17 B+C). Remarkably, also the reduced aggrecan cleavage under hypoxic conditions was confirmed, as detected by immunohistochemical staining for the neoepitope DIPEN (Figure 3.17 D), demonstrating the attenuating effects of hypoxia on MMP activity also in the larger scaffold system.

In summary, our results indicate oxygen tension to be an important cue in the development and maintenance of cartilaginous matrix as demonstrated in two models of chondrogenesis, i.e. pellet culture and 3D scaffolds. Hypoxia appears to not only promote ECM synthesis and maturation, but also to protect ECM from degradation by distinctly shifting the MMP/TIMP regulatory system towards a more matrix-protecting state, with attenuation of MMP expression and MMP-mediated aggrecan breakdown. Thus, this study contributes to the growing knowledge on the role of oxygen tension during chondrogenic differentiation of BMSCs.

3.4 TGF-β3 tethered to PMMA microspheres for chondrogenic differentiation of BMSCs in silk scaffolds

Articular cartilage defects caused by degenerative diseases are a major cause of disability in middle-aged and older people in industrialized countries and will be further increasing significantly over the next years due to obesity and the aging societies[261,282,283]. As injuries of articular cartilage are one of the most challenging issues of musculoskeletal medicine due to the poor capacity for intrinsic repair, huge efforts have been undertaken to develop alternative methods like growth factor application to restore the defect site. Traditional growth factor-based approaches for cartilage repair utilize soluble growth factor delivery which is limited for clinical applications due to high costs as a result of a short half-life[194,284] and associated undesirable side effects like osteoarthritis-like changes and the formation of osteophytes as reported for the intra-articular injection of TGF-β[285]. Therefore, a controlled delivery and localized presentation of the growth factor during tissue development or regeneration is crucial and desirable.

Immobilization of growth factors to biomaterials is an emerging field to present growth factors with improved stability and longevity to cells or the target tissue. It can prolonge growth factor availability and activity, reduce the amount of growth factor needed to gain similar biological responses compared to the delivery in its soluble form and allows a spatially restricted control of growth factor presentation[194]. In this study, TGF-β, a key mediator during chondrogenic differentiation of MSCs, has been immobilized on polymethylmethacrylate (PMMA) microspheres for a biomaterial-based approach for cartilage regeneration. The biomaterial silk fibroin was used as cell carrier, as it has gained increased attention in biomedical science in the last two decades due to its high biocompatibility and outstanding processing and mechanical properties. It has a high stability combined with impressive elasticity, but offers tunable biodegradability at the same time[207].

The combination of using chondrogenic progenitor cells like MSCs, which offer a high proliferation capacity and the ability to differentiate into chondrocytes[7,286], scaffold materials that act as support structures, and locally applied growth factors represents an attractive approach for tissue regeneration and development. Hence, in the present study, at first the general suitability of silk fibroin scaffolds for BMSC chondrogenesis was demonstrated. In a second step, the effects of TGF-β3-coupled PMMA microspheres on chondrogenesis were investigated in pellet culture. Ultimately, the potential of TGF-β3-coupled PMMA microsphere-loaded silk fibroin scaffolds that offer a locally restricted presentation of the growth factor, was investigated for chondrogenic differentiation of bone marrow-derived stromal cells towards the development of functionalized implants for cartilage defect repair.

Please note that the production of the 3D silk fibroin-based scaffolds and TGF-β3-coupled PMMA microspheres as well as the analysis of the coupling efficiency and biological activity of TGF-β3 were performed by Eva Gador. The biological evaluation of chondrogenesis in the implant upon seeding with BMSCs was content of this work but has already been published in the dissertation of Eva Gador[223].

3.4.1 SEM imaging of engineered constructs

Biphasic silk fibroin scaffolds with two porosities on a single scaffold were produced. To determine the structure and pore interconnectivity as well as cell seeding of the silk fibroin scaffold, the constructs were evaluated by SEM (Figure: 3.18). SEM imaging revealed a distinct interface between the two layers

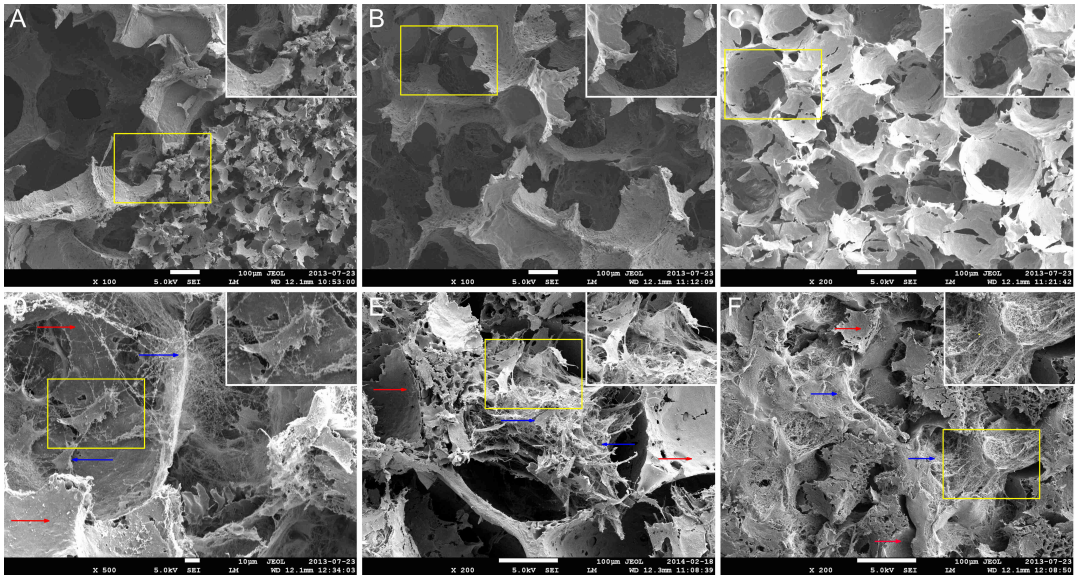

Figure 3.18: SEM images of blank and seeded silk scaffolds. (A-C) Cross sections of blank scaffolds showing (A) entire scaffold, (B) large pores (315–710 μm) and (C) small pores (100–160 μm) (D–F) Cross section images of BMSCs cultured for 21 days in chondrogenic medium on silk scaffolds. Close ups draw attention to important objects in the image: (A) Interface of the different layers, (B) large pore, (C) small pore, (D) cell attached to the scaffold surface, (E) ECM structures with moving cell, (F) pore filled with ECM. Red arrows indicate the silk scaffold, blue arrows indicate cells and ECM network. Scale bar 100 μm, except 10 μm for (D).

of the scaffold with different pore sizes (Figure 3.18 A). The diameters were shown to measure between 315–710 μm for the big pores and 100–160 μm for the small pores. The pores in each layer and the layer interface itself were observed to be interconnective (Figure 3.18 A–C). BMSC culture for 21 days in chondrogenic medium resulted in a homogeneous cell distribution. The cells attached to the scaffold and formed multiple layers of cells on the scaffold surface

(Figure 3.18 D+E) until the entire pores of the scaffold were fully filled with a dense tissue-like structure of cells and ECM (Figure 3.19 F + Figure 3.18 F).

3.4.2 Biocompatibility of silk scaffolds

In order to confirm the biocompatibility of the silk scaffolds, the constructs were analyzed by live/dead staining 4 h after seeding at day 0 and after 10 and 21 days of culture in chondrogenic medium. In fact, silk fibroin scaffolds turned

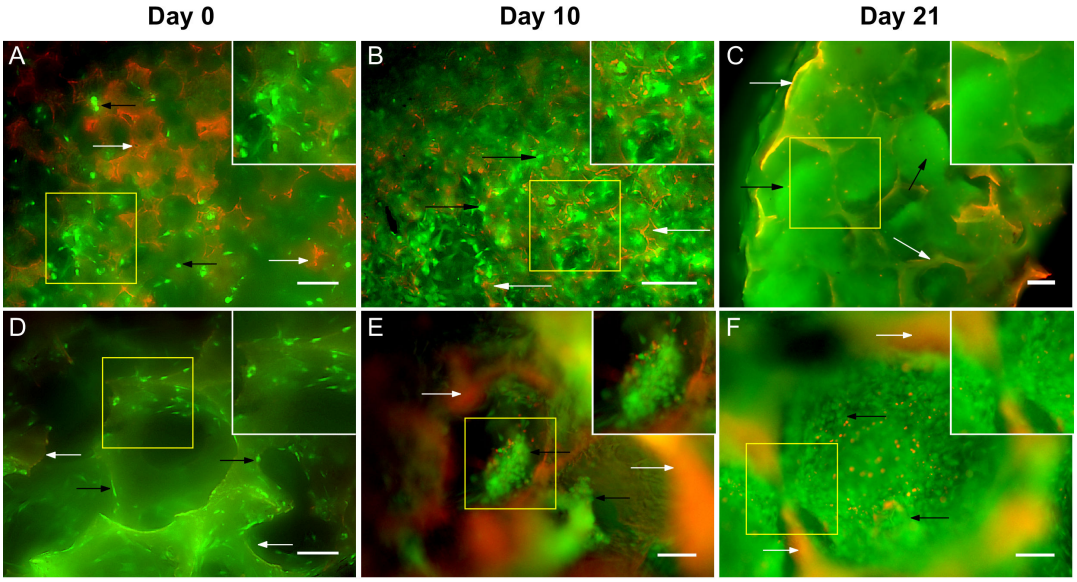

Figure 3.19: Biocompatibility test of silk scaffolds. Live/dead staining of BMSCs cultured for (A+D) 4 hours, (B+E) 10 days, and (C+F) 21 days in chondrogenic medium. Living cells are shown in green, dead cells in red, scaffolds in red–yellow interference. Close up show viable and dead cells distributed in small and large pores. (A–C) Cross section and overview of silk scaffold (4x magnification). (D–F) Cross sections of silk scaffolds at higher magnification (10x). White arrows indicate the silk scaffold, black arrows indicate cells. Scale bar 100 μm.

out to be highly biocompatible, the vast majority of cells was viable at any time (Figure 3.19). Even in the center of the scaffold only a negligible number of dead cells was detected at days 10 and 21. The cells formed small clusters after 10 days and tissue-like structures after 21 days of culture and were homogeneously distributed throughout the whole scaffold after 21 days.

3.4.3 Optimization of cell seeding

A homogeneous distribution of cells is crucial for rapid and uniform tissue regeneration in the construct. Therefore, we evaluated and improved our cell seeding technique for a high cell seeding efficiency and a spatially uniform cell distribution. It is important to note that these experiments were conducted before the pore interconnectivity of the scaffold had been finally optimized. As a consequence not all pores were filled with cells. Three different seeding methods

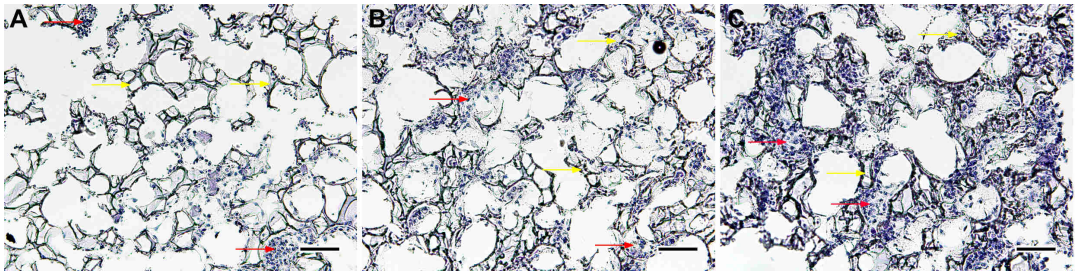

Figure 3.20: Optimization of scaffold seeding. (A) Seeding from top (unilateral). (B) Seeding from both sides (bilateral). (C) Seeding using a syringe-based method. Yellow arrows indicate the silk scaffold, red arrows indicate cells. BMSCs were cultured for 7 days in proliferation medium. Nuclei were stained with haematoxylin. Scale bar 100 μm.

(see 2.9.3) were compared whereupon histological staining demonstrated the best cell distribution for the syringe-based method (Figure 3.20 C). Consistent with these results the cell seeding efficiency (CSE) was highest for the syringe based method as well, with 86% compared to 73% and 56% for the bilateral and unilateral method, as shown by DNA analysis (Figure 3.21)

3.4.4 Chondrogenic differentiation of BMSCs in silk scaffolds

To investigate the general suitability of the silk fibroin scaffolds for chondrogenic differentiation of BMSCs, cells were cultured in chondrogenic medium in the presence or absence of TGF-β. After 10 and 21 days of culture, extracellular matrix key components of articular cartilage were detected using biochemical assays. BMSCs cultured with TGF-β displayed distinctly increased GAG and total collagen synthesis compared to the group without TGF-β (Figure 3.22).

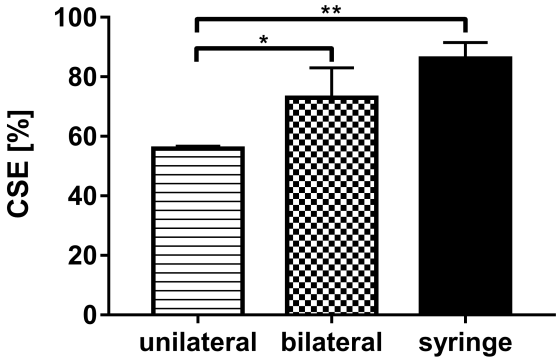

Figure 3.21: Optimization of the cell seeding efficiency. Scaffolds were seeded with BMSCs using different methods and cells were allowed to attach for 4 h in an incubator (37°C, 5% CO_2, 21% O_2). DNA content was analyzed and CSE was calculated by normalizing the sample value to the DNA value of the initial cell seeding number ($8x10^5$). Asterisks denote statistically significant differences between the groups (*p<0.05, **p<0.01).

These observations were supported by histological and immunohistochemical

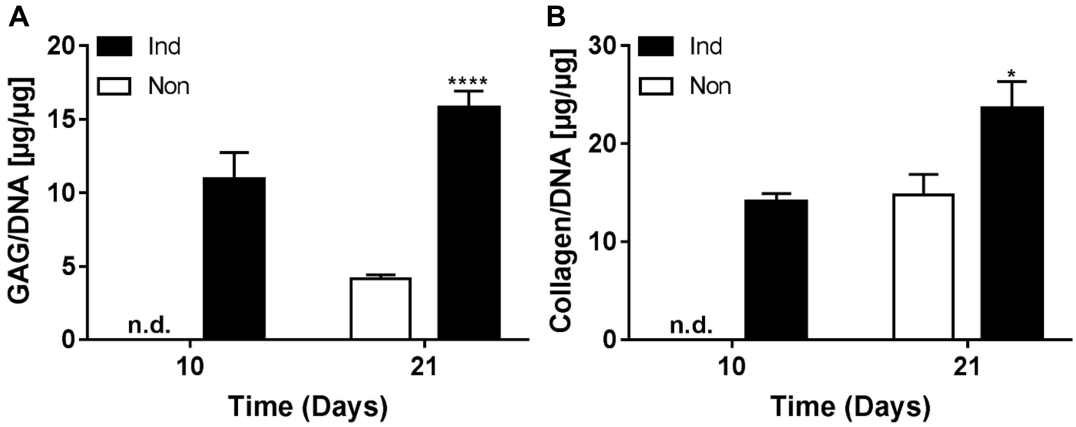

Figure 3.22: Biochemical analysis of major ECM components of BMSCs cultured in chondrogenic medium after 10 and 21 days in silk scaffolds. (A) GAG and (B) tcollagen synthesis. Data represented as mean ± SD (n=3). Asterisks denote statistically significant differences between the groups (*p<0.05, ****p<0.0001). n.d. = not determined.

staining for GAG and collagen type II (Figure 3.23). Chondrogenically induced BMSCs showed enhanced differentiation in comparison to the control group.

Furthermore, an up-regulation of specific chondrogenic marker genes *SOX9* and

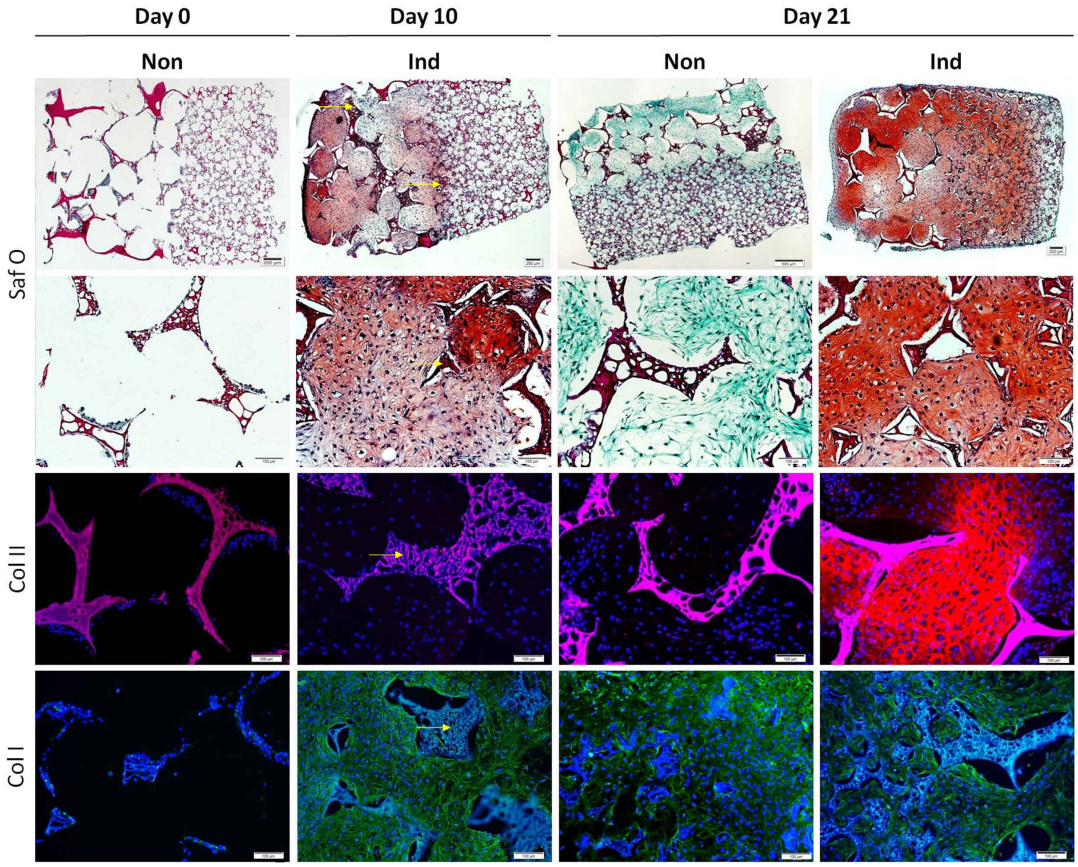

Figure 3.23: Histological and immunohistochemical evaluation of cartilaginous matrix components of BMSCs cultured in chondrogenic medium without or in the presence of TGF-β after 0, 10 and 21 days in silk scaffolds. Safranin O staining (GAG is shown in red, nuclei in dark blue) and immunohistochemical staining for collagen type II and I (the presence of collagen type II is shown in red, collagen type I in green, nuclei in blue). Yellow arrows indicate silk scaffolds.

ACAN on mRNA level could be detected in the induced group (Figure 3.24).

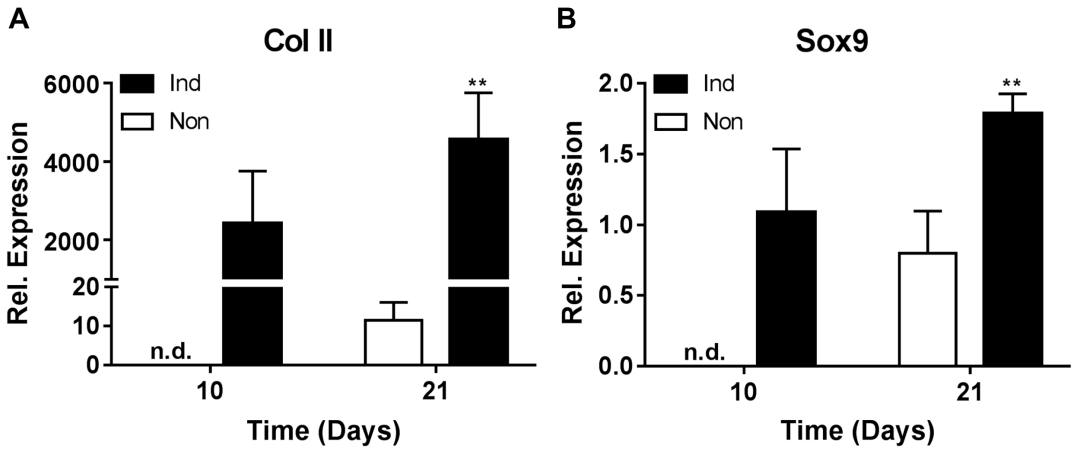

Figure 3.24: Analysis of chondrogenic gene expression using qRT-PCR of BMSCs cultured for 21 days in chondrogenic medium in the presence or absence of TGF-β in silk scaffolds. Gene expression levels of the different genes were normalized to *GAPDH* as housekeeping gene; the obtained values were further normalized to expression at day 0. Data represented as mean ± SD (n=3). Asterisks denote statistically significant differences between the groups (**p<0.01). n.d. = not determined.

3.4.5 TGF-β3-coupled PMMA microspheres induce chondrogenic differentiation of BMSCs in silk scaffolds

Stimulating effects of TGF-β3-coupled PMMA microspheres on BMSCs in pellet culture

In preliminary tests to prove the general suitability of functionalized PMMA microspheres to support chondrogenesis of BMSCs, BMSCs were cultured in chondrogenic medium with the addition of TGF-β3 functionalized PMMA microspheres in pellet culture. To investigate the chondrogenically stimulating effects of TGF-β3-tethered PMMA microspheres, major cartilaginous matrix components were analyzed by histological and immunohistochemical staining and biochemical assays. After 21 days of culture, BMSCs cultured with functionalized microspheres showed distinctly stronger staining for proteoglycans and collagen type II in histological and immunohistochemical analysis (Figure 3.25). Superior chondrogenesis of BMSCs cultured with TGF-β3-coupled microspheres was additionally demonstrated by quantitative biochemical analysis showing enhanced GAG and total collagen synthesis (Figure 3.26 A+B). As a result of increased ECM production and proliferation (data not shown) BMSC pellets cultured with TGF-β3-coupled microspheres were larger in size compared to BMSCs cultured with blank microspheres (Figure 3.25).

Chondrogenesis of BMSCs in TGF-β3-coupled PMMA microsphere-loaded silk scaffolds

To demonstrate the chondrogenic potential of the TGF-β3-coupled PMMA microspheres in a cartilage engineering relevant context, 3D silk fibroin-based scaffolds were loaded with BMSCs and TGF-β3 functionalized microspheres (coupled), microspheres without TGF-β3 (blank) or microspheres with TGF-β3 adsorbed to the microsphere surface (adsorbed) and were cultured for 21 days in chondrogenic medium. As seen in the preliminary tests in pellet culture, immunohistochemical staining showed a distinctly stronger staining for major cartilaginous collagen, collagen type II, and GAG in the ECM of BMSCs cultured in the presence of TGF-β3-coupled PMMA microspheres in comparison to the blank and adsorbed group, while staining for the fibrocartilage marker

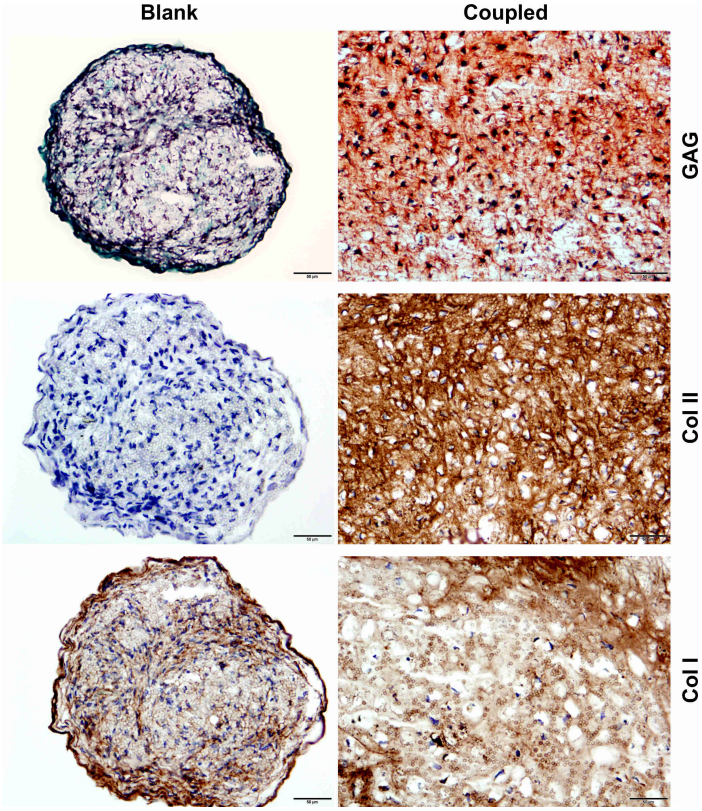

Figure 3.25: Histological and immunohistochemical analysis of cartilaginous matrix components of BMSCs cultured in chondrogenic medium with PMMA microspheres for 21 days. PMMA microspheres were used as blank microspheres (non-treated microspheres) or were tethered with TGF-β3 (18 ng TGF-β3 covalently coupled to microspheres). Safranin O staining (GAG is shown in red, nuclei in dark blue) and immunohistochemical staining for collagen type II and I (collagen type II and I were stained in brown, nuclei were stained with haematoxylin in blue-violet). Scale bar 50 μm.

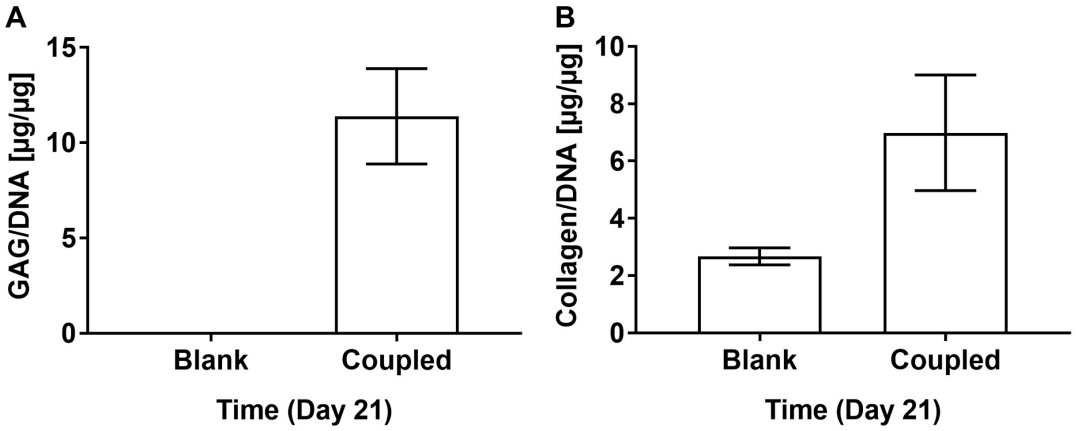

Figure 3.26: Biochemical analysis of major ECM components of BMSCs cultured in chondrogenic medium with PMMA microspheres in pellet culture after 21 days. PMMA microspheres were used as blank microspheres (non-treated microspheres) or were tethered with TGF-β3 (18 ng TGF-β3 covalently coupled to microspheres) to support chondrogenic differentiation. (A) GAG and (B) total collagen synthesis (n=2).

collagen type I was weaker in the coupled group in comparison to the adsorbed group (Figure 3.27). Enhanced GAG deposition was further analyzed using quantitative biochemical analysis confirming increased GAG synthesis when BMSCs were cultured with TGF-β3-coupled PMMA microspheres in silk scaffolds in comparison to BMSCs cultured in the presence of non-functionalized PMMA microspheres (Figure 3.28 A). Furthermore, TGF-β3-coupled PMMA microspheres significantly increased total collagen production compared to the blank group (Figure 3.28 B). Surprisingly, the adsorbed and coupled group showed similar GAG and total collagen production.

Gene expression analysis of chondrogenic marker genes

Gene expression analysis of chondrogenic marker genes was performed on day 21 using qRT-PCR (Figure 3.29). Expression of the chondrogenic master regulator *SOX9* was strongly increased when BMSCs were cultured with TGF-β3-functionalized microspheres, with an 16-fold increase as compared to the non-functionalized group and a 3-fold increase in comparison to the adsorbed group. Together with *SOX9*, the chondrogenic marker genes *COL2A* and *ACAN*

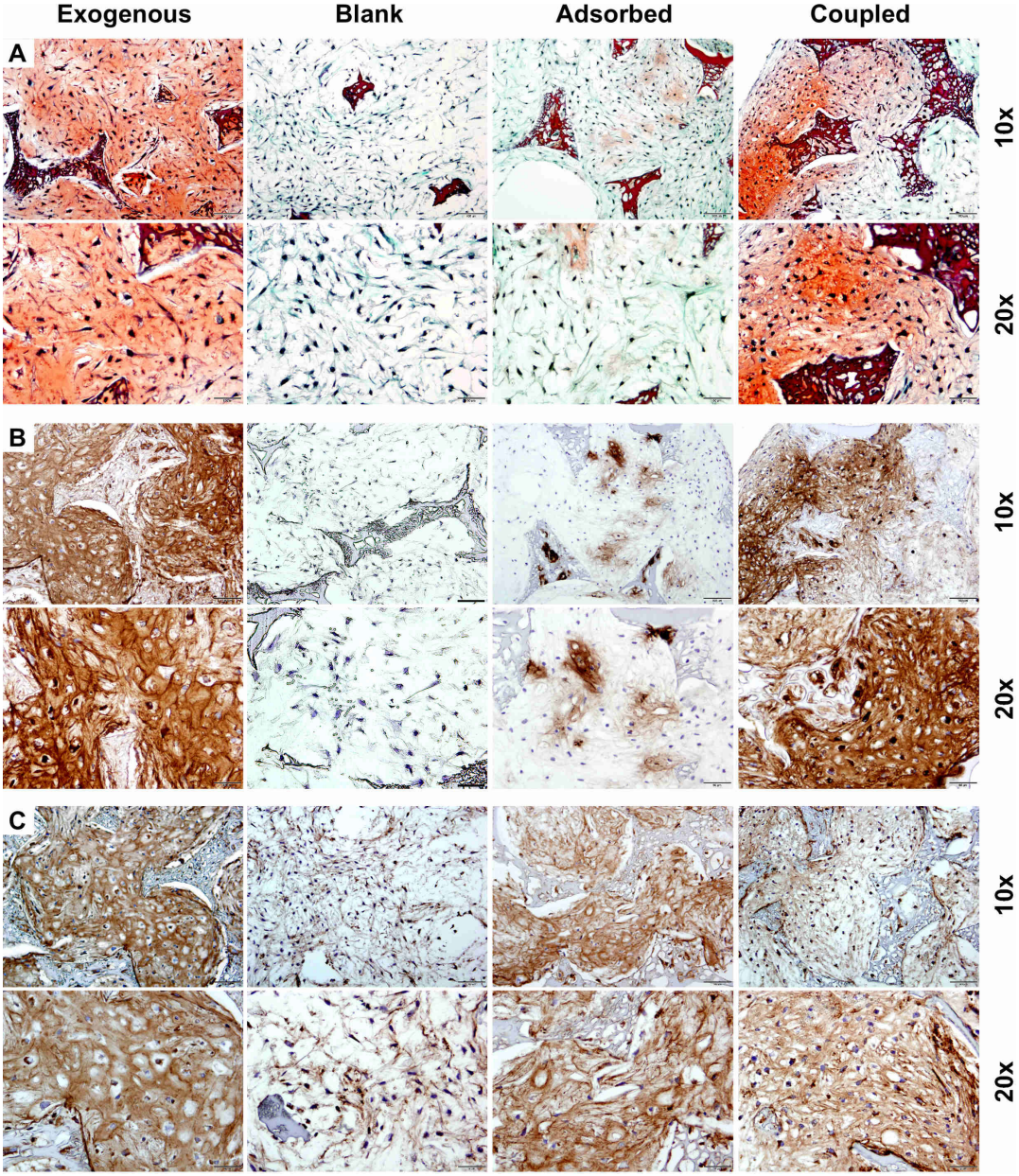

Figure 3.27: Histological and immunohistochemical evaluation of cartilaginous matrix components of BMSCs cultured in chondrogenic medium with PMMA microsphere-loaded silk scaffolds for 21 days. Blank (non-treated microspheres), adsorbed (13 ng TGF-β3 adsorbed to the PMMA surface) and coupled (78 ng TGF-β3 covalently coupled to microspheres) microspheres were evaluated for its chondrogenic potential. Exogenously delivered TGF-β3 (medium supplemented with 10 ng TGF-β3, 8 changes, 90 ng in total) served as standard positive control. (A) Safranin O staining (GAG is shown in red, nuclei in dark blue) and immunohistochemical staining for (B) collagen type II and (C) collagen type I (in brown, nuclei were stained with haematoxylin in blue-violet).

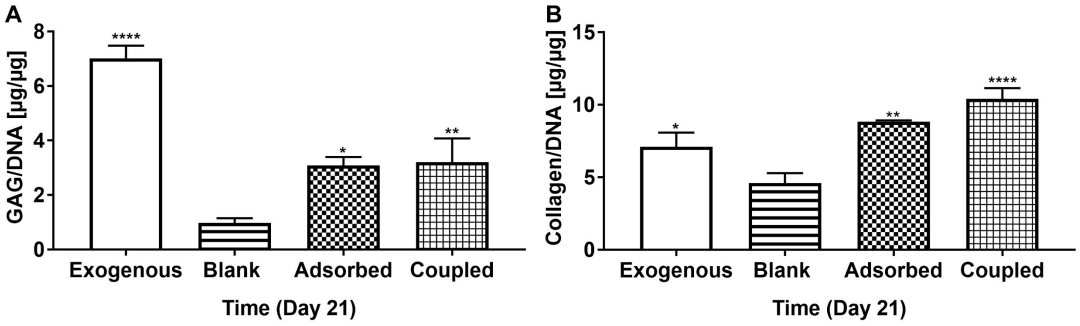

Figure 3.28: Biochemical analysis of GAG and total collagen amount of cartilaginous ECM of BMSCs cultured in chondrogenic medium with PMMA microspheres in silk scaffolds after 21 days. Blank (non-treated PMMA microspheres), adsorbed (PMMA microspheres with 13 ng TGF-β3 adsorbed to the PMMA surface) and coupled (PMMA microspheres covalently coupled with 78 ng TGF-β3) microspheres were evaluated for its potential to induce chondrogenesis of BMSCs. Exogenously delivered TGF-β3 (medium supplemented with 10 ng TGF-β3, 8 changes, 90 ng in total) served as standard positive control. (A) GAG and (B) total collagen synthesis. Data represented as mean ± SD (n=3). Asterisks denote statistically significant differences between the groups referring to to the blank (*$p<0.05$, **$p<0.01$, ****$p<0.001$).

also showed a distinctly higher expression, with 1940-fold and 19-fold increase upon exposure to the TGF-β3-coupled PMMA microspheres in comparison to the blank group, respectively, and a 14-fold and 6-fold increase compared to the adsorbed group, respectively. No differences could be detected between TGF-β3-coupled, blank and adsorbed microspheres for collagen type I and X gene expression.

3.4.6 Discussion

The lack of efficient treatment options for cartilage defects has accelerated research on cartilage engineering approaches combining chondrogenic progenitor cells, biomaterials and growth factors. However, the localized presentation of growth factors still represents a challenging task.
Therefore, this study aims to investigate the potential of TGF-β3-functionalized PMMA microspheres in combination with silk fibroin scaffolds to stimulate chondrogenic differentiation of BMSCs in particle loaded constructs.

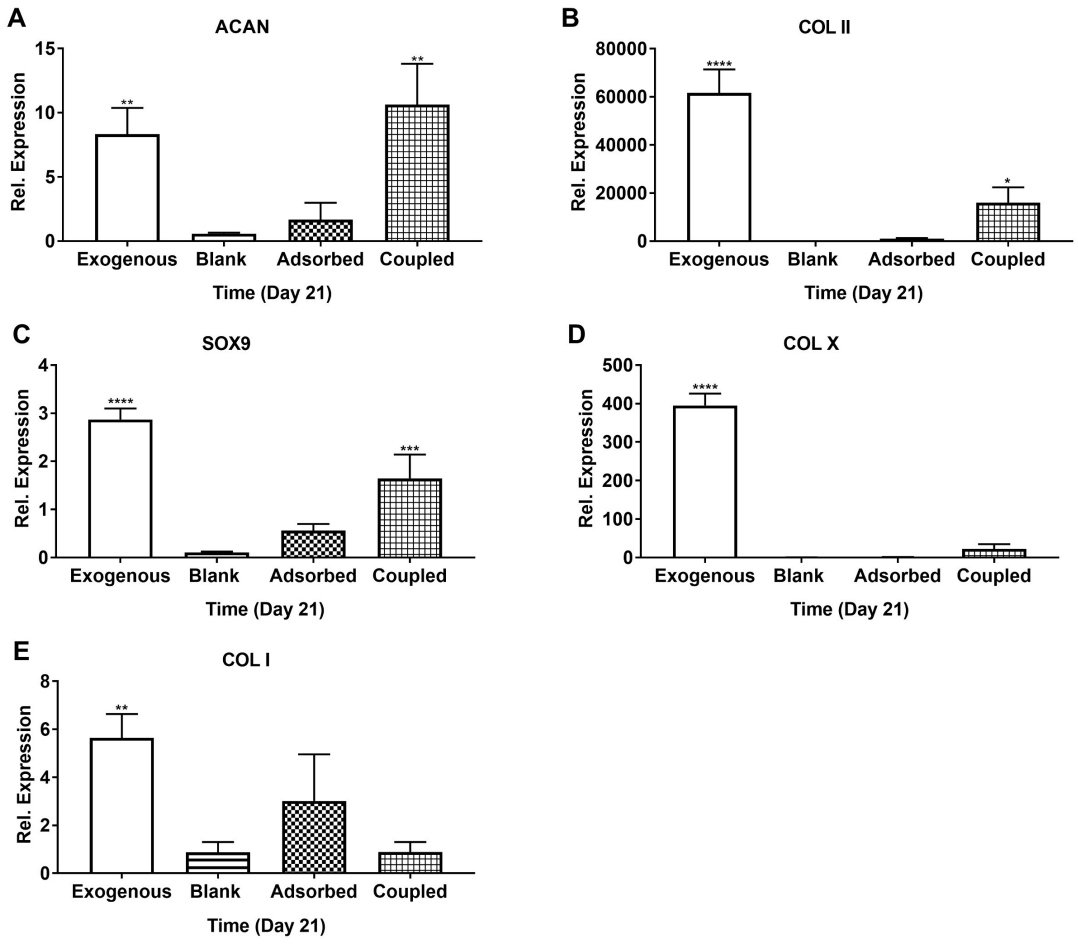

Figure 3.29: Examination of chondrogenic marker gene expression of BMSCs in PMMA microsphere loaded silk scaffolds cultured for 21 days in chondrogenic medium using qRT-PCR. Blank (non-treated PMMA microspheres), adsorbed (PMMA microspheres with 13 ng TGF-β3 adsorbed to the PMMA surface) and coupled (PMMA microspheres covalently coupled with 78 ng TGF-β3) microspheres were evaluated for its potential to induce chondrogenesis of BMSCs. Exogenously delivered TGF-β3 (medium supplemented with 10 ng TGF-β3, 8 changes, 90 ng in total) served as standard positive control. Gene expression levels of the different genes were normalized to *RPL13A* as housekeeping gene; the obtained values were further normalized to expression at day 0. Data represented as mean ± SD (n=3). Asterisks denote statistically significant differences between the groups referring to the blank as control group (*$p<0.05$, **$p<0.01$, ***$p<0.01$, ****$p<0.01$).

The newly developed 3D silk fibroin-based scaffolds were seeded with BMSCs using an optimized syringe-based method leading to a cell seeding efficiency of 86% compared to 60-75% from a recent report[287] and a homogeneous cell distribution (Figure 3.20 + 3.18). Pore interconnectivity of the scaffold was confirmed by SEM imaging (Figure 3.18). Consistent with former studies[281,288], the constructs elicited high biocompatibility as demonstrated in live/dead staining (Figure 3.19). Silk scaffolds provide a robust network with favorable mechanical characteristics and act as a support structure to enhance stability of engineered cartilage tissue[280,281]. The general suitability for chondrogenic differentiation of BMSCs of the newly designed silk scaffolds was proven in preliminary studies by culturing BMSC seeded constructs in chondrogenic medium supplemented with exogenous TGF-β (Figure 3.22 + Figure 3.23 + Figure 3.24). TGF-β is known to be a key component in cartilage development with TGF-β3 having the highest chondrogenic potential of all three isoforms[163]. It plays a central role in all stages of chondrogenesis from MSCs to chondroblasts and further to chondrocytes, including condensation, proliferation, ECM synthesis and differentiation[88,152–154]. Therefore, TGF-β3 represents an attractive candidate for cartilage defect regeneration. However, the clinical application of TGF-β still remains a critical step, as on the one hand growth factors in general display a short half-life, and on the other hand several studies reported severe side effects such as chondro-osteophyte formation, loss of proteoglycans and inflammatory joint diseases after intra-articular injection of TGF-β[285,289,290]. Hence, a local administration appears preferable[291].

In our study, we successfully applied TGF-β3-coupled PMMA microspheres in combination with the three-dimensional silk scaffold to induce chondrogenic differentiation of BMSCs for the development of artificial cartilage tissue. Remarkably, TGF-β3-coupled PMMA microsphere-loaded constructs significantly enhanced chondrogenesis and articular cartilage matrix development.
Safranin O staining for GAG (Figure 3.27 A) revealed substantially increased accumulation of proteoglycans in the ECM in comparison to BMSCs cultured in the presence of blank and adsorbed microspheres. This was well in agreement

with a recently published report for chondrogenesis using TGF-β functionalized magnetic beads[292] in pellets. Immunohistochemical staining for collagen type II (Figure 3.27 B) was distinctly enhanced when BMSCs were exposed to TGF-β3-tethered PMMA microspheres compared to BMSCs exposed to non-functionalized and adsorbed microspheres.
In consistency with the histological and immunohistochemical data for major cartilaginous matrix components, expression levels of the chondrogenic marker genes *COL2A* and *ACAN* were significantly up-regulated after 21 days when BMSCs were cultured on constructs loaded with TGF-β3 coupled microspheres compared to constructs loaded with blank and adsorbed microspheres as demonstrated in qRT-PCR analysis (Figure 3.29). Furthermore, elevated levels of the chondrogenic master regulator *SOX9*, an important factor for chondrocyte differentiation that facilitates the expression of collagen type II[293], confirmed the suitability of TGF-β3-functionalized PMMA microspheres to induce chondrogenesis on the molecular level.

The exact mechanism of action of TGF-β covalently coupled to biomaterial surfaces still remains poorly understood. TGF-β signals are transduced by binding to a heteromeric complex of type I and II receptors with serine/threonine kinase domains that interact with each other causing type I receptor phosphorylation and activation[164]. The activated receptor phosphorylates receptor-associated Smads (Smad2 and Smad3) which bind to Smad4, translocate to the nucleus and regulate target gene transcription[165,166]. We were able to prove TGF-β3 bioactivity after coupling in a SMAD reporter gene assay (data not shown) confirming TGF-β3-tethered PMMA microspheres to act via Smad-protein signaling pathways. Alternative TGF-β-mediated pathways to regulate chondrogenesis include the ERK and MAPK signaling pathway[167,168]. Interestingly, the chondrogenic potential of TGF-β3-coupled PMMA microspheres was similar to exogenously delivered TGF-β3 even though the functionalized microspheres (78 ng/mL TGF-β3) were added only once at the beginning to the BMSCs while the exogenously delivered TGF-β3 was added with every medium change (90 ng in total). The chondroinductive effect of TGF-β3-coupled PMMA microspheres was probably due to the extended activation of the TGF-β signaling pathways.

In general, growth factors interact with its receptor on the cell surface to form a complex which aggregates before it is internalized. The effect of growth factor binding can be attenuated by endocytosis of the receptor–ligand complex with subsequent degradation[294]. We assume that the complex of immobilized TGF-β3 and TGF-receptor cannot be internalized resulting in a persistent activation of the TGF-β signaling pathways. Another aspect to perpetuate the signaling cascade may be that by preventing the lateral diffusion of activated receptors in the cell membrane, immobilized TGF-β reduces the chance that the activated receptor encounters inhibitory regulators such as tyrosine phosphatases or serine/threonine kinases[295].
A number of signal pathways are activated via integrin-ECM/adhesion protein interaction. The underlying processes which are called "juxtacrine signaling"[296] do not induce integrin internalization, providing evidence that signal transduction does not necessarily requires ligand internalization[295,297,298]. Hence, we assume that TGF-β3-coupled PMMA microsphere binding to the TGF-receptor mimics juxtacrine stimulation of membrane-anchored growth factors, a process termed "artificial juxtacrine stimulation"[299], resulting in sustained chondrogenesis. Artificial juxtacrine stimulation has also been reported in studies using other immobilized growth factors, e.g. EGF for cell proliferation of Chinese hamster ovary cells[299,300] or recombinant human BMP-2 for bone formation[301].

In summary, our study demonstrates the potential of TGF-β3-coupled PMMA microspheres combined with silk fibroin scaffolds and BMSCs to engineer cartilage tissue constructs. In a clinical setting, the combination of silk scaffolds and PMMA microspheres loaded with biological cues such as TGF-β3 together with current treatment options for articular cartilage lesions, e.g. microfracture, represents an attractive approach to improve the clinical outcome for cartilage defect repair. Moreover, since this study can be regarded as a proof-of-principle study valued at cartilage tissue, functionalized PMMA microsphere loaded constructs offer the potential to serve as a versatile toolbox providing controlled delivery and spatially restricted presentation of growth factors for further diverse tissue engineering applications, e.g. bone reconstruction.

Chapter 4

Summary and Conclusion

Articular cartilage lesions that occur upon intensive sport, trauma or degenerative disease represent a severe therapeutic problem. At present, osteoarthritis is the most common joint disease worldwide, affecting around 10% of men and 18% of women over 60 years of age[302]. The poor self-regeneration capacity of cartilage and the lack of efficient therapeutic treatment options to regenerate durable articular cartilage tissue, provide the rationale for the development of new treatment options based on cartilage tissue engineering approaches[281]. The integrated use of cells, biomaterials and growth factors to guide tissue development has the potential to provide functional substitutes of lost or damaged tissues[2,3]. For the regeneration of cartilage, the availability of mesenchymal stromal cells (MSCs) or their recruitment into the defect site is fundamental[281]. Due to their high proliferation capacity, the possibility to differentiate into chondrocytes and their potential to attract other progenitor cells into the defect site, bone marrow-derived mesenchymal stromal cells (BMSCs) are still regarded as an attractive cell source for cartilage tissue engineering[80]. However, in order to successfully engineer cartilage tissue, a better understanding of basic principles of developmental processes and microenvironmental cues that guide chondrogenesis is required.

Therefore, in this work we studied the influence of one of the key components in cartilage development, the growth factor IGF-I,[176] on chondrogenic differentiation of bone marrow-derived stromal cells in the presence of TGF-β. We further investigated the chondroinductive effects of the truncated IGF-I analogue Des(1-3)IGF-I (desIGF) and analyzed the influence of IGF-binding proteins (IGFBPs) on IGF-I action and bioavailability. IGF-I was shown to induce chondrogenic differentiation of BMSCs in a dose-dependent manner. Biochemical analysis and histological and immunohistochemical staining for major cartilaginous matrix components revealed enhanced glycosaminoglycan (GAG) and collagen type II deposition in the extracellular matrix (ECM) with increasing concentrations of IGF-I, while unexpectedly high doses of 100 ng/mL IGF-I or even more were necessary to induce chondrogenesis. The growth factor desIGF is able to activate the IGF-IR and binds it with the same affinity as IGF-I, but its affinity for IGFBP is approximately 100 times reduced[183,244]. DesIGF turned out to be significantly

more potent and revealed superior chondrogenesis compared to IGF-I as demonstrated in histological and immunohistochemical staining, biochemical analysis and qRT-PCR. The application of the IGFBP inhibitor NBI-31772, a small molecule inhibitor that binds to IGFBPs and prevents IGF-I binding to IGFBPs or disrupts IGF-I/IGFBP interactions, increased proteoglycan synthesis in the presence of IGF-I in a dose-dependent manner as demonstrated in biochemical assay and histological staining, while desIGF-induced chondrogenesis was not affected. NBI-31772 appeared to partially rescue IGF-I chondroinductive action by displacing IGF-I from the IGF-I/IGFBP complex or by preventing IGF-I from IGFBP binding resulting in an effective counteraction of the IGFBP-induced reduction of IGF-I bioavailability.
In conclusion, using the truncated IGF-I analogue desIGF and the IGFBP inhibitor NBI-31772, it was demonstrated that high doses of IGF-I were necessary to induce chondrogenic differentiation of BMSCs due to an IGFBP induced reduction of IGF-I action and bioavailability. Our findings underline the importance of IGF-I in the development of articular cartilage matrix and highlight the central role of the IGF-I/IGFBP axis for IGF-I mediated chondrogenic differentiation of BMSCs (**Chapter 3.1**).

The ability of stem cells to differentiate along one lineage or another is, beside others, dependent on external cues[219]. One crucial external cue in stem cell fate is oxygen tension[220]. To analyse the impact of low oxygen tension on IGF-I mediated chondrogenic differentiation of BMSCs, BMSCs were exposed to hypoxic conditions (2%) during chondrogenic induction. IGF-I increased GAG and collagen production in chondrogenically differentiating BMSCs in a dose-dependent manner under hypoxic conditions as well. BMSCs cultured under low oxygen tension further displayed enhanced chondrogenesis compared to normoxic conditions as demonstrated by biochemical assays and histological and immunohistochemical staining for major cartilaginous matrix components GAG and collagen type II. Moreover, immunohistochemical staining and histomorphometric analysis indicated that low oxygen tension shifts the collagen type II to collagen type I (Col II/Col I) ratio towards a more collagen type II producing state for low IGF-I doses (**Chapter 3.2**).

Having shown that hypoxic conditions fostered cartilaginous matrix synthesis, consecutive work focused, for the first time, on hypoxic effects on degradation processes of the ECM during chondrogenic differentiation of BMSCs in pellet culture and silk fibroin scaffolds. Articular cartilage matrix is a dynamic structure that constantly undergoes remodeling processes to control tissue homeostasis[9,32]. These remodeling processes for matrix homeostasis are regulated by a careful balance between matrix synthesis, secretion, modification and enzymatic degradation[33], while especially cleavage of ECM components is the main process during ECM remodeling that regulates ECM composition and structure[35]. ECM-modulating enzymes and ECM development were investigated on molecular and protein levels. Additionally, MMP enzyme activity was monitored by general MMP activity assay and by immunohistochemical staining for the formation of specific MMP-mediated ECM-degradation products. BMSCs cultured in a hypoxic environment exhibited improved chondrogenesis with increased proteoglycan and collagen content in pellets and 3D silk fibroin-based scaffolds. Using qRT-PCR, different MMP expression patterns could be observed in both systems after exposure to hypoxic conditions as compared to normoxic conditions. Gene expression of the prominent cartilage-degrading enzyme *MMP13* was significantly reduced under hypoxia, whereas gene expression of *TIMP3*, the most prominently produced inhibitor of cartilage degradation, was significantly increased. Reduced expression of MMP13 was further confirmed on the protein level using immunohistochemistry. Remarkably, the MMP-generated aggrecan-neoepitope DIPEN was also distinctly reduced under hypoxic conditions as shown by immunohistochemical staining and histomorphometric quantification. This observation was further supported by reduced general MMP activity under hypoxia (**Chapter 3.3**).
The results of **Chapter 3.2 and 3.3** indicate oxygen tension to be an important cue in the development and maintenance of cartilaginous matrix as demonstrated in two independent cell culture models for chondrogenesis. Hypoxia appears not only to support ECM synthesis and maturation, but also to protect cartilaginous ECM from degradation contributing to higher proteoglycan content in the ECM.

While the previous chapters dealt with the analysis of critical factors that regu-

late chondrogenic cell fate and cartilaginous matrix development, the last chapter focused on the evaluation of a functionalized cartilage implant based on silk fibroin (**Chapter 3.4**). Current clinical therapies are unfortunately inadequate to completely regenerate the native hyaline cartilage structure[303]. Many topical tissue engineering approaches utilize soluble growth factor delivery which is limited in clinical applications due to the short growth factor half life and severe side effects[194,221]. Therefore, in a collaborative project with the research group of Prof. Dr. Dr. Lorenz Meinel at the Department of Pharmaceutical Technology and Biopharmacy of Würzburg University, a new platform combining TGF-β3-coupled polymethylmethacrylate (PMMA) microspheres with silk fibroin scaffolds was developed that provided a locally restricted presentation of the growth factor for the chondrogenic differentiation of BMSCs for cartilage defect repair. The developed 3D silk fibroin-based scaffold that acted as support structure and enhanced the mechanical strength of the engineered constructs, turned out to be interconnective and highly biocompatible, as indicated in SEM imaging and live/dead-staining. A homogeneous cell distribution in the construct was gained using a syringe-based seeding method allowing a coherent tissue formation. Chondrogenesis of BMSCs in functionalized constructs was evaluated using histology, immunohistochemistry, biochemical assays and qRT-PCR. BMSCs exposed to TGF-β3-coupled microspheres displayed enhanced chondrogenesis and cartilage matrix development compared to non-functionalized microspheres as indicated by stronger staining for GAG and collagen type II. These findings were confirmed by increased gene expression of chondrogenic marker genes *ACAN*, *COL2A* and *SOX9*. The combination of 3D silk fibroin-based scaffolds, TGF-β3-coupled microspheres and BMSCs was thereby shown suitable for the generation of cartilage tissue constructs and, combined with current treatment options, such as microfracture, may improve the clinical outcome of cartilage defect repair. Considering our study as a proof-of-principle valued at cartilage tissue, the functionalized PMMA microsphere-loaded constructs offer the potential to serve as a versatile platform providing controlled delivery and spatially restricted presentation of growth factors for further tissue engineering applications.

With the comprehensive investigation of two key factors that regulate chondro-

genic cell fate, IGF-I and oxygen tension, and the development of a functionalized artificial 3D cartilaginous tissue construct, this thesis contributes to a better understanding of the development and maintenance of articular cartilage matrix during chondrogenic differentiation of BMSCs. Moreover, the presented findings open up new opportunities towards the development of optimized clinically applicable tissue-engineered cartilaginous constructs.

Zusammenfassung und Schlussfolgerung

Verletzungen des Gelenkknorpels, die durch intensiven Sport, Trauma oder degenerative Krankheiten induziert wurden, stellen ein großes therapeutisches Problem dar. Heutzutage ist Arthrose die weltweit häufigste Gelenkerkrankung, die etwa 10% der männlichen und 18% der weiblichen Bevölkerung über 60 Jahre betrifft[302]. Die geringe intrinsische Heilungskapazität von Knorpelgewebe und das Fehlen effizienter Behandlungsmethoden, um dauerhaften Gelenkknorpel zu erzeugen, bilden die Grundlage für die Entwicklung neuartiger Behandlungsmethoden auf Basis des Tissue Engineering[281]. Hierbei verfügt speziell der integrierte Einsatz von Zellen, Biomaterialien und Wachstumsfaktoren über das Potential zerstörtes oder geschädigtes Gewebe zu ersetzen bzw. die Regeneration von neuem Gewebe zu fördern[2,3]. Für die Regeneration von Knorpelgewebe ist vor allem die Verfügbarkeit von mesenchymalen Stammzellen (MSC) und deren Rekrutierung in die Defektzone von großer Bedeutung[281]. Aufgrund ihrer hohen Proliferationsrate, der Fähigkeit in Chondrozyten zu differenzieren und des Potentials andere Vorläuferzellen in die Defektzone zu rekrutieren bilden MSCs auch heute noch einen attraktive Ansatz im Knorpel-Tissue Engineering[80].
Eine wichtige Voraussetzung für die erfolgreiche Entwicklung von Knorpelgewebe ist jedoch ein besseres Verständnis der grundlegenden Entwicklungsprozesse und der Einflussfaktoren der Mikroumgebung, die die Chondrogenese regulieren.

Aus diesem Grund wurde in dieser Arbeit eine der Schlüsselkomponenten in der Entwicklung von Knorpelgewebe, der Wachstumsfaktor IGF-I[176], hinsichtlich seines Einflusses auf die chondrogene Differenzierung von mesenchymalen Stammzellen aus dem Knochenmark (BMSC) in der Gegenwart von TGF-β untersucht. Des Weiteren wurden die chondro-induktiven Effekte des verkürzten IGF-I-Analogons Des(1-3)IGF-I (desIGF) und der Einfluss von IGF-Bindeproteinen (IGFBP) auf die Wirksamkeit und Bioverfügbarkeit von IGF-I untersucht. Es zeigte sich, dass IGF-I die chondrogene Differenzierung von BMSCs dosisabhänging induziert. In biochemischen Analysen und histologischen und immunhistochemischen Färbungen wurde deutlich, dass der Glykosaminoglykan- (GAG) und Kollagen II-Gehalt der extrazellulären Matrix (EZM) mit steigender

IGF-I Konzentration zunimmt, wobei unerwartet hohe Dosen von 100 ng/mL IGF-I und mehr für die Induktion der Chondrogenese notwendig waren. Der Wachstumsfaktor desIGF bindet und aktiviert den IGF-I-Rezeptor (IGF-IR) mit der gleichen Affinität wie das Wild-Typ IGF-I, seine Affinität für IGFBP ist aber ungefähr 100-fach reduziert[183,244]. DesIGF war deutlich potenter als IGF-I und induzierte eine deutlich verbesserte chondrogene Differenzierung der BMSC, was anhand histologischer und immunhistochemischer Färbungen, biochemischer Analysen und mittels qRT-PCR nachgewiesen wurde. Durch Applikation des IGFBP-Inhibitors NBI-31772, einem niedermolekularen Inhibitor der die IGF-I/ IGFBP Interaktion verhindert bzw. auflöst, konnte die Proteoglykansynthese NBI-31772-dosisabhängig erhöht werden. Es scheint, als führe die Zugabe von NBI-31772 zu einer Antagonisierung der IGFBP-induzierten Inhibition der IGF-I abhängigen GAG-Synthese, wobei der Inhibitor entweder IGF-I aus dem IGF-I/IGFBP-Komplex freisetzt oder die Bindung von IGF-I durch IGFBP verhindert.
Mit Hilfe des IGFBP Inhibitors NBI-31772 und des IGF-I-Analogons desIGF konnte dargelegt werden, dass hohe IGF-I Dosen zur Induktion der chondrogenen Differenzierung von BMSCs aufgrund einer IGFBP induzierten Reduktion der Wirksamkeit und Bioverfügbarkeit von IGF-I benötigt werden. Die dargestellten Ergebnisse bekräftigen die große Bedeutung von IGF-I in der Entwicklung der Knorpelmatrix und heben die zentrale Rolle der IGF-I/IGFBP Achse in der IGF-I vermittelten chondrogenen Differenzierung von BMSCs hervor (**Kapitel 3.1**).

Die Fähigkeit von Stammzellen in die unterschiedlichen Zelllinien zu differenzieren ist unter anderem von der Mikroumgebung abhängig[219]. Ein Haupteinflussfaktor hierbei ist der Sauerstoffpartialdruck[220]. Um den Einfluss von niedrigem Sauerstoffpartialdruck auf die IGF-I-vermittelte chondrogene Differenzierung von BMSCs zu untersuchen, wurden die BMSCs während der chondrogenen Induktion hypoxischen Bedingungen (2%) ausgesetzt. Dabei zeigte sich, dass IGF-I auch unter hypoxischen Bedingungen die GAG- und Kollagensynthese dosisabhängig steigert. Des Weiteren wiesen BMSCs, die während der Kultivierungsphase einem niedrigen Sauerstoffpartialdruck ausgesetzt wurden, eine

verstärkte Chondrogenese aus im Vergleich zu BMSCs, die unter Normoxie-Bedingungen kultiviert wurden. Dies wurde in biochemischen Analysen und histologischen und immunhistochemischen Untersuchungen bezüglich der Hauptbestandteile der Knorpelmatrix, GAG und Kollagen II, deutlich. Sowohl die immunhistochemischen als auch die histomorphometrischen Untersuchungen legten zusätzlich den Schluss nahe, dass sich unter niedrigem Sauerstoffpartialdruck das Verhältnis von Kollagen II zu Kollagen I bei niedrigen IGF-I Konzentrationen vermehrt in Richtung Kollagen II-Produktion verlagert und es zu einer geringeren Expression des Bindegewebsknorpelmarkers Kollagen I kommt (**Kapitel 3.2**).

Nachdem nachgewiesen wurde, dass hypoxische Bedingungen die Knorpelmatrixsynthese unterstützen, lag der Fokus der nachfolgenden Arbeiten erstmalig überhaupt auf Extrazellulärmatrix-abbauenden Prozessen während der chondrogenen Differenzierung von BMSCs in Pelletkultur und Seidenfibroin-Implantaten. Die Knorpelmatrix ist eine dynamische Struktur, die, um die Homöostase des Knorpelgewebes zu kontrollieren und zu gewährleisten, ständigen Umbauprozessen unterworfen ist[9,32]. Die Umbauprozesse für die Matrix-Homöostase werden durch eine sorgfältige Balance aus Matrixsynthese, -sekretion, -modifikation und enzymatischer Degradation reguliert[33], wobei hauptsächlich die Spaltung der EZM-Komponenten den Prozess des EZM-Umbaus ausmachen, der die Zusammensetzung und Struktur der EZM kontrolliert[35]. Um die Abbauprozesse näher zu untersuchen, wurden EZM-modulierende Enzyme und die EZM-Entwicklung auf molekularer und Proteinebene charakterisiert. Zusätzlich wurde die Gesamt-MMP-Aktivität mittels MMP-Aktivitätsassay und die daraus resultierende Entstehung von MMP-Spaltprodukten mittels immunhistochemischer Färbungen untersucht. In Pelletkultur und 3D Seidenfibroin-Implantaten konnte zunächst gezeigt werden, dass hypoxische Bedingungen die Chondrogenese von BMSCs fördern und zu einem Anstieg von Proteogylkanen und Kollagenen in der EZM führen. Des Weiteren wurden in beiden Kultursystemen unterschiedliche MMP Expressionsmuster unter Hypoxie im Vergleich zur Normoxie mittels qRT-PCR beobachtet. Während die Genexpression von *MMP13*, dem Enzym welches maßgeblich für den Knorpelabbau verantwortlich ist, signifikant geringer war,

war unter hypoxischen Bedingungen die Genexpression von *TIMP3*, dem am häufigsten produzierten und bedeutendsten Inhibitor des Knorpelabbaus, signifikant erhöht. Zusätzlich zeigte sich in der Immunhistochemie eine deutlich geringere MMP13-Proteinexpression. Besonders bemerkenswert unter Hypoxie war die Reduktion des MMP-abhängigen Aggrekan-Neoepitops DIPEN, welches mittels immunhistochemischer Färbung nachgewiesen und zusätzlich histomorphometrisch quantifiziert wurde. Diese Beobachtung spiegelte sich auch in einer verringerten Gesamt-MMP-Aktivität unter Hypoxie wider.
Die Ergebnisse aus **Kapitel 3.2 und 3.3** belegen in zwei unabhängigen Zellkultursystemen die Bedeutung des Sauerstoffpartialdrucks als wichtigen Effektor in der Entwicklung und Aufrechterhaltung der Knorpelmatrix. Demnach wirken hypoxische Bedingungen nicht nur unterstützend auf die EZM-Synthese und deren Aufbau, sondern schützen die Knorpelmatrix auch vor Abbauprozessen, was letztendlich in einem höheren Anteil von Proteoglykanen in der EZM resultiert.

Nachdem sich die vorangegangenen Kapitel mit wichtigen Einflussfaktoren der chondrogenen Differenzierung und Knorpelmatrixentwicklung von BMSCs beschäftigt haben, ging es im letzten Kapitel dieser Arbeit (**Kapitel 3.4**) um die Evaluation eines funktionalisierten Knorpelimplantats auf Seidenfibroin-Basis. Heutige Behandlungsmethoden sind leider noch nicht in der Lage nativen Knorpel vollständig zu regenerieren[303]. Die meisten derzeitigen Tissue-Engineering Ansätze applizieren Wachstumsfaktoren in löslicher Form, obwohl dies mit einer verminderten Halbwertszeit des Wachstumsfaktors und mit starken Nebenwirkungen verbunden sein kann[194,221]. Aus diesen Gründen wurde hier in einem Kooperationsprojekt mit der Arbeitsgruppe von Prof. Dr. Dr. Lorenz Meinel vom Institut für Pharmazeutische Technologie und Biopharmazie der Universität Würzburg, eine neue Plattform entwickelt, die in Kombination von TGF-β3-gekoppelten Polymethylmethacrylat (PMMA)-Mikrosphären mit 3D Seidenfibroin-Implantaten eine räumlich begrenzte Präsentation der Wachstumsfaktoren für die chondrogene Differenzierung von BMSCs in der Knorpelregeneration ermöglicht. Die neu entwickelten 3D Seidenfibroin-Implantate dienen zudem als tragende Strukturen zur Erhöhung der mechanischen Stabilität der Konstrukte. Wie im SEM und in der Lebend-Tod Färbung nachgewiesen werden

konnte, waren die Implantate interkonnektiv und äußerst biokompatibel. Mit Hilfe einer spritzenbasierten Besiedelungsmethode konnte eine homogene Verteilung der Zellen erzielt werden, die eine kohärente Gewebeentwicklung ermöglicht. Die Chondrogenese der BMSCs im funktionalisierten Konstrukt wurde mittels Histologie, Immunhistochemie, biochemischer Assays und qRT-PCR untersucht. Nachdem die BMSCs mit TGF-β3-gekoppelten Mikrosphären kultiviert wurden, wiesen sie im Vergleich zur Gruppe mit nicht-funktionalisierten Mikrosphären in der histologischen und immunhistochemischen Untersuchung bezüglich GAG und Kollagen II eine deutlich erhöhte Chondrogenese und Knorpelmatrixentwicklung aus. Diese Beobachtungen konnten durch eine erhöhte Genexpression der chondrogenen Markergenen *ACAN*, *COL2A* und *SOX9* unterstützend belegt werden. Die Kombination aus 3D Seidenfibroin-Implantat, TGF-β3 gekoppelten PMMA-Mikrosphären und BMSCs erwies sich demnach als erfolgreich für die Entwicklung von Knorpelgewebskonstrukten und könnte in Kombination mit Behandlungsmethoden wie der Mikrofrakturierung den Therapieerfolg verbessern. Betrachtet man diese Studie als "proof-of-principle", welches erfolgreich anhand eines Knorpelimplantats exemplarisch dargelegt werden konnte, bieten die mit funktionalisierten PMMA-Mikrosphären beladenen Implantate das Potential einer vielfältigen Plattform, die die kontrollierte Bereitstellung und lokal begrenzte Präsentation von Wachstumsfaktoren ermöglicht und die Möglichkeit bietet auch in anderen Tissue-Engineering-Bereichen Anwendung zu finden.

Mit der umfassenden Untersuchung zweier Schlüsselfaktoren, IGF-I und Sauerstoffpartialdruck, die maßgeblich die chondrogene Entwicklung von Stammzellen regulieren, und der Entwicklung eines funktionalisierten künstlichen 3D Knorpelimplantats leistet diese Dissertation einen wichtigen Beitrag zum besseren Verständnis von zellulären Entwicklungsprozessen der Knorpelmatrix während der chondrogenen Differenzierung von BMSCs. Die hier vorgestellten Erkenntnisse bieten sowohl Grundlage als auch Perspektiven, neue Wege bei der Entwicklung innovativer Implantate für die Regeneration von Knorpelgewebe zu gehen.

Bibliography

1. Lanza, R., Langer, R. & Vacanti, J. in *Principles of Tissue Engineering* Fourth Edition (Academic Press, Boston, 2014).
2. Langer, R & Vacanti, J. Tissue engineering. *Science* **260,** 920–926 (1993).
3. Rustad, K. C., Sorkin, M., Levi, B., Longaker, M. T. & Gurtner, G. C. Strategies for organ level tissue engineering. *Organogenesis* **6,** 151–157 (2010).
4. Nerem, R. M. *Advances in Tissue Engineering* (eds Polak, J., Mantalaris, S. & Harding, S.) (Imperial Collage Press, 2012).
5. Temenoff, J. S. & Mikos, A. G. Review: tissue engineering for regeneration of articular cartilage. *Biomaterials* **21,** 431–40 (2000).
6. O'Driscoll, S. W. Current Concepts Review - The Healing and Regeneration of Articular Cartilage. *J Bone Joint Surg Am* **80,** 1795 (1998).
7. Hunziker, E., Lippuner, K., Keel, M. & Shintani, N. An educational review of cartilage repair: precepts & practice – myths & misconceptions – progress & prospects. *Osteoarthritis and Cartilage* **23,** 334–350 (2015).
8. Zhang, L., Hu, J. & Athanasiou, K. A. The Role of Tissue Engineering in Articular Cartilage Repair and Regeneration. *Critical reviews in biomedical engineering* **37,** 1–57 (2009).
9. Buckwalter, J. A. & Mankin, H. J. Articular cartilage: tissue design and chondrocyte-matrix interactions. *Instr Course Lect* **47,** 477–486 (1998).
10. Cohen, N. P., Foster, R. J. & Mow, V. C. Composition and dynamics of articular cartilage: structure, function, and maintaining healthy state. *J Orthop Sports Phys Ther* **28,** 203–215 (1998).
11. Mow, V. C., Ratcliffe, A. & Poole, A. R. Cartilage and diarthrodial joints as paradigms for hierarchical materials and structures. *Biomaterials* **13,** 67–97 (1992).
12. Sophia Fox, A. J., Bedi, A. & Rodeo, S. A. The basic science of articular cartilage: structure, composition, and function. *Sports Health* **1,** 461–468 (2009).

13. Kuettner, K. E. Biochemistry of articular cartilage in health and disease. *Clin Biochem* **25,** 155–163 (1992).

14. O'Hara, B. P., Urban, J. P. & Maroudas, A. Influence of cyclic loading on the nutrition of articular cartilage. *Ann Rheum Dis* **49,** 536–539 (1990).

15. Woo, S. L. & Buckwalter, J. A. AAOS/NIH/ORS workshop. Injury and repair of the musculoskeletal soft tissues. Savannah, Georgia, June 18-20, 1987. *J Orthop Res* **6,** 907–931 (1988).

16. Correa, D. & Lietman, S. A. Articular cartilage repair: Current needs, methods and research directions. *Seminars in Cell & Developmental Biology* **62,** 67 –77 (2017).

17. Warman, M. L. Human genetic insights into skeletal development, growth, and homeostasis. *Clin Orthop Relat Res,* S40–S54 (2000).

18. Hughes, L. C., Archer, C. W. & I. ap Gwynn, I. The ultrastructure of mouse articular cartilage: collagen orientation and implications for tissue functionality. A polarised light and scanning electron microscope study and review. *Eur Cell Mater* **9,** 68–84 (June 2005).

19. Poole, A. R., Kojima, T., Yasuda, T., Mwale, F., Kobayashi, M. & Laverty, S. Composition and structure of articular cartilage: a template for tissue repair. *Clin Orthop Relat Res,* S26–S33 (2001).

20. Guilak, F. & Mow, V. C. The mechanical environment of the chondrocyte: a biphasic finite element model of cell-matrix interactions in articular cartilage. *J Biomech* **33,** 1663–1673 (2000).

21. Muir, H. The chondrocyte, architect of cartilage. Biomechanics, structure, function and molecular biology of cartilage matrix macromolecules. *Bioessays* **17,** 1039–1048 (1995).

22. Mow, V. C. & Guo, X. E. Mechano-electrochemical properties of articular cartilage: their inhomogeneities and anisotropies. *Annu Rev Biomed Eng* **4,** 175–209 (2002).

23. Bhosale, A. M. & Richardson, J. B. Articular cartilage: structure, injuries and review of management. *Br Med Bull* **87,** 77–95 (2008).

24. Wachtel, E. & Maroudas, A. The effects of pH and ionic strength on intrafibrillar hydration in articular cartilage. *Biochim Biophys Acta* **1381,** 37–48 (1998).

25. Mow, V. C., Kuei, S. C., Lai, W. M. & Armstrong, C. G. Biphasic creep and stress relaxation of articular cartilage in compression? Theory and experiments. *J Biomech Eng* **102,** 73–84 (1980).

26. Eyre, D. R. Collagen: molecular diversity in the body's protein scaffold. *Science* **207,** 1315–1322 (1980).

27. Maroudas, A. *Physiochemical properties of Carticular cartilage.* In: Freeman MAR, ed. Adult Articular Cartilage. 215–290 (Cambridge University Press, 1979).

28. Mörgelin, M., Paulsson, M., Hardingham, T. E., Heinegård, D. & Engel, J. Cartilage proteoglycans. Assembly with hyaluronate and link protein as studied by electron microscopy. *Biochem J* **253,** 175–185 (1988).

29. Buckwalter, L. H. E. J. Rosenberg. Articular Cartilage And Knee Joint Function: Basic Science And Arthroscopy. *New York, NY: Raven Press* (1990).

30. Chen, S. & Birk, D. E. The regulatory roles of small leucine-rich proteoglycans in extracellular assembly. *The FEBS journal* **280,** 2120–2137 (2013).

31. Boivin, W. A., Shackleford, M., Vanden Hoek, A., Zhao, H., Hackett, T. L., Knight, D. A. & Granville, D. J. Granzyme B Cleaves Decorin, Biglycan and Soluble Betaglycan, Releasing Active Transforming Growth Factor-1. *PLoS ONE* **7,** e33163– (2012).

32. Hynes, R. O. The extracellular matrix: not just pretty fibrils. *Science* **326,** 1216–1219 (2009).

33. Roycik, M. D., Fang, X. & Sang, Q.-X. A fresh prospect of extracellular matrix hydrolytic enzymes and their substrates. *Curr Pharm Des* **15,** 1295–1308 (2009).

34. Järveläinen, H., Sainio, A., Koulu, M., Wight, T. N. & Penttinen, R. Extracellular matrix molecules: potential targets in pharmacotherapy. *Pharmacol Rev* **61,** 198–223 (2009).

35. Bonnans, C., Chou, J. & Werb, Z. Remodelling the extracellular matrix in development and disease. *Nat Rev Mol Cell Biol* **15,** 786–801 (2014).

36. Mott, J. D. & Werb, Z. Regulation of matrix biology by matrix metalloproteinases. *Curr Opin Cell Biol* **16,** 558–564 (2004).

37. Visse, R. & Nagase, H. Matrix metalloproteinases and tissue inhibitors of metalloproteinases: structure, function, and biochemistry. *Circ Res* **92,** 827–839 (2003).

38. Franco, C., Patricia, H.-R., Timo, S., Claudia, B. & Marcela, H. Matrix Metalloproteinases as Regulators of Periodontal Inflammation. *International Journal of Molecular Sciences* **18,** 440– (2017).

39. Hamano, Y., Zeisberg, M., Sugimoto, H., Lively, J. C., Maeshima, Y., Yang, C., Hynes, R. O., Werb, Z., Sudhakar, A. & Kalluri, R. Physiological levels of tumstatin, a fragment of collagen IV alpha3 chain, are generated by MMP-9 proteolysis and suppress angiogenesis via alphaV beta3 integrin. *Cancer Cell* **3,** 589–601 (2003).

40. Mannello, F. & Gazzanelli, G. Tissue inhibitors of metalloproteinases and programmed cell death: conundrums, controversies and potential implications. *Apoptosis* **6,** 479–482 (2001).

41. Mannello, F., Luchetti, F., Falcieri, E. & Papa, S. Multiple roles of matrix metalloproteinases during apoptosis. *Apoptosis* **10,** 19–24 (2005).

42. Mannello, F., Tonti, G. A. M., Bagnara, G. P. & Papa, S. Role and function of matrix metalloproteinases in the differentiation and biological characterization of mesenchymal stem cells. *Stem Cells* **24,** 475–481 (2006).

43. Lu, P., Takai, K., Weaver, V. M. & Werb, Z. Extracellular matrix degradation and remodeling in development and disease. *Cold Spring Harb Perspect Biol* **3** (2011).

44. Apte, S. S. A disintegrin-like and metalloprotease (reprolysin-type) with thrombospondin type 1 motif (ADAMTS) superfamily: functions and mechanisms. *J Biol Chem* **284,** 31493–31497 (2009).

45. Kuno, K. & Matsushima, K. ADAMTS-1 protein anchors at the extracellular matrix through the thrombospondin type I motifs and its spacing region. *J Biol Chem* **273,** 13912–13917 (1998).

46. Kashiwagi, M., Enghild, J. J., Gendron, C., Hughes, C., Caterson, B., Itoh, Y. & Nagase, H. Altered proteolytic activities of ADAMTS-4 expressed by C-terminal processing. *J Biol Chem* **279,** 10109–10119 (2004).

47. Porter, S., Clark, I. M., Kevorkian, L. & Edwards, D. R. The ADAMTS metalloproteinases. *Biochem J* **386,** 15–27 (2005).

48. Longpré, J.-M. & Leduc, R. Identification of prodomain determinants involved in ADAMTS-1 biosynthesis. *J Biol Chem* **279,** 33237–33245 (2004).

49. Koo, B.-H., Longpré, J.-M., Somerville, R. P. T., Alexander, J. P., Leduc, R. & Apte, S. S. Cell-surface processing of pro-ADAMTS9 by furin. *J Biol Chem* **281,** 12485–12494 (2006).

50. Longpré, J.-M., McCulloch, D. R., Koo, B.-H., Alexander, J. P., Apte, S. S. & Leduc, R. Characterization of proADAMTS5 processing by proprotein convertases. *Int J Biochem Cell Biol* **41,** 1116–1126 (2009).

51. Fosang, A. J., Stanton, H., Little, C. B. & Atley, L. M. Neoepitopes as biomarkers of cartilage catabolism. *Inflamm Res* **52,** 277–282 (2003).

52. Little, C. B., Hughes, C. E., Curtis, C. L., Janusz, M. J., Bohne, R., Wang-Weigand, S., Taiwo, Y. O., Mitchell, P. G., Otterness, I. G., Flannery, C. R. & Caterson, B. Matrix metalloproteinases are involved in C-terminal and interglobular domain processing of cartilage aggrecan in late stage cartilage degradation. *Matrix Biol* **21,** 271–288 (2002).

53. Sandy, J. D., Neame, P. J., Boynton, R. E. & Flannery, C. R. Catabolism of aggrecan in cartilage explants. Identification of a major cleavage site within the interglobular domain. *J Biol Chem* **266,** 8683–8685 (1991).

54. Ilic, M. Z., Handley, C. J., Robinson, H. C. & Mok, M. T. Mechanism of catabolism of aggrecan by articular cartilage. *Arch Biochem Biophys* **294,** 115–122 (1992).

55. Tortorella, M. D., Pratta, M., Liu, R. Q., Austin, J., Ross, O. H., Abbaszade, I., Burn, T. & Arner, E. Sites of aggrecan cleavage by recombinant human aggrecanase-1 (ADAMTS-4). *J Biol Chem* **275,** 18566–18573 (2000).

56. Patterson, M. L., Atkinson, S. J., Knäuper, V. & Murphy, G. Specific collagenolysis by gelatinase A, MMP-2, is determined by the hemopexin domain and not the fibronectin-like domain. *FEBS Lett* **503,** 158–162 (2001).

57. Ohuchi, E., Imai, K., Fujii, Y., Sato, H., Seiki, M. & Okada, Y. Membrane type 1 matrix metalloproteinase digests interstitial collagens and other extracellular matrix macromolecules. *J Biol Chem* **272,** 2446–2451 (1997).

58. Charni-Ben Tabassi, N., Desmarais, S., Bay-Jensen, A. C., Delaisse, J. M., Percival, M. D. & Garnero, P. The type II collagen fragments Helix-II and CTX-II reveal different enzymatic pathways of human cartilage collagen degradation. *Osteoarthritis Cartilage* **16,** 1183–91 (2008).

59. Catterall, J., Dewitt Parr, S., Fagerlund, K. & Caterson, B. CTX-II is a marker of cartilage degradation but not of bone turnover. *Osteoarthritis and Cartilage* **21** (2013).

60. Duclos, M. E., Roualdes, O., Cararo, R., Rousseau, J. C., Roger, T. & Hartmann, D. J. Significance of the serum CTX-II level in an osteoarthritis animal model: a 5-month longitudinal study. *Osteoarthritis Cartilage* **18,** 1467–1476 (2010).

61. Kashiwagi, M., Tortorella, M., Nagase, H. & Brew, K. TIMP-3 is a potent inhibitor of aggrecanase 1 (ADAMTS4) and aggrecanase 2 (ADAMTS5). *J Biol Chem* **276,** 12501–12504 (2001).

62. Neuhold, L. A., Killar, L., Zhao, W., Sung, M. L., Warner, L., Kulik, J., Turner, J., Wu, W., Billinghurst, C., Meijers, T., Poole, A. R., Babij, P. & DeGennaro, L. J. Postnatal expression in hyaline cartilage of constitutively active human collagenase-3 (MMP-13) induces osteoarthritis in mice. *J Clin Invest* **107,** 35–44 (2001).

63. Mitchell, P. G., Magna, H. A., Reeves, L. M., Lopresti-Morrow, L. L., Yocum, S. A., Rosner, P. J., Geoghegan, K. F. & Hambor, J. E. Cloning, expression, and type II collagenolytic activity of matrix metalloproteinase-13 from human osteoarthritic cartilage. *J Clin Invest* **97,** 761–768 (1996).

64. Bouloumié, A., Sengenès, C., Portolan, G., Galitzky, J. & Lafontan, M. Adipocyte produces matrix metalloproteinases 2 and 9: involvement in adipose differentiation. *Diabetes* **50,** 2080–2086 (2001).

65. Friedenstein, A. J., Chailakhjan, R. K. & Lalykina, K. S. The development of fibroblast colonies in monolayer cultures of guinea-pig bone marrow and spleen cells. *Cell Tissue Kinet* **3,** 393–403 (1970).

66. Caplan, A. I. Mesenchymal stem cells. *J Orthop Res* **9,** 641–650 (1991).

67. Pittenger, M. F., Mackay, A. M., Beck, S. C., Jaiswal, R. K., Douglas, R., Mosca, J. D., Moorman, M. A., Simonetti, D. W., Craig, S. & Marshak, D. R. Multilineage potential of adult human mesenchymal stem cells. *Science* **284,** 143–7 (1999).

68. Johnstone, B., Alini, M., Cucchiarini, M., Dodge, G. R., Eglin, D., Guilak, F., Madry, H., Mata, A., Mauck, R. L., Semino, C. E. & Stoddart, M. J. Tissue engineering for articular cartilage repair - the state of the art. *Eur Cell Mater* **25,** 248–67 (2013).

69. Dominici, M., Le Blanc, K., Mueller, I., Slaper-Cortenbach, I., Marini, F., Krause, D., Deans, R., Keating, A., Prockop, D. & Horwitz, E. Minimal criteria for defining multipotent mesenchymal stromal cells. The International Society for Cellular Therapy position statement. *Cytotherapy* **8,** 315–7 (2006).

70. Koga, H., Engebretsen, L., Brinchmann, J. E., Muneta, T. & Sekiya, I. Mesenchymal stem cell-based therapy for cartilage repair: a review. *Knee Surg Sports Traumatol Arthrosc* **17,** 1289–1297 (2009).

71. Das, R., Jahr, H., van Osch, G. J. & Farrell, E. The role of hypoxia in bone marrow-derived mesenchymal stem cells: considerations for regenerative medicine approaches. *Tissue Eng Part B Rev* **16,** 159–68 (2010).

72. Viganò, M., Sansone, V., d'Agostino, M. C., Romeo, P., Perucca Orfei, C. & de Girolamo, L. Mesenchymal stem cells as therapeutic target of biophysical stimulation for the treatment of musculoskeletal disorders. *Journal of Orthopaedic Surgery and Research* **11,** 163 (2016).

73. Jones, B. J. & McTaggart, S. J. Immunosuppression by mesenchymal stromal cells: From culture to clinic. *Experimental Hematology* **36,** 733–741 (2008).

74. Caplan, A. I. & Correa, D. The MSC: An Injury Drugstore. *Cell Stem Cell* **9,** 11–15 (2011).

75. Salibian, A. A., Widgerow, A. D., Abrouk, M. & Evans, G. R. Stem cells in plastic surgery: a review of current clinical and translational applications. *Arch Plast Surg* **40,** 666–675 (2013).

76. Robert, H. Chondral repair of the knee joint using mosaicplasty. *Orthopaedics & Traumatology: Surgery & Research* **97,** 418 –429 (2011).

77. Corpus, K. T., Bajaj, S., Daley, E. L., Lee, A., Kercher, J. S., Salata, M. J., Verma, N. N. & Cole, B. J. Long-Term Evaluation of Autologous Chondrocyte Implantation: Minimum 7-Year Follow-Up. *Cartilage* **3,** 342–50 (2012).

78. Briggs, T. W., Mahroof, S., David, L. A., Flannelly, J., Pringle, J. & Bayliss, M. Histological evaluation of chondral defects after autologous chondrocyte implantation of the knee. *J Bone Joint Surg Br* **85,** 1077–83 (2003).

79. Redondo, M. L., Beer, A. J. & Yanke, A. B. Cartilage Restoration: Microfracture and Osteochondral Autograft Transplantation. *J Knee Surg* (2018).

80. Yu, D.-A., Han, J. & Kim, B.-S. Stimulation of chondrogenic differentiation of mesenchymal stem cells. *Int J Stem Cells* **5,** 16–22 (2012).

81. Keller, B., Yang, T., Chen, Y., Munivez, E., Bertin, T., Zabel, B. & Lee, B. Interaction of TGFβ and BMP signaling pathways during chondrogenesis. *PLoS One* **6,** e16421 (2011).

82. Hartmann, C. & Tabin, C. J. Wnt-14 plays a pivotal role in inducing synovial joint formation in the developing appendicular skeleton. *Cell* **104,** 341–351 (2001).

83. Rountree, R. B., Schoor, M., Chen, H., Marks, M. E., Harley, V., Mishina, Y. & Kingsley, D. M. BMP receptor signaling is required for postnatal maintenance of articular cartilage. *PLoS Biol* **2,** e355 (2004).

84. Tickle, C. Molecular basis of vertebrate limb patterning. *Am J Med Genet* **112,** 250–255 (2002).

85. Pacifici, M., Koyama, E., Iwamoto, M. & Gentili, C. Development of articular cartilage: what do we know about it and how may it occur? *Connect Tissue Res* **41,** 175–184 (2000).

86. Cserjesi, P., Brown, D., Ligon, K. L., Lyons, G. E., Copeland, N. G., Gilbert, D. J., Jenkins, N. A. & Olson, E. N. Scleraxis: a basic helix-loop-helix protein that prefigures skeletal formation during mouse embryogenesis. *Development* **121,** 1099–1110 (1995).

87. Bi, W., Deng, J. M., Zhang, Z., Behringer, R. R. & de Crombrugghe, B. Sox9 is required for cartilage formation. *Nat Genet* **22,** 85–89 (1999).

88. Cole, N. J., Tanaka, M., Prescott, A. & Tickle, C. Expression of limb initiation genes and clues to the morphological diversification of threespine stickleback. *Curr Biol* **13,** R951–R952 (2003).

89. Hall, B. K. & Miyake, T. The membranous skeleton: the role of cell condensations in vertebrate skeletogenesis. *Anat Embryol (Berl)* **186,** 107–124 (1992).

90. Sandell, L. J., Sugai, J. V. & Trippel, S. B. Expression of collagens I, II, X, and XI and aggrecan mRNAs by bovine growth plate chondrocytes in situ. *J Orthop Res* **12,** 1–14 (1994).

91. Demoor, M., Ollitrault, D., Gomez-Leduc, T., Bouyoucef, M., Hervieu, M., Fabre, H., Lafont, J., Denoix, J.-M., Audigié, F., Mallein-Gerin, F., Legendre, F. & Galera, P. Cartilage tissue engineering: molecular control of chondrocyte differentiation for proper cartilage matrix reconstruction. *Biochim Biophys Acta* **1840,** 2414–2440 (2014).

92. Li, J., Zhao, Z., Liu, J., Huang, N., Long, D., Wang, J., Li, X. & Liu, Y. MEK/ERK and p38 MAPK regulate chondrogenesis of rat bone marrow mesenchymal stem cells through delicate interaction with TGF-beta1/Smads pathway. *Cell Prolif* **43,** 333–343 (2010).

93. Lengerke, C., Schmitt, S., Bowman, T. V., Jang, I. H., Maouche-Chretien, L., McKinney-Freeman, S., Davidson, A. J., Hammerschmidt, M., Rentzsch, F., Green, J. B. A., Zon, L. I. & Daley, G. Q. BMP and Wnt specify hematopoietic fate by activation of the Cdx-Hox pathway. *Cell Stem Cell* **2,** 72–82 (2008).

94. Kyriacos, A., Eric, D., Jerry, H., Grayson, D. & A. Hari, R. Articular Cartilage (2013).

95. Robi, K., Jakob, N., Matevz, K. & Matjaz, V. Novel Therapies for the Management of Sports Injuries. *Current Issues in Sports and Exercise Medicine* (2013).

96. Hall, B. K. & Miyake, T. Divide, accumulate, differentiate: cell condensation in skeletal development revisited. *Int J Dev Biol* **39,** 881–893 (1995).

97. Shum, L., Coleman, C. M., Hatakeyama, Y. & Tuan, R. S. Morphogenesis and dysmorphogenesis of the appendicular skeleton. *Birth Defects Research Part C: Embryo Today: Reviews* **69,** 102–122 (2003).

98. Leonard, C. M., Fuld, H. M., Frenz, D. A., Downie, S. A., Massagué, J. & Newman, S. A. Role of transforming growth factor-beta in chondrogenic pattern formation in the embryonic limb: stimulation of mesenchymal condensation and fibronectin gene expression by exogenenous TGF-beta and evidence for endogenous TGF-beta-like activity. *Dev Biol* **145,** 99–109 (1991).

99. Chisa Hidaka, M. B. G. Regulatory mechanisms of chondrogenesis and implications for understanding articular cartilage homeostasis. *Current Rheumatology Reviews* **4,** 136–147 (2008).

100. Pacifici, M., Koyama, E., Shibukawa, Y., Wu, C., Tamamura, Y., Enomoto-Iwamoto, M. & Iwamoto, M. Cellular and molecular mechanisms of synovial joint and articular cartilage formation. *Ann N Y Acad Sci* **1068,** 74–86 (2006).

101. Pacifici, M., Koyama, E. & Iwamoto, M. Mechanisms of synovial joint and articular cartilage formation: recent advances, but many lingering mysteries. *Birth Defects Res C Embryo Today* **75,** 237–248 (2005).

102. Johnstone, B., Hering, T. M., Caplan, A. I., Goldberg, V. M. & Yoo, J. U. In vitro chondrogenesis of bone marrow-derived mesenchymal progenitor cells. *Exp Cell Res* **238,** 265–272 (1998).

103. Sekiya, I., Colter, D. C. & Prockop, D. J. BMP-6 enhances chondrogenesis in a subpopulation of human marrow stromal cells. *Biochem Biophys Res Commun* **284,** 411–418 (2001).

104. Embree, M. C., Kilts, T. M., Ono, M., Inkson, C. A., Syed-Picard, F., Karsdal, M. A., Oldberg, A., Bi, Y. & Young, M. F. Biglycan and Fibromodulin Have Essential Roles in Regulating Chondrogenesis and Extracellular Matrix Turnover in Temporomandibular Joint Osteoarthritis. *The American Journal of Pathology* **176,** 812–826 (2010).

105. DuRaine, G., Neu, C. P., Chan, S. M. T., Komvopoulos, K., June, R. K. & Reddi, A. H. Regulation of the friction coefficient of articular cartilage by TGF-beta1 and IL-1beta. *J Orthop Res* **27,** 249–256 (2009).

106. Neu, C. P., Khalafi, A., Komvopoulos, K., Schmid, T. M. & Reddi, A. H. Mechanotransduction of bovine articular cartilage superficial zone protein by transforming growth factor beta signaling. *Arthritis Rheum* **56,** 3706–3714 (2007).

107. Fortier, L. A., Mohammed, H. O., Lust, G. & Nixon, A. J. Insulin-like growth factor-I enhances cell-based repair of articular cartilage. *J Bone Joint Surg Br* **84,** 276–288 (2002).

108. Luyten, F. P., Hascall, V. C., Nissley, S. P., Morales, T. I. & Reddi, A. H. Insulin-like growth factors maintain steady-state metabolism of proteoglycans in bovine articular cartilage explants. *Arch Biochem Biophys* **267,** 416–25 (1988).

109. Barry, F., Boynton, R. E., Liu, B. & Murphy, J. M. Chondrogenic differentiation of mesenchymal stem cells from bone marrow: differentiation-dependent gene expression of matrix components. *Exp Cell Res* **268,** 189–200 (2001).

110. Steck, E., Bertram, H., Abel, R., Chen, B., Winter, A. & Richter, W. Induction of intervertebral disc-like cells from adult mesenchymal stem cells. *Stem Cells* **23,** 403–411 (2005).

111. Ichinose, S., Yamagata, K., Sekiya, I., Muneta, T. & Tagami, M. Detailed examination of cartilage formation and endochondral ossification using human mesenchymal stem cells. *Clin Exp Pharmacol Physiol* **32,** 561–570 (2005).

112. Pelttari, K., Steck, E. & Richter, W. The use of mesenchymal stem cells for chondrogenesis. *Injury* **39 Suppl 1,** S58–S65 (2008).

113. Estes, B. T., Diekman, B. O., Gimble, J. M. & Guilak, F. Isolation of adipose-derived stem cells and their induction to a chondrogenic phenotype. *Nat Protoc* **5,** 1294–1311 (2010).

114. Kolf, C. M., Cho, E. & Tuan, R. S. Mesenchymal stromal cells. Biology of adult mesenchymal stem cells: regulation of niche, self-renewal and differentiation. *Arthritis Res Ther* **9,** 204 (2007).

115. Fehrer, C., Brunauer, R., Laschober, G., Unterluggauer, H., Reitinger, S., Kloss, F., Gülly, C., Gassner, R. & Lepperdinger, G. Reduced oxygen tension attenuates differentiation capacity of human mesenchymal stem cells and prolongs their lifespan. *Aging Cell* **6,** 745–757 (2007).

116. Lennon, D. P., Edmison, J. M. & Caplan, A. I. Cultivation of rat marrow-derived mesenchymal stem cells in reduced oxygen tension: effects on in vitro and in vivo osteochondrogenesis. *J Cell Physiol* **187,** 345–355 (2001).

117. Busuttil, R. A., Rubio, M., Dollé, M. E. T., Campisi, J. & Vijg, J. Oxygen accelerates the accumulation of mutations during the senescence and immortalization of murine cells in culture. *Aging Cell* **2,** 287–294 (2003).

118. Mohyeldin, A., Garzón-Muvdi, T. & Quiñones-Hinojosa, A. Oxygen in stem cell biology: a critical component of the stem cell niche. *Cell Stem Cell* **7,** 150–161 (2010).

119. Fermor, B., Christensen, S. E., Youn, I., Cernanec, J. M., Davies, C. M. & Weinberg, J. B. Oxygen, nitric oxide and articular cartilage. *Eur Cell Mater* **13,** 56–65; discussion 65 (2007).

120. Cross, M., Alt, R. & Niederwieser, D. The case for a metabolic stem cell niche. *Cells Tissues Organs* **188,** 150–159 (2008).

121. Grayson, W. L., Zhao, F., Bunnell, B. & Ma, T. Hypoxia enhances proliferation and tissue formation of human mesenchymal stem cells. *Biochem Biophys Res Commun* **358,** 948–953 (2007).

122. Ren, H., Cao, Y., Zhao, Q., Li, J., Zhou, C., Liao, L., Jia, M., Zhao, Q., Cai, H., Han, Z. C., Yang, R., Chen, G. & Zhao, R. C. Proliferation and differentiation of bone marrow stromal cells under hypoxic conditions. *Biochem Biophys Res Commun* **347,** 12–21 (2006).

123. Carrancio, S., Lopez-Holgado, N., Sanchez-Guijo, F. M., Villaron, E., Barbado, V., Tabera, S., Diez-Campelo, M., Blanco, J., San Miguel, J. F. & Del Canizo, M. C. Optimization of mesenchymal stem cell expansion procedures by cell separation and culture conditions modification. *Exp Hematol* **36,** 1014–21 (2008).

124. Mylotte, L. A., Duffy, A. M., Murphy, M., O'Brien, T., Samali, A., Barry, F. & Szegezdi, E. Metabolic flexibility permits mesenchymal stem cell survival in an ischemic environment. *Stem Cells* **26,** 1325–1336 (2008).

125. Ezashi, T., Das, P. & Roberts, R. M. Low O2 tensions and the prevention of differentiation of hES cells. *Proc Natl Acad Sci U S A* **102,** 4783–4788 (2005).

126. Yamamoto, Y., Fujita, M., Tanaka, Y., Kojima, I., Kanatani, Y., Ishihara, M. & Tachibana, S. Low oxygen tension enhances proliferation and maintains stemness of adipose tissue-derived stromal cells. *Biores Open Access* **2,** 199–205 (2013).

127. Berniakovich, I. & Giorgio, M. Low oxygen tension maintains multipotency, whereas normoxia increases differentiation of mouse bone marrow stromal cells. *Int J Mol Sci* **14,** 2119–2134 (2013).

128. D'Ippolito, G., Diabira, S., Howard, G. A., Roos, B. A. & Schiller, P. C. Low oxygen tension inhibits osteogenic differentiation and enhances stemness of human MIAMI cells. *Bone* **39,** 513–522 (2006).

129. Majmundar, A. J., Wong, W. J. & Simon, M. C. Hypoxia-inducible factors and the response to hypoxic stress. *Mol Cell* **40,** 294–309 (2010).

130. Semenza, G. L. Hypoxia-inducible factors in physiology and medicine. *Cell* **148,** 399–408 (2012).

131. Jaakkola, P., Mole, D. R., Tian, Y. M., Wilson, M. I., Gielbert, J., Gaskell, S. J., von Kriegsheim, A., Hebestreit, H. F., Mukherji, M., Schofield, C. J., Maxwell, P. H., Pugh, C. W. & Ratcliffe, P. J. Targeting of HIF-alpha to the von Hippel-Lindau ubiquitylation complex by O2-regulated prolyl hydroxylation. *Science* **292,** 468–472 (2001).

132. Schofield, C. J. & Ratcliffe, P. J. Oxygen sensing by HIF hydroxylases. *Nat Rev Mol Cell Biol* **5,** 343–354 (2004).

133. Lord-Dufour, S., Copland, I. B., Levros, L.-C. Jr, Post, M., Das, A., Khosla, C., Galipeau, J., Rassart, E. & Annabi, B. Evidence for transcriptional regulation of the glucose-6-phosphate transporter by HIF-1alpha: Targeting G6PT with mumbaistatin analogs in hypoxic mesenchymal stromal cells. *Stem Cells* **27,** 489–497 (2009).

134. Kanichai, M., Ferguson, D., Prendergast, P. J. & Campbell, V. A. Hypoxia promotes chondrogenesis in rat mesenchymal stem cells: a role for AKT and hypoxia-inducible factor (HIF)-1alpha. *J Cell Physiol* **216,** 708–715 (2008).

135. Thoms, B. L., Dudek, K. A., Lafont, J. E. & Murphy, C. L. Hypoxia promotes the production and inhibits the destruction of human articular cartilage. *Arthritis Rheum* **65,** 1302–1312 (2013).

136. Schipani, E., Ryan, H. E., Didrickson, S., Kobayashi, T., Knight, M. & Johnson, R. S. Hypoxia in cartilage: HIF-1alpha is essential for chondrocyte growth arrest and survival. *Genes Dev* **15,** 2865–2876 (2001).

137. Wang, D. W., Fermor, B., Gimble, J. M., Awad, H. A. & Guilak, F. Influence of oxygen on the proliferation and metabolism of adipose derived adult stem cells. *J Cell Physiol* **204,** 184–191 (2005).

138. Khan, W. S., Adesida, A. B., Tew, S. R., Lowe, E. T. & Hardingham, T. E. Bone marrow-derived mesenchymal stem cells express the pericyte marker 3G5 in culture and show enhanced chondrogenesis in hypoxic conditions. *J Orthop Res* **28,** 834–840 (2010).

139. Martin-Rendon, E., Hale, S. J. M., Ryan, D., Baban, D., Forde, S. P., Roubelakis, M., Sweeney, D., Moukayed, M., Harris, A. L., Davies, K. & Watt, S. M. Transcriptional profiling of human cord blood CD133+ and cultured bone marrow mesenchymal stem cells in response to hypoxia. *Stem Cells* **25,** 1003–1012 (2007).

140. Müller, J., Benz, K., Ahlers, M., Gaissmaier, C. & Mollenhauer, J. Hypoxic conditions during expansion culture prime human mesenchymal stromal precursor cells for chondrogenic differentiation in three-dimensional cultures. *Cell Transplant* **20,** 1589–1602 (2011).

141. Markway, B. D., Tan, G.-K., Brooke, G., Hudson, J. E., Cooper-White, J. J. & Doran, M. R. Enhanced chondrogenic differentiation of human bone marrow-derived mesenchymal stem cells in low oxygen environment micropellet cultures. *Cell Transplant* **19,** 29–42 (2010).

142. Coyle, C. H., Izzo, N. J. & Chu, C. R. Sustained hypoxia enhances chondrocyte matrix synthesis. *J Orthop Res* **27,** 793–799 (2009).

143. Robins, J. C., Akeno, N., Mukherjee, A., Dalal, R. R., Aronow, B. J., Koopman, P. & Clemens, T. L. Hypoxia induces chondrocyte-specific gene expression in mesenchymal cells in association with transcriptional activation of Sox9. *Bone* **37,** 313–322 (2005).

144. Ströbel, S., Loparic, M., Wendt, D., Schenk, A. D., Candrian, C., Lindberg, R. L. P., Moldovan, F., Barbero, A. & Martin, I. Anabolic and catabolic responses of human articular chondrocytes to varying oxygen percentages. *Arthritis Res Ther* **12,** R34 (2010).

145. Gawlitta, D., van Rijen, M. H. P., Schrijver, E. J. M., Alblas, J. & Dhert, W. J. A. Hypoxia impedes hypertrophic chondrogenesis of human multipotent stromal cells. *Tissue Eng Part A* **18,** 1957–1966 (2012).

146. Hirao, M., Tamai, N., Tsumaki, N., Yoshikawa, H. & Myoui, A. Oxygen tension regulates chondrocyte differentiation and function during endochondral ossification. *J Biol Chem* **281,** 31079–31092 (2006).

147. Leijten, J. C. H., Moreira Teixeira, L. S., Landman, E. B. M., van Blitterswijk, C. A. & Karperien, M. Hypoxia inhibits hypertrophic differentiation and endochondral ossification in explanted tibiae. *PLoS One* **7,** e49896 (2012).

148. Holzwarth, C., Vaegler, M., Gieseke, F., Pfister, S. M., Handgretinger, R., Kerst, G. & Müller, I. Low physiologic oxygen tensions reduce proliferation and differentiation of human multipotent mesenchymal stromal cells. *BMC Cell Biol* **11,** 11 (2010).

149. Goldring, M. B., Tsuchimochi, K. & Ijiri, K. The control of chondrogenesis. *J Cell Biochem* **97,** 33–44 (2006).

150. DuRaine, G. D., Chan, S. M. T. & Reddi, A. H. Effects of TGF-β1 on alternative splicing of Superficial Zone Protein in articular cartilage cultures. *Osteoarthritis Cartilage* **19,** 103–110 (2011).

151. Spagnoli, A., Longobardi, L. & O'Rear, L. Cartilage disorders: potential therapeutic use of mesenchymal stem cells. *Endocr Dev* **9,** 17–30 (2005).

152. Grimaud, E., Heymann, D. & Rédini, F. Recent advances in TGF-beta effects on chondrocyte metabolism. Potential therapeutic roles of TGF-beta in cartilage disorders. *Cytokine Growth Factor Rev* **13,** 241–257 (2002).

153. Serra, R., Johnson, M., Filvaroff, E. H., LaBorde, J., Sheehan, D. M., Derynck, R. & Moses, H. L. Expression of a truncated, kinase-defective TGF-beta type II receptor in mouse skeletal tissue promotes terminal chondrocyte differentiation and osteoarthritis. *J Cell Biol* **139,** 541–552 (1997).

154. Bosnakovski, D., Mizuno, M., Kim, G., Takagi, S., Okumura, M. & Fujinaga, T. Chondrogenic differentiation of bovine bone marrow mesenchymal stem cells (MSCs) in different hydrogels: influence of collagen type II extracellular matrix on MSC chondrogenesis. *Biotechnol Bioeng* **93,** 1152–1163 (2006).

155. Chimal-Monroy, J. & Díaz de León, L. Expression of N-cadherin, N-CAM, fibronectin and tenascin is stimulated by TGF-beta1, beta2, beta3 and beta5 during the formation of precartilage condensations. *Int J Dev Biol* **43,** 59–67 (1999).

156. Oberlender, S. A. & Tuan, R. S. Expression and functional involvement of N-cadherin in embryonic limb chondrogenesis. *Development* **120,** 177–187 (1994).

157. Widelitz, R. B., Jiang, T. X., Murray, B. A. & Chuong, C. M. Adhesion molecules in skeletogenesis: II. Neural cell adhesion molecules mediate precartilaginous mesenchymal condensations and enhance chondrogenesis. *J Cell Physiol* **156,** 399–411 (1993).

158. Yamaguchi, A. Regulation of differentiation pathway of skeletal mesenchymal cells in cell lines by transforming growth factor-beta superfamily. *Semin Cell Biol* **6,** 165–173 (1995).

159. Darling, E. M. & Athanasiou, K. A. Growth factor impact on articular cartilage subpopulations. *Cell Tissue Res* **322,** 463–473 (2005).

160. Kwon, H., Paschos, N. K., Hu, J. C. & Athanasiou, K. Articular cartilage tissue engineering: the role of signaling molecules. *Cell Mol Life Sci* **73,** 1173–1194 (2016).

161. Zhang, X., Ziran, N., Goater, J. J., Schwarz, E. M., Puzas, J. E., Rosier, R. N., Zuscik, M., Drissi, H. & O'Keefe, R. J. Primary murine limb bud mesenchymal cells in long-term culture complete chondrocyte differentiation: TGF-beta delays hypertrophy and PGE2 inhibits terminal differentiation. *Bone* **34,** 809–817 (2004).

162. Lebrin, F., Deckers, M., Bertolino, P. & Ten Dijke, P. TGF-beta receptor function in the endothelium. *Cardiovasc Res* **65,** 599–608 (2005).

163. Mueller, M. B., Fischer, M., Zellner, J., Berner, A., Dienstknecht, T., Prantl, L., Kujat, R., Nerlich, M., Tuan, R. S. & Angele, P. Hypertrophy in mesenchymal stem cell chondrogenesis: effect of TGF-beta isoforms and chondrogenic conditioning. *Cells Tissues Organs* **192,** 158–166 (2010).

164. Wrana, J. L., Attisano, L., Cárcamo, J., Zentella, A., Doody, J., Laiho, M., Wang, X. F. & Massagué, J. TGF beta signals through a heteromeric protein kinase receptor complex. *Cell* **71,** 1003–1014 (1992).

165. Zhang, Y., Feng, X. H. & Derynck, R. Smad3 and Smad4 cooperate with c-Jun/c-Fos to mediate TGF-beta-induced transcription. *Nature* **394,** 909–913 (1998).

166. de Caestecker, M. The transforming growth factor-beta superfamily of receptors. *Cytokine Growth Factor Rev* **15,** 1–11 (2004).

167. Derynck, R. & Zhang, Y. E. Smad-dependent and Smad-independent pathways in TGF-beta family signalling. *Nature* **425,** 577–584 (2003).

168. Bakin, A. V., Rinehart, C., Tomlinson, A. K. & Arteaga, C. L. p38 mitogen-activated protein kinase is required for TGFbeta-mediated fibroblastic transdifferentiation and cell migration. *J Cell Sci* **115,** 3193–3206 (2002).

169. Huang, F. & Chen, Y.-G. Regulation of TGF-β receptor activity. *Cell & Bioscience* **2,** 9 (2012).

170. Schoenle, E., Zapf, J., Humbel, R. E. & Froesch, E. R. Insulin-like growth factor I stimulates growth in hypophysectomized rats. *Nature* **296,** 252–253 (1982).

171. Vetter, U., Zapf, J., Heit, W., Helbing, G., Heinze, E., Froesch, E. R. & Teller, W. M. Human fetal and adult chondrocytes. Effect of insulinlike growth factors I and II, insulin, and growth hormone on clonal growth. *J Clin Invest* **77,** 1903–1908 (1986).

172. Longobardi, L., O'Rear, L., Aakula, S., Johnstone, B., Shimer, K., Chytil, A., Horton, W. A., Moses, H. L. & Spagnoli, A. Effect of IGF-I in the chondrogenesis of bone marrow mesenchymal stem cells in the presence or absence of TGF-beta signaling. *J Bone Miner Res* **21,** 626–36 (2006).

173. Martin, J. A., Scherb, M. B., Lembke, L. A. & Buckwalter, J. A. Damage control mechanisms in articular cartilage: the role of the insulin-like growth factor I axis. *Iowa Orthop J* **20,** 1–10 (2000).

174. Berenbaum, F., Thomas, G., Poiraudeau, S., Bérériat, G., Corvol, M. T. & Masliah, J. Insulin-like growth factors counteract the effect of interleukin 1 beta on type II phospholipase A2 expression and arachidonic acid release by rabbit articular chondrocytes. *FEBS Lett* **340,** 51–55 (1994).

175. Worster, A. A., Brower-Toland, B. D., Fortier, L. A., Bent, S. J., Williams, J. & Nixon, A. J. Chondrocytic differentiation of mesenchymal stem cells sequentially exposed to transforming growth factor-beta1 in monolayer and insulin-like growth factor-I in a three-dimensional matrix. *J Orthop Res* **19,** 738–49 (2001).

176. Martel-Pelletier, J., Di Battista, J. A., Lajeunesse, D. & Pelletier, J. P. IGF/IGFBP axis in cartilage and bone in osteoarthritis pathogenesis. *Inflamm Res* **47,** 90–100 (1998).

177. Yoon, D. M. & Fisher, J. P. Effects of exogenous IGF-1 delivery on the early expression of IGF-1 signaling molecules by alginate embedded chondrocytes. *Tissue Eng Part A* **14,** 1263–1273 (2008).

178. Hawsawi, Y., El-Gendy, R., Twelves, C., Speirs, V. & Beattie, J. Insulin-like growth factor - oestradiol crosstalk and mammary gland tumourigenesis. *Biochim Biophys Acta* **1836,** 345–353 (2013).

179. Oh, C.-D. & Chun, J.-S. Signaling mechanisms leading to the regulation of differentiation and apoptosis of articular chondrocytes by insulin-like growth factor-1. *J Biol Chem* **278,** 36563–36571 (2003).

180. Fukumoto, T., Sperling, J. W., Sanyal, A., Fitzsimmons, J. S., Reinholz, G. G., Conover, C. A. & O'Driscoll, S. W. Combined effects of insulin-like growth factor-1 and transforming growth factor-beta1 on periosteal mesenchymal cells during chondrogenesis in vitro. *Osteoarthritis Cartilage* **11,** 55–64 (2003).

181. Sunic, D., Belford, D. A., McNeil, J. D. & Wiebkin, O. W. Insulin-like growth factor binding proteins (IGF-BPs) in bovine articular and ovine growth-plate chondrocyte cultures: their regulation by IGFs and modulation of proteoglycan synthesis. *Biochim Biophys Acta* **1245,** 43–48 (1995).

182. Gillespie, C., Read, L. C., Bagley, C. J. & Ballard, F. J. Enhanced potency of truncated insulin-like growth factor-I (des(1-3)IGF-I) relative to IGF-I in lit/lit mice. *J Endocrinol* **127,** 401–405 (1990).

183. Ballard, F. J., Wallace, J. C., Francis, G. L., Read, L. C. & Tomas, F. M. Des(1-3)IGF-I: a truncated form of insulin-like growth factor-I. *Int J Biochem Cell Biol* **28,** 1085–1087 (1996).

184. Clemmons, D. R., Busby, W. H., Arai, T., Nam, T. J., Clarke, J. B., Jones, J. I. & Ankrapp, D. K. Role of insulin-like growth factor binding proteins in the control of IGF actions. *Prog Growth Factor Res* **6,** 357–366 (1995).

185. Clemmons, D. R. Role of IGF Binding Proteins in Regulating Metabolism. *Trends in Endocrinology & Metabolism* **27,** 375–391 (2016).

186. Firth, S. M. & Baxter, R. C. Cellular actions of the insulin-like growth factor binding proteins. *Endocr Rev* **23,** 824–854 (2002).

187. De Mellow, J. S. & Baxter, R. C. Growth hormone-dependent insulin-like growth factor (IGF) binding protein both inhibits and potentiates IGF-I-stimulated DNA synthesis in human skin fibroblasts. *Biochem Biophys Res Commun* **156,** 199–204 (1988).

188. Galasso, O., De Gori, M., Nocera, A., Brunetti, A. & Gasparini, G. Regulatory functions of insulin-like growth factor binding proteins in osteoarthritis. *Int J Immunopathol Pharmacol* **24,** 55–9 (2011).

189. Olney, R. C., Tsuchiya, K., Wilson, D. M., Mohtai, M., Maloney, W. J., Schurman, D. J. & Smith, R. L. Chondrocytes from osteoarthritic cartilage have increased expression of insulin-like growth factor I (IGF-I) and IGF-binding protein-3 (IGFBP-3) and -5, but not IGF-II or IGFBP-4. *J Clin Endocrinol Metab* **81,** 1096–1103 (1996).

190. Morales, T. I. The insulin-like growth factor binding proteins in uncultured human cartilage: increases in insulin-like growth factor binding protein 3 during osteoarthritis. *Arthritis Rheum* **46,** 2358–2367 (2002).

191. Doré, S., Pelletier, J. P., DiBattista, J. A., Tardif, G., Brazeau, P. & Martel-Pelletier, J. Human osteoarthritic chondrocytes possess an increased number of insulin-like growth factor 1 binding sites but are unresponsive to its stimulation. Possible role of IGF-1-binding proteins. *Arthritis Rheum* **37,** 253–263 (1994).

192. Tardif, G., Reboul, P., Pelletier, J. P., Geng, C., Cloutier, J. M. & Martel-Pelletier, J. Normal expression of type 1 insulin-like growth factor receptor by human osteoarthritic chondrocytes with increased expression and synthesis of insulin-like growth factor binding proteins. *Arthritis Rheum* **39,** 968–978 (1996).

193. Iwanaga, H., Matsumoto, T., Enomoto, H., Okano, K., Hishikawa, Y., Shindo, H. & Koji, T. Enhanced expression of insulin-like growth factor-binding proteins in human osteoarthritic cartilage detected by immunohistochemistry and in situ hybridization. *Osteoarthritis Cartilage* **13,** 439–448 (2005).

194. Masters, K. S. Covalent growth factor immobilization strategies for tissue repair and regeneration. *Macromol Biosci* **11,** 1149–63 (2011).

195. Hermanson, G. T. *Bioconjugate Techniques* Third edition (Academic Press, 2013).

196. Wang, C., Yan, Q., Liu, H.-B., Zhou, X.-H. & Xiao, S.-J. Different EDC/NHS Activation Mechanisms between PAA and PMAA Brushes and the Following Amidation Reactions. *Langmuir* **27,** 12058–12068 (2011).

197. Ogiwara, K., Nagaoka, M., Cho, C.-S. & Akaike, T. Effect of photo-immobilization of epidermal growth factor on the cellular behaviors. *Biochem Biophys Res Commun* **345,** 255–259 (2006).

198. Leslie-Barbick, J. E., Shen, C., Chen, C. & West, J. L. Micron-scale spatially patterned, covalently immobilized vascular endothelial growth factor on hydrogels accelerates endothelial tubulogenesis and increases cellular angiogenic responses. *Tissue Eng Part A* **17,** 221–229 (2011).

199. Tigli, R. S. & Gumusderelioglu, M. Evaluation of RGD- or EGF-immobilized chitosan scaffolds for chondrogenic activity. *Int J Biol Macromol* **43,** 121–128 (2008).

200. Kleps, I., Ignat, T., Miu, M., Craciunoiu, F., Trif, M., Simion, M., Bragaru, A. & Dinescu, A. Nanostructured silicon particles for medical applications. *J Nanosci Nanotechnol* **10,** 2694–2700 (2010).

201. Henry, A. C., Tutt, T. J., Galloway, M., Davidson, Y. Y., McWhorter, C. S., Soper, S. A. & McCarley, R. L. Surface modification of poly(methyl methacrylate) used in the fabrication of microanalytical devices. *Anal Chem* **72,** 5331–5337 (2000).

202. Ni, M., Tong, W. H., Choudhury, D., Rahim, N. A., Iliescu, C. & Yu, H. Cell culture on MEMS platforms: a review. *Int J Mol Sci* **10,** 5411–41 (2009).

203. Kuehn, K.-D., Ege, W. & Gopp, U. Acrylic bone cements: composition and properties. *Orthop Clin North Am* **36,** 17–28, v (2005).

204. Gogia, J. S., Meehan, J. P., Di Cesare, P. E. & Jamali, A. A. Local Antibiotic Therapy in Osteomyelitis. *Seminars in Plastic Surgery* **23,** 100–107 (2009).

205. Omenetto, F. G. & Kaplan, D. L. New Opportunities for an Ancient Material. *Science* **329,** 528–531 (2010).

206. Altman, G. H., Diaz, F., Jakuba, C., Calabro, T., Horan, R. L., Chen, J., Lu, H., Richmond, J. & Kaplan, D. L. Silk-based biomaterials. *Biomaterials* **24,** 401 –416 (2003).

207. Kundu, B., Rajkhowa, R., Kundu, S. C. & Wang, X. Silk fibroin biomaterials for tissue regenerations. *Advanced Drug Delivery Reviews* **65,** 457 –470 (2013).

208. Vepari, C. & Kaplan, D. L. Silk as a Biomaterial. *Progress in polymer science* **32,** 991–1007 (2007).

209. Wang, Y., Blasioli, D. J., Kim, H.-J., Kim, H. S. & Kaplan, D. L. Cartilage tissue engineering with silk scaffolds and human articular chondrocytes. *Biomaterials* **27,** 4434 –4442 (2006).

210. Li, H., Fan, J., Sun, L., Liu, X., Cheng, P. & Fan, H. Functional regeneration of ligament-bone interface using a triphasic silk-based graft. *Biomaterials* **106,** 180 –192 (2016).

211. Hofmann, S., Hagenmuller, H., Koch, A. M., Muller, R., Vunjak-Novakovic, G., Kaplan, D. L., Merkle, H. P. & Meinel, L. Control of in vitro tissue-engineered bone-like structures using human mesenchymal stem cells and porous silk scaffolds. *Biomaterials* **28,** 1152–62 (2007).

212. Wang, Y., Kim, U. J., Blasioli, D. J., Kim, H. J. & Kaplan, D. L. In vitro cartilage tissue engineering with 3D porous aqueous-derived silk scaffolds and mesenchymal stem cells. *Biomaterials* **26,** 7082–94 (2005).

213. Liao, J., Shi, K., Ding, Q., Qu, Y., Luo, F. & Qian, Z. *Recent Developments in Scaffold-Guided Cartilage Tissue Regeneration* 2014.

214. Weiss, S., Hennig, T., Bock, R., Steck, E. & Richter, W. Impact of growth factors and PTHrP on early and late chondrogenic differentiation of human mesenchymal stem cells. *J Cell Physiol* **223,** 84–93 (2010).

215. Kim, H. J. & Im, G. I. Chondrogenic differentiation of adipose tissue-derived mesenchymal stem cells: greater doses of growth factor are necessary. *J Orthop Res* **27,** 612–9 (2009).

216. Indrawattana, N., Chen, G., Tadokoro, M., Shann, L. H., Ohgushi, H., Tateishi, T., Tanaka, J. & Bunyaratvej, A. Growth factor combination for chondrogenic induction from human mesenchymal stem cell. *Biochem Biophys Res Commun* **320,** 914–9 (2004).

217. Baddoo, M., Hill, K., Wilkinson, R., Gaupp, D., Hughes, C., Kopen, G. C. & Phinney, D. G. Characterization of mesenchymal stem cells isolated from murine bone marrow by negative selection. *J Cell Biochem* **89,** 1235–1249 (2003).

218. Zhou, Q., Li, B., Zhao, J., Pan, W., Xu, J. & Chen, S. IGF-I induces adipose derived mesenchymal cell chondrogenic differentiation in vitro and enhances chondrogenesis in vivo. *In Vitro Cellular & Developmental Biology - Animal,* 1–9 (2016).

219. Zipori, D. Mesenchymal stem cells: harnessing cell plasticity to tissue and organ repair. *Blood Cells Mol Dis* **33,** 211–5 (2004).

220. Boyette, L. B., Creasey, O. A., Guzik, L., Lozito, T. & Tuan, R. S. Human bone marrow-derived mesenchymal stem cells display enhanced clonogenicity but impaired differentiation with hypoxic preconditioning. *Stem Cells Transl Med* **3,** 241–254 (2014).

221. McCall, J. D., Luoma, J. E. & Anseth, K. S. Covalently tethered transforming growth factor beta in PEG hydrogels promotes chondrogenic differentiation of encapsulated human mesenchymal stem cells. *Drug Deliv Transl Res* **2,** 305–312 (2012).

222. Uebersax, L., Hagenmuller, H., Hofmann, S., Gruenblatt, E., Muller, R., Vunjak-Novakovic, G., Kaplan, D. L., Merkle, H. P. & Meinel, L. Effect of scaffold design on bone morphology in vitro. *Tissue Eng* **12,** 3417–29 (2006).

223. Gador, E. *Strategies to improve the biological performance of protein therapeutics* PhD thesis (2018).

224. Wittmann, K., Storck, K., Muhr, C., Mayer, H., Regn, S., Staudenmaier, R., Wiese, H., Maier, G., Bauer-Kreisel, P. & Blunk, T. Development of volume-stable adipose tissue constructs using polycaprolactone-based polyurethane scaffolds and fibrin hydrogels. *J Tissue Eng Regen Med* (2013).

225. Eyrich, D., Wiese, H., Maier, G., Skodacek, D., Appel, B., Sarhan, H., Tessmar, J., Staudenmaier, R., Wenzel, M. M., Goepferich, A. & Blunk, T. In vitro and in vivo cartilage engineering using a combination of chondrocyte-seeded long-term stable fibrin gels and polycaprolactone-based polyurethane scaffolds. *Tissue Eng* **13,** 2207–2218 (2007).

226. Kim, Y. J., Sah, R. L., Doong, J. Y. & Grodzinsky, A. J. Fluorometric assay of DNA in cartilage explants using Hoechst 33258. *Anal Biochem* **174,** 168–76 (1988).

227. Farndale, R. W., Buttle, D. J. & Barrett, A. J. Improved quantitation and discrimination of sulphated glycosaminoglycans by use of dimethylmethylene blue. *Biochim Biophys Acta* **883,** 173–177 (1986).

228. Woessner Jr, J. F. The determination of hydroxyproline in tissue and protein samples containing small proportions of this imino acid. *Archives of Biochemistry and Biophysics* **93,** 440–447 (1961).

229. Hollander, A. P., Heathfield, T. F., Webber, C., Iwata, Y., Bourne, R., Rorabeck, C. & Poole, A. R. Increased damage to type II collagen in osteoarthritic articular cartilage detected by a new immunoassay. *J Clin Invest* **93,** 1722–1732 (1994).

230. Smith, M. M., Sakurai, G., Smith, S. M., Young, A. A., Melrose, J., Stewart, C. M., Appleyard, R. C., Peterson, J. L., Gillies, R. M., Dart, A. J., Sonnabend, D. H. & Little, C. B. Modulation of aggrecan and ADAMTS expression in ovine tendinopathy induced by altered strain. *Arthritis Rheum* **58,** 1055–66 (2008).

231. Roy-Beaudry, M., Martel-Pelletier, J., Pelletier, J. P., M'Barek, K. N., Christgau, S., Shipkolye, F. & Moldovan, F. Endothelin 1 promotes osteoarthritic cartilage degradation via matrix metalloprotease 1 and matrix metalloprotease 13 induction. *Arthritis Rheum* **48,** 2855–64 (2003).

232. Jensen, E. C. Quantitative Analysis of Histological Staining and Fluorescence Using ImageJ. *The Anatomical Record* **296,** 378–381 (2013).

233. De Ceuninck, F., Caliez, A., Dassencourt, L., Anract, P. & Renard, P. Pharmacological disruption of insulin-like growth factor 1 binding to IGF-binding proteins restores anabolic responses in human osteoarthritic chondrocytes. *Arthritis Res Ther* **6,** R393–403 (2004).

234. Bonnevie, E. D., Puetzer, J. L. & Bonassar, L. J. Enhanced boundary lubrication properties of engineered menisci by lubricin localization with insulin-like growth factor I treatment. *Journal of Biomechanics* **47,** 2183–2188 (2014).

235. Madry, H., Kaul, G., Zurakowski, D., Vunjak-Novakovic, G. & Cucchiarini, M. Cartilage constructs engineered from chondrocytes overexpressing IGF-I improve the repair of osteochondral defects in a rabbit model. *Eur Cell Mater* **25,** 229–47 (2013).

236. Sakimura, K., Matsumoto, T., Miyamoto, C., Osaki, M. & Shindo, H. Effects of insulin-like growth factor I on transforming growth factor beta1 induced chondrogenesis of synovium-derived mesenchymal stem cells cultured in a polyglycolic acid scaffold. *Cells Tissues Organs* **183,** 55–61 (2006).

237. Steinert, A. F., Palmer, G. D., Pilapil, C., Nöth, U., Evans, C. H. & Ghivizzani, S. C. Enhanced in vitro chondrogenesis of primary mesenchymal stem cells by combined gene transfer. *Tissue Eng Part A* **15,** 1127–1139 (2009).

238. Pei, M., Aaron, R. & D.M., C. TGFβ1 dependent Chondrogenic Effect of IGF-I and FGF-2 on Syonovial Fibroblasts. *51st Annual meeting of the Orthopaedic Research Society* (2005).

239. Pei, M., He, F. & Vunjak-Novakovic, G. Synovium-derived stem cell-based chondrogenesis. *Differentiation* **76,** 1044–1056 (2008).

240. Im, G.-I., Shin, Y.-W. & Lee, K.-B. Do adipose tissue-derived mesenchymal stem cells have the same osteogenic and chondrogenic potential as bone marrow-derived cells? *Osteoarthritis Cartilage* **13,** 845–853 (2005).

241. Mastrogiacomo, M., Cancedda, R. & Quarto, R. Effect of different growth factors on the chondrogenic potential of human bone marrow stromal cells. *Osteoarthritis Cartilage* **9 Suppl A,** S36–S40 (2001).

242. Walsh, S., Jefferiss, C. M., Stewart, K. & Beresford, J. N. IGF-I does not affect the proliferation or early osteogenic differentiation of human marrow stromal cells. *Bone* **33,** 80–89 (2003).

243. Islam, A., Hansen, A. K., Mennan, C. & Martinez-Zubiaurre, I. Mesenchymal stromal cells from human umbilical cords display poor chondrogenic potential in scaffold-free three dimensional cultures. *Eur Cell Mater* **31,** 407–424 (2016).

244. Francis, G. L., Ross, M., Ballard, F. J., Milner, S. J., Senn, C., McNeil, K. A., Wallace, J. C., King, R. & Wells, J. R. Novel recombinant fusion protein analogues of insulin-like growth factor (IGF)-I indicate the relative importance of IGF-binding protein and receptor binding for enhanced biological potency. *J Mol Endocrinol* **8,** 213–23 (1992).

245. Liu, X. J., Xie, Q., Zhu, Y. F., Chen, C. & Ling, N. Identification of a nonpeptide ligand that releases bioactive insulin-like growth factor-I from its binding protein complex. *J Biol Chem* **276,** 32419–32422 (2001).

246. Martin, J. A., Ellerbroek, S. M. & Buckwalter, J. A. Age-related decline in chondrocyte response to insulin-like growth factor-I: the role of growth factor binding proteins. *J Orthop Res* **15,** 491–498 (1997).

247. Fortier, L. A., Nixon, A. J., Williams, J. & Cable, C. S. Isolation and chondrocytic differentiation of equine bone marrow-derived mesenchymal stem cells. *Am J Vet Res* **59,** 1182–7 (1998).

248. Blunk, T., Sieminski, A. L., Gooch, K. J., Courter, D. L., Hollander, A. P., Nahir, A. M., Langer, R., Vunjak-Novakovic, G. & Freed, L. E. Differential effects of growth factors on tissue-engineered cartilage. *Tissue Eng* **8,** 73–84 (2002).

249. Chung, C., Beecham, M., Mauck, R. L. & Burdick, J. A. The influence of degradation characteristics of hyaluronic acid hydrogels on in vitro neocartilage formation by mesenchymal stem cells. *Biomaterials* **30,** 4287–4296 (2009).

250. Bian, L., Guvendiren, M., Mauck, R. L. & Burdick, J. A. Hydrogels that mimic developmentally relevant matrix and N-cadherin interactions enhance MSC chondrogenesis. *Proc Natl Acad Sci USA* **110,** 10117–10122 (2013).

251. Wu, S.-C., Chang, J.-K., Wang, C.-K., Wang, G.-J. & Ho, M.-L. Enhancement of chondrogenesis of human adipose derived stem cells in a hyaluronan-enriched microenvironment. *Biomaterials* **31,** 631–640 (2010).

252. Schwartz, Z., Griffon, D. J., Fredericks, L. P., Lee, H.-B. & Weng, H.-Y. Hyaluronic acid and chondrogenesis of murine bone marrow mesenchymal stem cells in chitosan sponges. *Am J Vet Res* **72,** 42–50 (2011).

253. Markway, B. D., Cho, H. & Johnstone, B. Hypoxia promotes redifferentiation and suppresses markers of hypertrophy and degeneration in both healthy and osteoarthritic chondrocytes. *Arthritis Res Ther* **15,** R92 (2013).

254. Anderson, D. E., Markway, B. D., Weekes, K. J., McCarthy, H. E. & Johnstone, B. Physioxia Promotes the Articular Chondrocyte-Like Phenotype in Human Chondroprogenitor-Derived Self-Organized Tissue. *Tissue Engineering Part A* **24,** 264–274 (2018).

255. Anderson, D. E., Markway, B. D., Bond, D., McCarthy, H. E. & Johnstone, B. Responses to altered oxygen tension are distinct between human stem cells of high and low chondrogenic capacity. *Stem Cell Research & Therapy* **7,** 154 (2016).

256. Fortier, L. A. & Nixon, A. J. Chondrocytic differentiation of mesenchymal cells in long-term three-dimensional fibrin cultures treated with IGF-I. *42nd Annual Meeting, Orthopaedic Research Society* (1996).

257. Ciarmatori, S., Kiepe, D., Haarmann, A., Huegel, U. & Tonshoff, B. Signaling mechanisms leading to regulation of proliferation and differentiation of the mesenchymal chondrogenic cell line RCJ3.1C5.18 in response to IGF-I. *J Mol Endocrinol* **38,** 493–508 (2007).

258. Adesida, A. B., Mulet-Sierra, A. & Jomha, N. M. Hypoxia mediated isolation and expansion enhances the chondrogenic capacity of bone marrow mesenchymal stromal cells. *Stem Cell Res Ther* **3,** 9 (2012).

259. Lee, H. H., Chang, C. C., Shieh, M. J., Wang, J. P., Chen, Y. T., Young, T. H. & Hung, S. C. Hypoxia enhances chondrogenesis and prevents terminal differentiation through PI3K/Akt/FoxO dependent anti-apoptotic effect. *Sci Rep* **3,** 2683 (2013).

260. Jonitz, A., Lochner, K., Tischer, T., Hansmann, D. & Bader, R. TGF-β1 and IGF-1 influence the re-differentiation capacity of human chondrocytes in 3D pellet cultures in relation to different oxygen concentrations. *Int J Mol Med* **30,** 666–672 (2012).

261. Meretoja, V. V., Dahlin, R. L., Wright, S., Kasper, F. K. & Mikos, A. G. The effect of hypoxia on the chondrogenic differentiation of co-cultured articular chondrocytes and mesenchymal stem cells in scaffolds. *Biomaterials* **34,** 4266–73 (2013).

262. Chen, L., Tredget, E. E., Wu, P. Y. & Wu, Y. Paracrine factors of mesenchymal stem cells recruit macrophages and endothelial lineage cells and enhance wound healing. *PLoS One* **3,** e1886 (2008).

263. Tucci, M., Nygard, K., Tanswell, B. V., Farber, H. W., Hill, D. J. & Han, V. K. Modulation of insulin-like growth factor (IGF) and IGF binding protein biosynthesis by hypoxia in cultured vascular endothelial cells. *J Endocrinol* **157,** 13–24 (1998).

264. Sartori-Cintra, A. R., Mara, C. S. d., Argolo, D. L. & Coimbra, I. B. Regulation of hypoxia-inducible factor-1α (HIF-1α) expression by interleukin-1β (IL-1 β), insulin-like growth factors I (IGF-I) and II (IGF-II) in human osteoarthritic chondrocytes. *Clinics (Sao Paulo)* **67,** 35–40 (2012).

265. Beckert, S., Glatzle, J., Mayer, P., Königsrainer, A., Hunt, T. K. & Coerper, S. in *Chirurgisches Forum 2007: für experimentelle und klinische Forschung 124. Kongress der Deutschen Gesellschaft für Chirurgie München, 01.05. – 04.05.2007* (eds Steinau, H. U., Schackert, H. K. & Bauer, H.) 341–343 (Springer Berlin Heidelberg, 2007).

266. Gelse, K., Muhle, C., Knaup, K., Swoboda, B., Wiesener, M., Hennig, F., Olk, A. & Schneider, H. Chondrogenic differentiation of growth factor-stimulated precursor cells in cartilage repair tissue is associated with increased HIF-1alpha activity. *Osteoarthritis Cartilage* **16,** 1457–65 (2008).

267. Kim, J. H., Yoon, S. M., Song, S. U., Park, S. G., Kim, W.-S., Park, I. G., Lee, J. & Sung, J.-H. Hypoxia Suppresses Spontaneous Mineralization and Osteogenic Differentiation of Mesenchymal Stem Cells via IGFBP3 Up-Regulation. *Int J Mol Sci* **17** (2016).

268. Moromisato, D. Y., Moromisato, M. Y., Zanconato, S. & Roberts, C. Jr. Effect of hypoxia on lung, heart, and liver insulin-like growth factor-I gene and receptor expression in the newborn rat. *Crit Care Med* **24,** 919–924 (1996).

269. Nurwidya, F., Takahashi, F., Kobayashi, I., Murakami, A., Kato, M., Minakata, K., Nara, T., Hashimoto, M., Yagishita, S., Baskoro, H., Hidayat, M., Shimada, N. & Takahashi, K. Treatment with insulin-like growth factor 1 receptor inhibitor reverses hypoxia-induced epithelial-mesenchymal transition in non-small cell lung cancer. *Biochem Biophys Res Commun* **455,** 332–338 (2014).

270. Bertram, H., Boeuf, S., Wachters, J., Boehmer, S., Heisel, C., Hofmann, M. W., Piecha, D. & Richter, W. Matrix metalloprotease inhibitors suppress initiation and progression of chondrogenic differentiation of mesenchymal stromal cells in vitro. *Stem Cells Dev* **18,** 881–892 (2009).

271. Boeuf, S., Graf, F., Fischer, J., Moradi, B., Little, C. B. & Richter, W. Regulation of aggrecanases from the ADAMTS family and aggrecan neoepitope formation during in vitro chondrogenesis of human mesenchymal stem cells. *Eur Cell Mater* **23,** 320–332 (2012).

272. Fosang, A. J., Last, K., Stanton, H., Weeks, D. B., Campbell, I. K., Hardingham, T. E. & Hembry, R. M. Generation and novel distribution of matrix metalloproteinase-derived aggrecan fragments in porcine cartilage explants. *J Biol Chem* **275,** 33027–33037 (2000).

273. Reboul, P., Pelletier, J. P., Tardif, G., Cloutier, J. M. & Martel-Pelletier, J. The new collagenase, collagenase-3, is expressed and synthesized by human chondrocytes but not by synoviocytes. A role in osteoarthritis. *J Clin Invest* **97,** 2011–2019 (1996).

274. Markway, B. D., Cho, H., Anderson, D. E., Holden, P., Ravi, V., Little, C. B. & Johnstone, B. Reoxygenation enhances tumour necrosis factor alpha-induced degradation of the extracellular matrix produced by chondrogenic cells. *Eur Cell Mater* **31,** 425–439 (2016).

275. Kenagy, R. D., Plaas, A. H. & Wight, T. N. Versican degradation and vascular disease. *Trends Cardiovasc Med* **16,** 209–215 (2006).

276. Little, C. B., Barai, A., Burkhardt, D., Smith, S. M., Fosang, A. J., Werb, Z., Shah, M. & Thompson, E. W. Matrix metalloproteinase 13–deficient mice are resistant to osteoarthritic cartilage erosion but not chondrocyte hypertrophy or osteophyte development. *Arthritis & Rheumatism* **60,** 3723–3733 (2009).

277. Portron, S., Hivernaud, V., Merceron, C., Lesoeur, J., Masson, M., Gauthier, O., Vinatier, C., Beck, L. & Guicheux, J. Inverse regulation of early and late chondrogenic differentiation by oxygen tension provides cues for stem cell-based cartilage tissue engineering. *Cell Physiol Biochem* **35,** 841–857 (2015).

278. Gendron, C., Kashiwagi, M., Hughes, C., Caterson, B. & Nagase, H. TIMP-3 inhibits aggrecanase-mediated glycosaminoglycan release from cartilage explants stimulated by catabolic factors. *FEBS Lett* **555,** 431–436 (2003).

279. Lozito, T. P. & Tuan, R. S. Mesenchymal stem cells inhibit both endogenous and exogenous MMPs via secreted TIMPs. *J Cell Physiol* **226,** 385–396 (2011).

280. Hofmann, S., Knecht, S., Langer, R., Kaplan, D. L., Vunjak-Novakovic, G., Merkle, H. P. & Meinel, L. Cartilage-like tissue engineering using silk scaffolds and mesenchymal stem cells. *Tissue Eng* **12,** 2729–2738 (2006).

281. Meinel, L., Hofmann, S., Karageorgiou, V., Zichner, L., Langer, R., Kaplan, D. & Vunjak-Novakovic, G. Engineering cartilage-like tissue using human mesenchymal stem cells and silk protein scaffolds. *Biotechnol Bioeng* **88,** 379–391 (2004).

282. Ahmed, T. A. & Hincke, M. T. Strategies for articular cartilage lesion repair and functional restoration. *Tissue Eng Part B Rev* **16,** 305–29 (2010).

283. Henrotin, Y. & Dubuc, J.-E. Cartilage repair in osteoarthritic patients: utopia or real opportunity? *F1000 Med Rep* **1** (2009).

284. Vögelin, E., Jones, N. F., Huang, J. I., Brekke, J. H. & Toth, J. M. Practical illustrations in tissue engineering: surgical considerations relevant to the implantation of osteoinductive devices. *Tissue Eng* **6,** 449–460 (2000).

285. Van Beuningen, H., Glansbeek, H., van der Kraan, P. & van den Berg, W. Osteoarthritis-like changes in the murine knee joint resulting from intra-articular transforming growth factor-beta injections. *Osteoarthritis and Cartilage* **8,** 25 –33 (2000).

286. Ronzière, M. C., Perrier, E., Mallein-Gerin, F. & Freyria, A.-M. Chondrogenic potential of bone marrow- and adipose tissue-derived adult human mesenchymal stem cells. *Biomed Mater Eng* **20,** 145–158 (2010).

287. Correia, C., Bhumiratana, S., Yan, L.-P., Oliveira, A. L., Gimble, J. M., Rockwood, D., Kaplan, D. L., Sousa, R. A., Reis, R. L. & Vunjak-Novakovic, G. Development of silk-based scaffolds for tissue engineering of bone from human adipose-derived stem cells. *Acta Biomaterialia* **8,** 2483 –2492 (2012).

288. Meinel, L., Karageorgiou, V., Fajardo, R., Snyder, B., Shinde-Patil, V., Zichner, L., Kaplan, D., Langer, R. & Vunjak-Novakovic, G. Bone tissue engineering using human mesenchymal stem cells: effects of scaffold material and medium flow. *Ann Biomed Eng* **32,** 112–22 (2004).

289. Van den Berg, W. B., van Osch, G. J. V. M., van der Kraan, P. M. & van Beuningen, H. M. Cartilage destruction and osteophytes in instability-induced murine osteoarthritis: Role of TGFβ in osteophyte formation? *Agents and Actions* **40,** 215–219 (1993).

290. Elford, P. R., Graeber, M., Ohtsu, H., Aeberhard, M., Legendre, B., Wishart, W. L. & MacKenzie, A. R. Induction of swelling, synovial hyperplasia and cartilage proteoglycan loss upon intra-articular injection of transforming growth factor β-2 in the rabbit. *Cytokine* **4,** 232 –238 (1992).

291. Fuchs, T. F., Surke, C, Stange, R, Quandte, S, Wildemann, B, Raschke, M. J. & Schmidmaier, G. Local Delivery of Growth Factors Using Coated Suture Material. *The Scientific World Journal* **2012,** 109216 (2012).

292. Motoyama, M., Deie, M., Kanaya, A., Nishimori, M., Miyamoto, A., Yanada, S., Adachi, N. & Ochi, M. In vitro cartilage formation using TGF-beta-immobilized magnetic beads and mesenchymal stem cell-magnetic bead complexes under magnetic field conditions. *J Biomed Mater Res A* **92,** 196–204 (2010).

293. Hino, K., Saito, A., Kido, M., Kanemoto, S., Asada, R., Takai, T., Cui, M., Cui, X. & Imaizumi, K. Master Regulator for Chondrogenesis, Sox9, Regulates Transcriptional Activation of the Endoplasmic Reticulum Stress Transducer BBF2H7/CREB3L2 in Chondrocytes. *The Journal of Biological Chemistry* **289,** 13810–13820 (2014).

294. Baldwin, S. P. & Saltzman, W. M. Materials for protein delivery in tissue engineering. *Advanced Drug Delivery Reviews* **33,** 71 –86 (1998).

295. Ito, Y., Li, J. S., Takahashi, T., Imanishi, Y., Okabayashi, Y., Kido, Y. & Kasuga, M. Enhancement of the mitogenic effect by artificial juxtacrine stimulation using immobilized EGF. *J Biochem* **121,** 514–20 (1997).

296. Gilbert, T. W. Strategies for tissue and organ decellularization. *J Cell Biochem* **113,** 2217–22 (2012).

297. Hynes, R. O. Integrins: Versatility, modulation, and signaling in cell adhesion. *Cell* **69,** 11–25 (1992).

298. Yamada, K. M. & Miyamoto, S. Integrin transmembrane signaling and cytoskeletal control. *Current Opinion in Cell Biology* **7,** 681 –689 (1995).

299. Ito, Y., Chen, G. & Imanishi, Y. Artificial juxtacrine stimulation for tissue engineering. *J Biomater Sci Polym Ed* **9,** 879–890 (1998).

300. Singh, A. B. & Harris, R. C. Autocrine, paracrine and juxtacrine signaling by EGFR ligands. *Cellular Signalling* **17,** 1183 –1193 (2005).

301. Liu, H.-W., Chen, C.-H., Tsai, C.-L. & Hsiue, G.-H. Targeted delivery system for juxtacrine signaling growth factor based on rhBMP-2-mediated carrier-protein conjugation. *Bone* **39,** 825 –836 (2006).

302. Glyn-Jones, S, Palmer, A. J. R., Agricola, R, Price, A. J., Vincent, T. L., Weinans, H & Carr, A. J. Osteoarthritis. *The Lancet* **386,** 376 –387 (2015).

303. Kock, L., van Donkelaar, C. C. & Ito, K. Tissue engineering of functional articular cartilage: the current status. *Cell and Tissue Research* **347,** 613–627 (2012).

Appendix

A.1 Abbreviations

3D	Three-dimensional
ADAMTS	Disintegrin and metalloproteinase with thrombospondin motifs
ANOVA	Analysis of variance
APS	Ammonium persulfate
ASC	Adipose-derived stromal cell
ATP	Adenosine triphosphate
bFGF	Basic-FGF (FGF-2)
BMP	Bone morphogenetic protein
BMSC	Bone marrow-derrived mesenchymal stromal cell
BSA	Bovine serum albumin
Calcein	Calcein acetoxymethyl ester
CD	Cluster of differentiation
cDNA	Copy/complementary deoxyribonucleic acid
Col I	Collagen type I
Col II	Collagen type II
CPD	Critical point drying
CS	Chondroitin sulphate
CSE	Cell seeding efficiency
CTGF	Connective tissue growth factor
CTX-II	MMP-mediated collagen type II cleavage product
DAB	3,3'-dimethylamino-benzaldehyde
DAPI	4',6-diamidino-2-phenylindole
desIGF	Des(1-3)IGF-I
DIPEN	MMP-mediated aggrecan cleavage product
DMEM/F-12	Dulbecco's Modified Eagle's Medium/Ham's
DMMB	Dimethylmethylene blue
DMSO	Dimethyl sulfoxide
DNA	Deoxyribonucleic acid
ECM	Extracellular matrix
EDC	1-Ethyl-3-(3-dimethylaminopropyl)carbodiimide

EDTA	Ethylenediaminetetraacetic acid
EGF	Epidermal growth factor
ELISA	Enzyme Linked Immunosorbent Assay
ER	Endoplasmic reticulum
ERK	Extracellular signal-regulated kinase
ESC	Embryonic stem cell
EthD	Ethidium bromide homodimer III
FBS	Fetal bovine serum
FGF	Fibroblast growth factors
FRET	Resonance energy transfer
GAG	Gylcosaminoglycan
GAPDH	Glyceraldehyde-3-phosphate dehydrogenase
GDF	Growth/differentiation factor
H&E	Haematoxylin and eosin
HB-EGF	EGF-like growth factor
HEPES	4-(2-hydroxyethyl)-1-piperazineethanesulfonic
hES	Human embryonic stem cells
HIF	Hypoxia inducible factor
HRP	Horseradish peroxidase
IGD	Interglobular domain
IGF	Insulin-like growth factor
IGFBP	Insulin-like growth factor binding protein
IGF-IR	Insulin-like growth factor receptor
IHC	Immunohistochemistry
IHH	Indian hedgehog
IL-Iβ	Interleukin-1 beta
ITS	Insulin, transferin, selenium
KS	Keratan sulphate
MAPK	Mitogen-activated protein kinase
MCP-3	Monocyte chemotactic protein-3
MMP	Matrix metalloproteinase
MSC	Mesenchymal stromal cell
MT	Membrane-type
NHS	N-Hydroxysuccinimide
NIH	National Institutes of Health
OA	Osteoarthritis
P2	Second passage cells
PBS	Phosphate-buffered saline
PEG	Polyethylene glycol
PI3K	phosphoinositide 3-kinase

PMMA	Poly(methyl methacrylate)
PS	Penicillin-streptomycin
qRT-PCR	Quantitative real-time polymerase chain reaction
RNA	Ribonucleic acid
rpm	Revolutions per minute
SD	Standard deviation
SDS-PAGE	Dodecyl sulfate polyacrylamide gel electrophoresis
SEM	Scanning electron microscopy
TEMED	Tetramethylethylenediamine
TGF-β	Transforming growth factor beta
TIMP	Tissue inhibitor of metalloproteinases
TNF-α	Tumor necrosis factor alpha
TRIS	Tris(hydroxymethyl)aminomethan
TS	Thrombospondin
VEGF	Vascular endothelial growth factor
WB	Western blot

A.2 Scientific contributions

Journal articles

1. Böck, T., Schill, V., **Krähnke, M.**, Tessmar, J., Blunk, T., Groll, J. TGF-β1-modified hyaluronic acid / poly(glycidol) hydrogels for chondrogenic differentiation of human mesenchymal stromal cells. Macromolecular Bioscience 2018, published online in Wiley Online Library doi: 10.1002/mabi.201700390

Oral presentations

1. **Krähnke M.**, Richter L., Böck T., Ahlbrecht R., Steinert A., Groll J., Tessmar J., Blunk T. Differential effects of IGF-I and des(1-3)IGF-I during chondrogenic differentiation of bone marrow-derived stromal cells. Kongresses für Orthopädie und Unfallchirurgie (DKOU) 2017, Berlin, Germany.

2. **Krähnke M.**, Böck T., Heusler E., Meinel L., Meffert R., Blunk T. Extracellular matrix-modulating enzyme expression and proteoglycan degradation are regulated by oxygen tension during chondrogenesis of bone marrow-derived stromal cells. Tissue Engineering and Regenerative Medicine International Society (TERMIS) 2017, Davos, Switzerland.

3. **Krähnke M.**, Böck T., Meffert R., Blunk T. Hypoxia affects Extracellular Matrix-Modulating Enzymes and Reduces Proteoglycan Degradation during Chondrogenesis of Bone Marrow-Derived Stromal Cells. Kongresses für Orthopädie und Unfallchirurgie (DKOU) 2016, Berlin, Germany.

4. **Krähnke M.**, Böck T., Meffert R., Blunk T. Impact of Hypoxia on Extracellular Matrix-Modulating Enzymes during Chondrogenesis of Bone Marrow-Derived Stromal Cells. 19. chirurgische Forschungstage der Deutschen Gesellschaft für Orthopädie und Unfallchirurgie (DGOU) 2015, Würzburg, Germany

5. Böck, T., Schill, V., Stichler, S., **Krähnke, M.**, Steinert, A., Tessmar, J., Blunk, T., Groll, J. Chondromimetic polyglycidol-based hydrogels for MSC chondrogenesis. 4th International Conference Strategies in Tissue Engineering 2015, Würzburg, Germany.

6. Böck, T., Schill, V., **Krähnke, M.**, Gilbert, F., Steinert, A., Tessmar, J., Blunk, T., Groll J. Maßgeschneiderte biomimetische und bioaktive

Hydrogele für die Knorpelregeneration mit mesenchymalen Stammzellen. Deutscher Kongresses für Orthopädie und Unfallchirurgie (DKOU) 2014, Berlin, Germany.

7. Böck, T., Schill, V., **Krähnke, M.**, Steinert, A. Tessmar, J., Blunk, T., Groll, J. Tailored hyaluronic acid-based hydrogels for cartilage regeneration. 11th World Congress of the International Cartilage Repair Society (ICRS) 2013, Izmir, Turkey.

Poster presentations

1. **Krähnke M.**, Blunk T. Impact of hypoxia on extracellular matrix-modulating enzymes during chondrogenesis of bone marrow-derived stromal cells. P-054. 4th International Conference Strategies in Tissue Engineering 2015, Würzburg, Germany.

2. **Krähnke M.**, Heusler E., Blunk T., Meinel L. Towards osteochondral tissue engineering utilizing 3D silk fibroin scaffolds. P-055. 4th International Conference Strategies in Tissue Engineering 2015, Würzburg, Germany.

3. Böck, T., Schill, V., Stichler, S., **Krähnke, M.**, Steinert, A., Tessmar, J., Blunk, T., Groll, J. Chondromimetic peptide- and growth factor-modified polyglycidolbased hydrogels for MSC chondrogenesis. PO11-633. Deutscher Kongresses für Orthopädie und Unfallchirurgie (DKOU) 2015, Berlin, Germany.

4. Böck, T., Schill, V., Stichler, S., **Krähnke, M.**, Steinert, A., Tessmar, J., Blunk, T., Groll, J. Versatile polyglycidol-based hydrogel platform for MSC chondrogenesis. P53. 12th World Congress of the International Cartilage Repair Society (ICRS) 2015, Chicago, United States of America.

5. **Krähnke, M.**, Heusler, E., Böck, T., Blunk, T., Meinel, L. Multifunktionale osteochondrale Implantate - Chondrogene und osteogene Differenzierung von mesenchymalen Stammzellen in biphasischen Seidenfibroin-Implantaten. Deutscher Kongresses für Orthopädie und Unfallchirurgie (DKOU) 2014, Berlin, Germany.

6. Böck, T., Schill, V., **Krähnke, M.**, Gilbert, F., Steinert, A., Tessmar, J., Blunk, T., Groll, J. Biomimetic hyaluronic acid-based hydrogels for cartilage regeneration. Eureka - 9th International Symposium organized by the students of the GSLS 2014, Würzburg, Germany.

7. **Krähnke, M.**, Heusler, E., Böck, T., Blunk, T., Meinel, L. Towards Engineering Osteochondral Implants – Chondrogenic and Osteogenic Differentiation of Mesenchymal Stem Cells in Silk Fibroin Scaffolds. PP-066. World Conference on Regenerative Medicine 2013, Leipzig, Germany.

8. Böck, T., Schill, V., **Krähnke, M.**, Gilbert, F., Steinert, A., Tessmar, J., Blunk, T., Groll, J. Tailored hyaluronic acid-based hydrogels with varying crosslinker concentration for cartilage regeneration – chondrogenic differentiation of mesenchymal stem cells. PP-358. World Conference on Regenerative Medicine 2013, Leipzig, Germany.

A.3 Acknowledgments

An dieser Stelle ist es mir eine Freude, mich bei all denjenigen zu bedanken, die es mir ermöglicht haben diese Doktorarbeit anzufertigen und natürlich auch bei denjenigen, die mich auf diesem langen Weg begleitet haben.

Zuallererst möchte ich mich ganz herzlich bei meinem Professor Torsten Blunk für die tolle Betreuung über die gesamte Zeit der Arbeit bedanken. Vielen Dank für den Freiraum den du uns immer gegeben hast, damit wir unseren Ideen nachgehen konnten und für den Input den du hast einfließen lassen. Danke auch für die Möglichkeit in halb Europa an diversen Kongressen und Konferenzen teilnehmen zu können! Nicht zu vergessen natürlich die lustigen Teambuilding-maßnahmen auf unterschiedlichsten Ausflügen und Weinfesten.

Als nächstes möchte ich mich herzlichst bei Herrn Prof. Meinel für die Übernahme der Erstprüferschaft und die gute Zusammenarbeit in unserem Projekt bedanken.

Vielen Dank auch an meine Kooperationspartnerin Eva Gador (Heusler) für die angenehme Zusammenarbeit über das gesamte Projekt hin und für die Versorgung mit Seidenscaffolds und TGFβ-gekoppelten PMMA-Beads.

Ein ganz besonderer Dank geht natürlich an meine lieben Mitstreiter aus dem Kompetenzteam Tissue Engineering: Katha, Miri, Nane, Oli und Thomas. Ihr wart mir die allerliebsten Laborkollegen die es gibt und seid mir sehr ans Herz gewachsen. Vielen Dank für die vielen lustigen Momente und die zum Teil lichterloh brennende Arbeitsatmosphäre in Labor und Büro, die den derweil deprimierenden und rückschlagbehafteten Forschungsalltag erträglich gemacht haben und mich immer gerne auf die Arbeit haben kommen lassen. Nicht zu vergessen auch die vielen Erlebnisse abseits der Klinik.
Vielen Dank an meine Studenten und Mediziner, die mit herausragender fachlicher Kompetenz (Zitat: „Denken ist nicht so meine Stärke“) ihren Beitrag zu dieser Arbeit geleistet haben: Caroline, Lisa, Rasmus, Felix und Alex. Selbstverständlich auch alle anderen im Labor: Katharina, Wiebke, Daniel, Nathalie, Lisa, Sylvia, Renate, Irina, Andrea, Susanne und falls ich jemanden vergessen habe, seid mir bitte nicht böse.

Unserer guten Seele im Labor, Sabine, sei ganz herzlich für die Hilfe beim Schneiden der Histoproben und RNA-Aufreinigung gedankt und Claudia für das Einbetten in Paraffin.

Ein großes Dankeschön geht an André Steinert und Fabian Gilbert aus dem König-Ludwig-Haus für die Versorgung mit Hüftköpfen.

Dem IZKF Würzburg danke ich für die Förderung des Projektes.

Dem Sekretariat um das Dreigestirn Frau Riechwald, Neumann und Hofmann sei für die tatkräftige Unterstützung bei jedweden organisatorischen Dingen gedankt.

Ein großer Dank geht natürlich auch an meine Familie, meinen Eltern Iris und Bernd und meinen beiden Schwestern Marielle und Meike. Ihr habt es mir erst ermöglicht, das zu tun, was ich immer machen wollte. Außerdem ist es schön zu wissen, dass zumindest irgendjemand glaubt, dass ich mal den Nobelpreis verliehen bekomme :).

Zu guter letzt gilt mein ganz besonderer Dank meiner wunderbaren Frau Jule. Danke, dass du immer für mich da bist!